General Disclaimer

One or more of the Following Statements may affect this Document

- This document has been reproduced from the best copy furnished by the organizational source. It is being released in the interest of making available as much information as possible.

- This document may contain data, which exceeds the sheet parameters. It was furnished in this condition by the organizational source and is the best copy available.

- This document may contain tone-on-tone or color graphs, charts and/or pictures, which have been reproduced in black and white.

- This document is paginated as submitted by the original source.

- Portions of this document are not fully legible due to the historical nature of some of the material. However, it is the best reproduction available from the original submission.

NAS CR-167924

(NASA-CR-167924) A NEW ANTENNA CONCEPT FOR SATELLITE COMMUNICATIONS (NTL, Inc., Colmmack, N.Y.) 111 p HC A06/MF A01

N82-31584

Unclas
G3/32 28837

A NEW ANTENNA CONCEPT FOR SATELLITE COMMUNICATIONS

By G. Skahill and D. Ciccolella

NTL, Inc.

Prepared for

NATIONAL AERONAUTICS AND SPACE ADMINISTRATION

NASA Lewis Research Center

Contract NAS3-22887

1. Report No.	2. Government Accession No.	3. Recipient's Catalog No.
NASA CR 167924		

4. Title and Subtitle	5. Report Date
A New Antenna Concept for Satellite Communication	June 1982
	6. Performing Organization Code

7. Author(s)	8. Performing Organization Report No.
G. Skahill and D. Ciccolella	
	10. Work Unit No.

9. Performing Organization Name and Address	11. Contract or Grant No.
NTL, Inc. 358 Veterans Memorial Highway Commack, NY 11725	NAS 3-22887
	13. Type of Report and Period Covered
12. Sponsoring Agency Name and Address	Contractor Report
NASA Lewis Research Center Cleveland, OH 44135	14. Sponsoring Agency Code

15. Supplementary Notes

Technical Monitor, Richard Lee, Space Communications Division
NASA Lewis Research Center

16. Abstract

A novel antenna configuration of two reflecting surfaces and a phased array is examined for application to satellite communications and shown to be superior in every respect to earlier designs for service to the continental United States from synchronous orbit. The vignetting that afflicts other two reflector optical systems is eliminated by use of a reflecting field element. The remaining aberrations, predominantly coma, are isolated in the time delay distribution at the surface of the array and can be compensated by ordinary array techniques. The optics exhibits infinite bandwidth and the frequency range is limited only by the design of the array.

17. Key Words (Suggested by Author(s))	18. Distribution Statement
Antennas Reflector antennas Two reflector antennas Scanning antennas Limited sector antennas	Unclassified - Unlimited

19. Security Classif. (of this report)	20. Security Classif. (of this page)	21. No. of Pages	22. Price*
Unclassified	Unclassified	119	

* For sale by the National Technical Information Service, Springfield, Virginia 22161

CONTENTS

CONTENTS

ILLUSTRATIONS

ILLUSTRATIONS

ILLUSTRATIONS

ILLUSTRATIONS

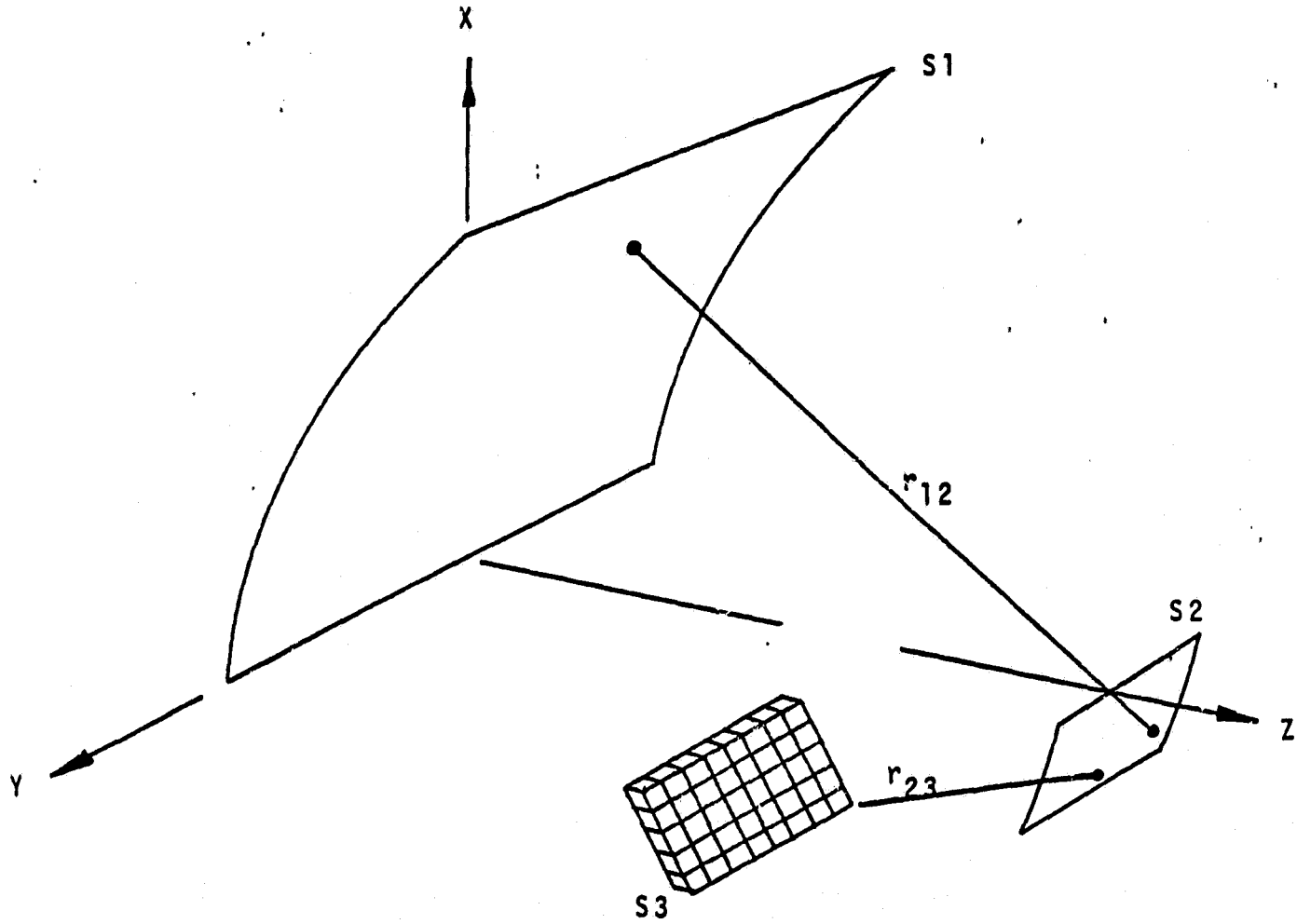

FIGURE 1-1. MICROWAVE TELESCOPE

1.0 INTRODUCTION

1.1 SUMMARY OF RESULTS

NTL has developed a proprietary antenna design for transforming a small aperture antenna capable of wide angle scanning to a large aperture antenna with reduced angle scanning. It consists of a large primary reflector, a small subreflector, and a phased array feed (Figure 1-1) and its performance is clearly superior to previous limited field scanners.

This document reports on an examination of the applicability of the NTL antenna to the satellite terminals of 30/20 GHz SATCOM configured to provide service to CONUS from synchronous orbit. Excellent pattern control was demonstrated over a field of ± 4 degrees (Figure 1-2) by ± 2 degrees (Figure 1-3) using a compact antenna system employing control of only the phase of the elements of the array.

A number of unique and attractive performance features were also demonstrated. For example:

- The NTL design minimizes the impact of phaser granularity and phaser errors by transforming them into amplitude effects on the primary aperture, thereby minimizing degradation of the radiation patterns.

FIGURE 1-2. EAST-WEST SCANNING PERFORMANCE USING PHASE CONTROL ONLY OF ARRAY ELEMENTS (SCAN -4, 0, +4 DEGREES)

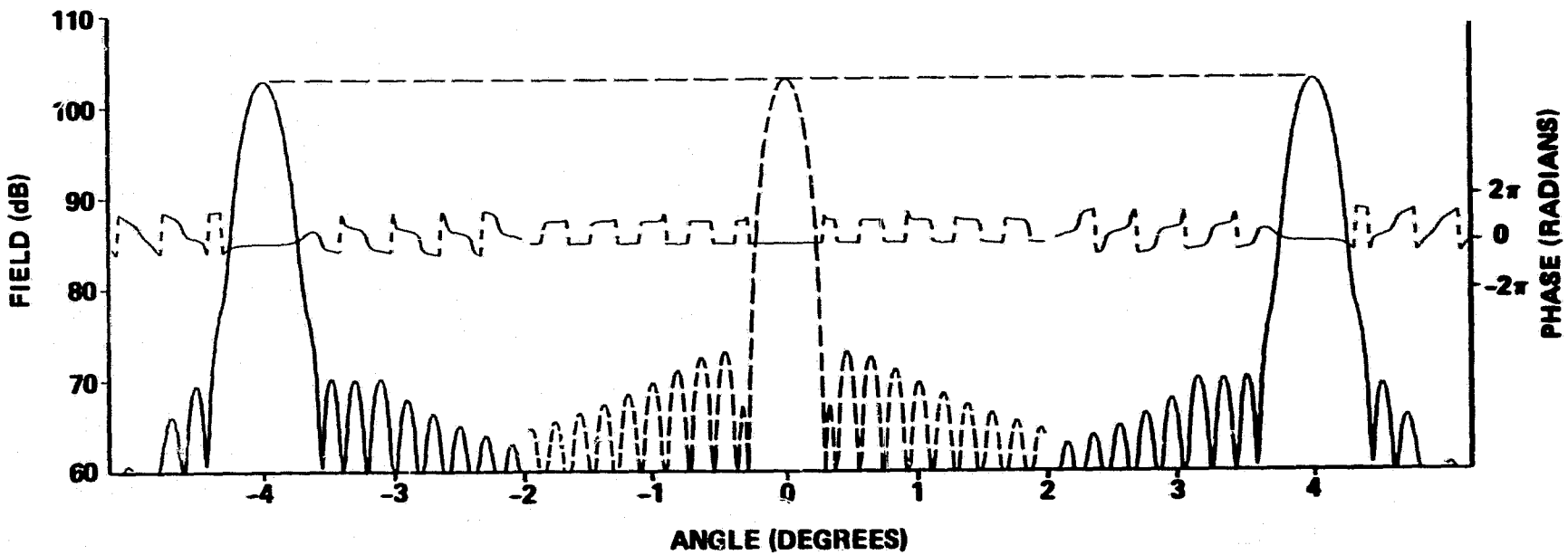

FIGURE 1-3. NORTH-SOUTH SCANNING PERFORMANCE USING PHASE CONTROL ONLY OF ARRAY ELEMENTS (SCAN -1, +1, +3 DEGREES)

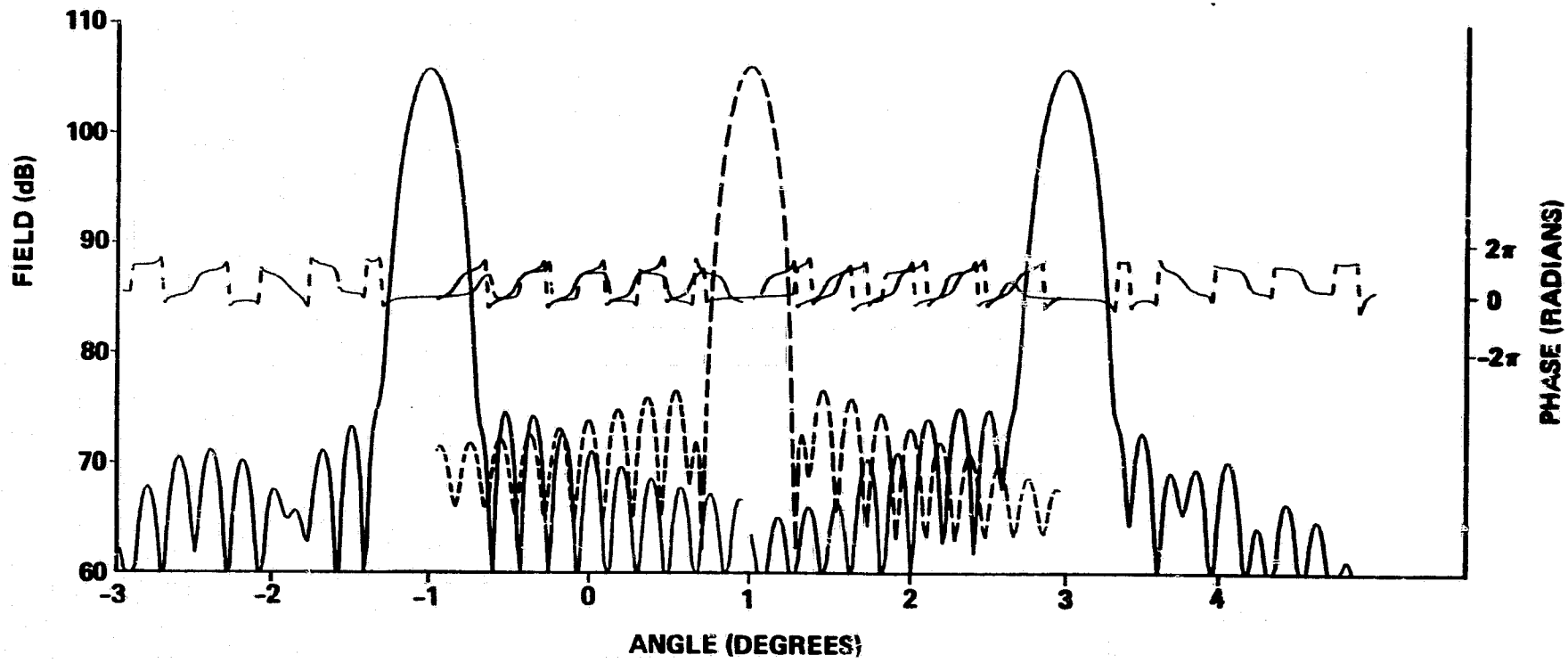

Slowly varying phase errors on the surface of the array transform to aperture errors of the same shape and amplitude with scale magnification (Figure 1-4).

- The two reflector optical system exhibits infinite bandwidth and the frequency sensitivity of the antenna is that of the phased array. Any amplitude and time delay distribution on the aperture transforms to a frequency invariant excitation of the phased array. As a result, the NTL antenna, unlike similar configurations, exhibits angle limited performance. The number of beamwidths covered can be increased arbitrarily by increasing the frequency.

- Vignetting losses are eliminated, permitting the entire surface areas of the primary reflector and the phased array to be utilized for all beam positions. Because of this feature the scanning aberrations can be compensated entirely by controlling the phase distribution on the phased array. Because of this feature amplitude control of the array elements is not required.

- Multiple beam/scanning beam/multiple scanning beam performance will be the same as can be obtained from an

FIGURE 1-4. OPTICAL TRANSFORMATIONS

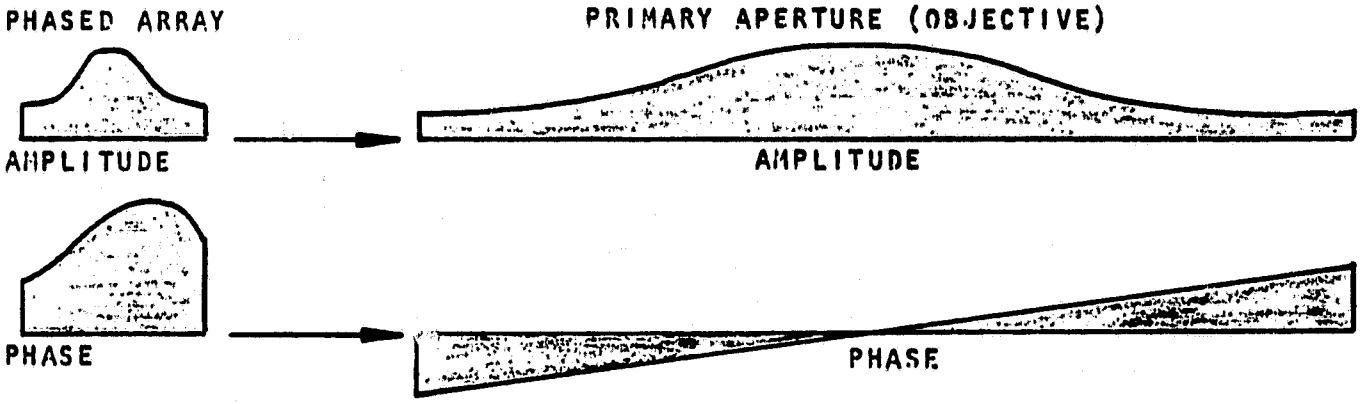

ERROR FREE TRANSFORMATION

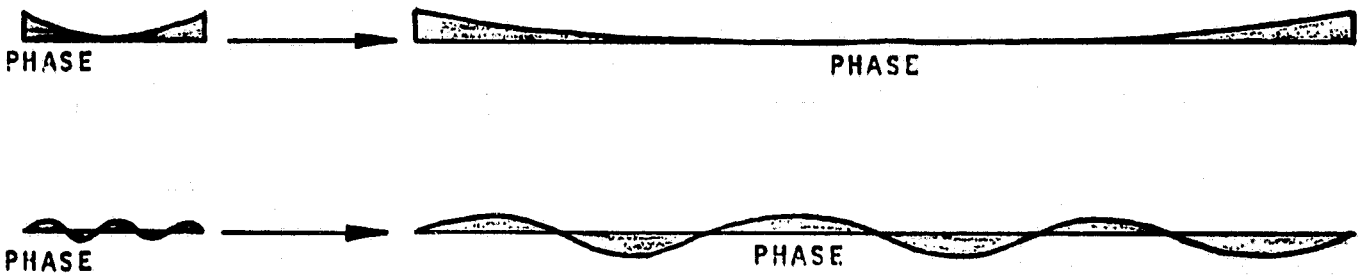

IMPACT OF SLOWLY VARYING PHASE ERRORS

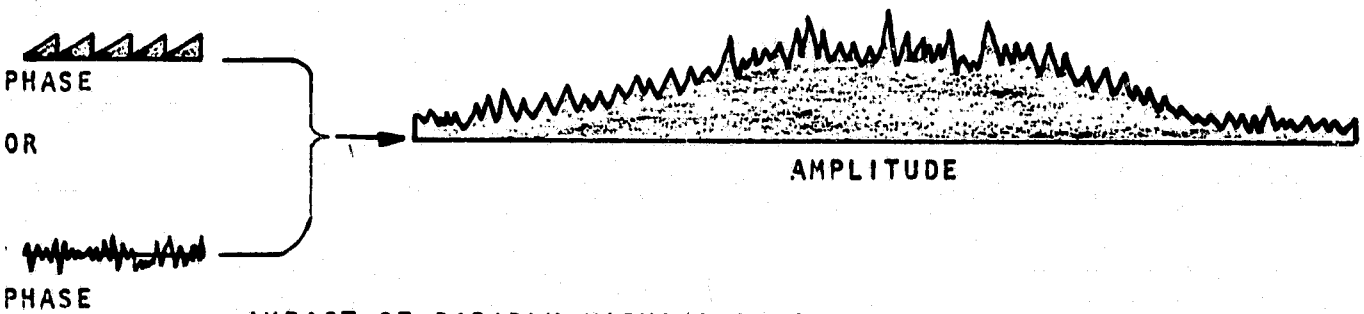

IMPACT OF RAPIDLY VARYING PHASE ERRORS

equivalent phased array antenna subject to our ability to control the polarization conversion (Section 4.2). These results have been drawn from detailed examination of an offset configuration with an f-number of 1.5 and magnification of 5 (array area is 4 percent of the aperture area). Three dimensional performance was estimated by successive two-dimensional analyses of compatible offset and symmetrical geometries (Figure 1-5). These methods have proven successful at characterizing the performance of offset reflector systems although more elaborate, three dimensional, analytical models are required for accurate system design.

1.2 CONCLUSIONS

NTL's antenna design offers performance which is clearly superior to other limited field scanners (Section 3). Its applicability to 30/20 GHz SATCOM is outstanding and it merits consideration in the planning for that system.

1.3 RECOMMENDATIONS

Further analytical activity is indicated in several areas:

- Accurate design of the two-reflector optical system requires efficient three dimensional analytical models

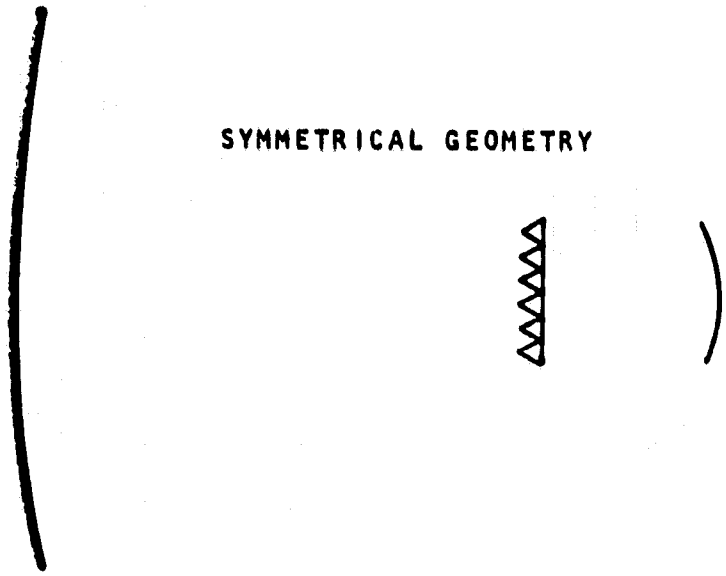

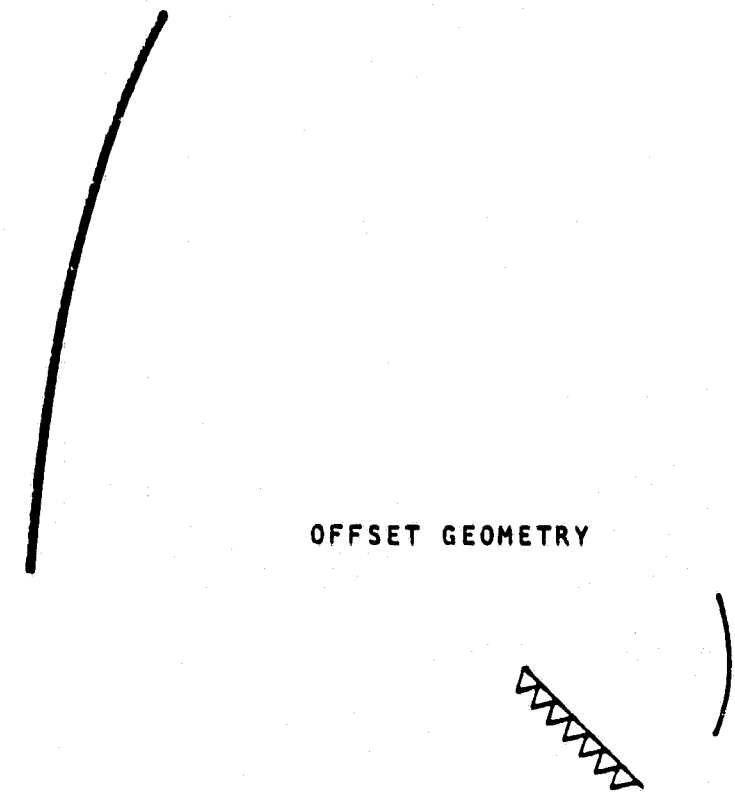

FIGURE 1-5

TWO DIMENSIONAL ANALYSIS
MODELS

capable of successive diffraction calculations to characterize the distributions on all surfaces. Several elements of these models are already available but they need to be pulled together into a coordinated design tool.

- A modest production activity using the existing two-dimensional analyses will result in a deeper understanding of the unusual transformation properties of this optical system.

- Extensive three dimensional studies are recommended for designing satellite systems and proof-of-concept experiments.

- The recommended analytical developments can be used as a basis for designing an experimental test bed and in specifying/directing test plans and conditions.

1.4 REPORT ORGANIZATION

The optical configuration of the NTL antenna is described in Section 2. Comparisons with similar systems are presented in Section 3 with some observations on why it offers such

profoundly improved performance parameters. Analytical methods are described in Section 4. Section 5 contains a large amount of data characterizing a selected system's performance relative to the requirements of 30/20 GHz SATCOM.

2.0 THE NTL ANTENNA CONCEPT

2.1 TELESCOPE OPTICS

In common two element telescopes electromagnetic energy from a distant source is collected by a primary (or objective) element which directs it to a focus (Figure 2-1).

FIGURE 2-1. A COMMON TELESCOPE

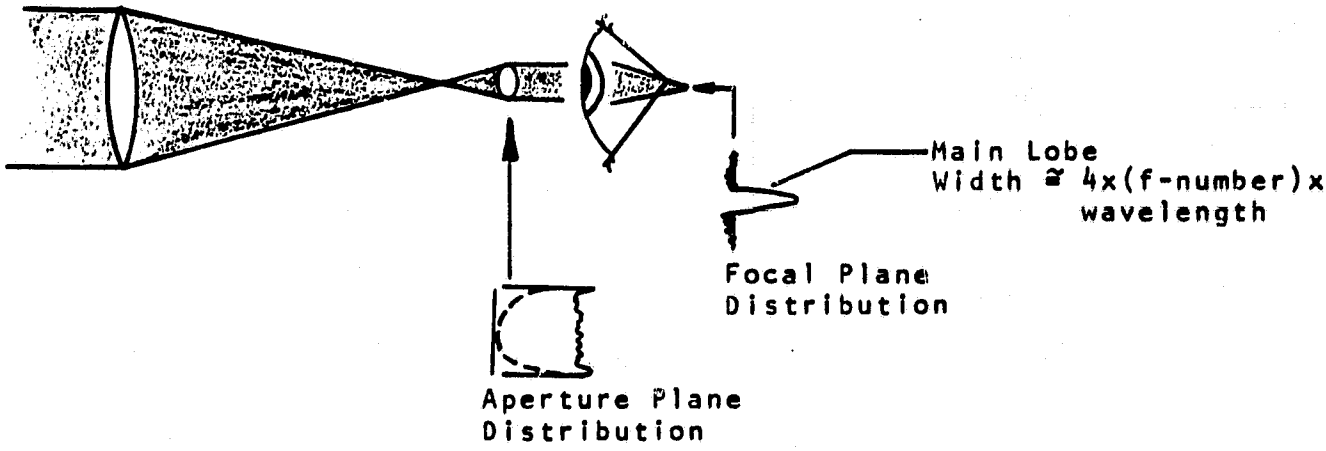

A smaller eyepiece, usually deployed so the focal region is between the elements, recollimates the energy for processing by an eye. In this system the elements define aperture planes wherein the energy is distributed over many wavelenths; in the focal planes the energy from a single remote source exhibits the familiar diffraction patterns with most of the energy concentrated in a central lobe. A retina, or film, or a detector array can be placed in a focal plane to provide processed data over a small range of incident angles.

At radio frequencies a phased array can be placed in an aperture plane. In this situation the outputs of a multiple beam array correspond to different angles of incidence and they constitute a focal plane (Figure 2-2).

FIGURE 2-2. TWO ELEMENT TELESCOPE EMPLOYING A PHASED ARRAY EYEPIECE/EYE

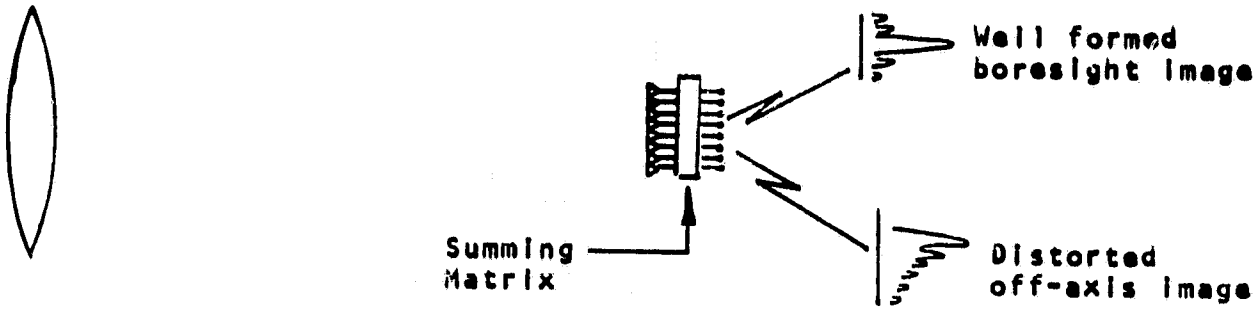

In a single beam array the output corresponds to a single angle of incidence which can be scanned by reconfiguring the phase coefficients of the summing manifold. Multiple scanning beam systems can be constructed by using a matrix in which the summing coefficients for each output port can be reconfigured "independently". Multiple beam systems are able to operate with low losses and true independence only if the far-field radiation patterns corresponding to each pair of output ports are nearly orthogonal.

Two types of performance degradation can be observed when a two element telescope is scanned. "Vignetting" is the aberration in which the rotated angle of incidence causes

some of the energy to miss the eyepiece (Figure 2-3).

FIGURE 2-3. VIGNETTING IN A COMMON TELESCOPE

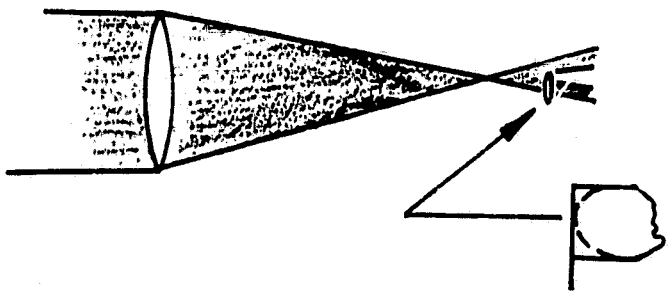

The other type of aberration results in distorted focal plane images because the phase path lengths have been disturbed relative to the boresight condition (Figure 2-4).

FIGURE 2-4. DISTORTED FOCAL PLANE IMAGE CAUSED BY SCANNING

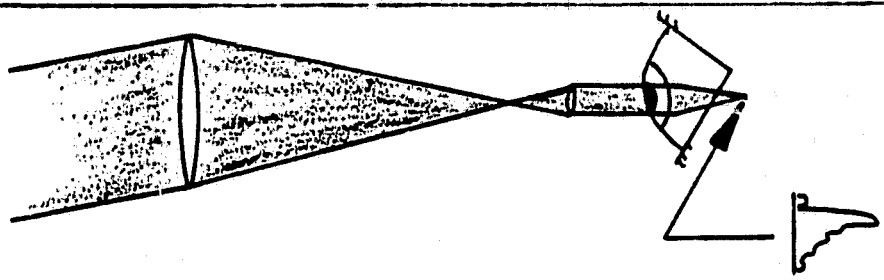

Vignetting is aggravated by increasing the length of the system (larger f-number). Focal plane distortion is aggravated by shortening the system.

2.2 FIELD ELEMENTS

Opticians have resolved the scanning aberrations in long focus systems by locating a field element (so named because it is on the field side of the eyepiece) at or near the focal plane of the primary surface. The field element images the objective to the eyepiece which means it has one focus at the center of the objective and another at the center of the eyepiece.

When the system is long enough the vignetting is eliminated and a perfectly collimated output is obtained (Figure 2-5).

FIGURE 2-5. A THREE ELEMENT TELESCOPE

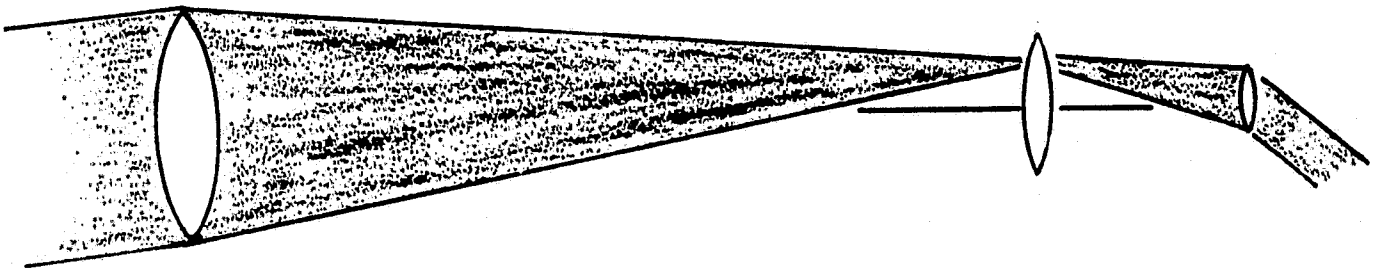

Attempts to shorten these systems have not been successful because the other aberrations begin to dominate. Improved results have been obtained by rotations of the smaller elements

with incident angle (Figure 2-6). However these systems still require a large f-number for quality image formation.

FIGURE 2-6. THREE ELEMENT TELESCOPE WITH ROTATIONS

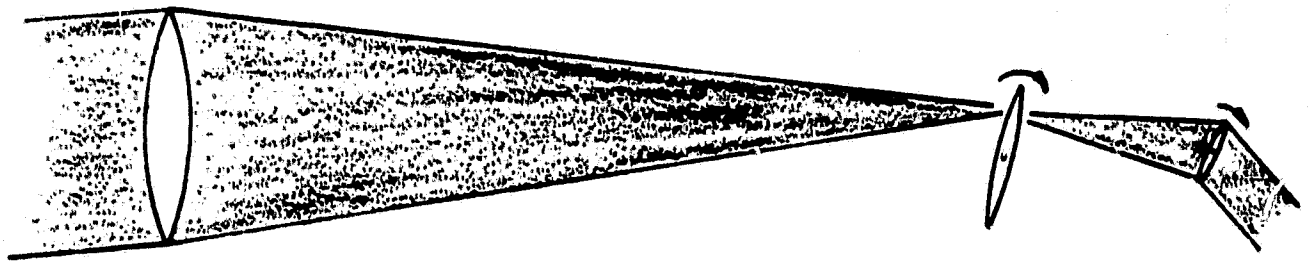

2.3 SHORT FOCUS TELESCOPES

Microwave antenna systems must feature low f-numbers to be practical. Brute force shortening of the common telescope described in Section 2.2 results in severely distorted focal plane images and does not seem to be a fruitful path for the antenna designer. Despite the appearances, however, brute force shortening is the way to go!

What is different about microwave antenna design that permits the use of compact geometries that are forbidden to the optical designers? The answer lies in our ability to control phase and in an unexpected and unique property of the three

element telescope (Figure 2-7).

FIGURE 2-7. THREE ELEMENT TELESCOPE LOCALIZES EYEPIECE SCANNING ABERRATION IN THE PHASE DISTRIBUTION!

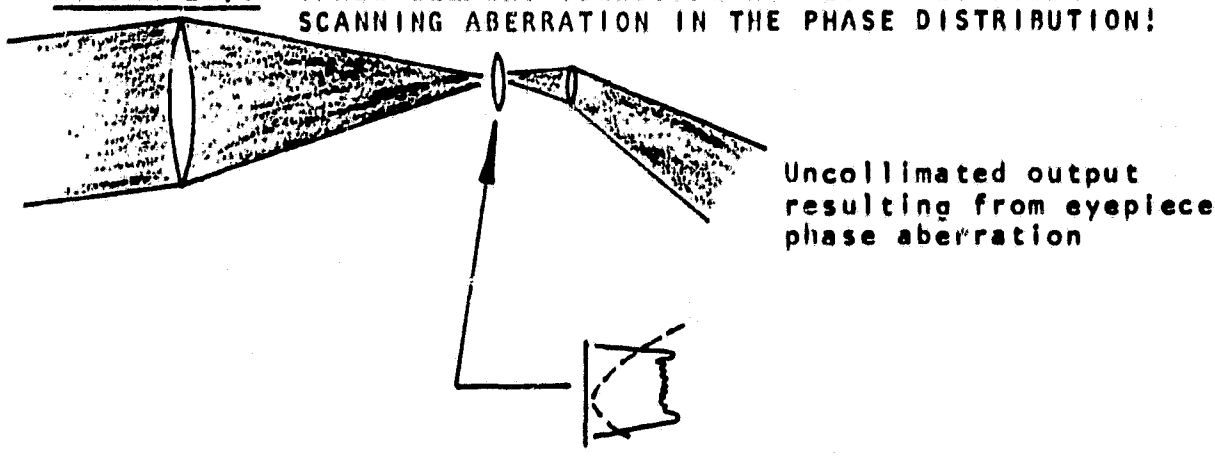

The focal plane distortions that are the result of scanning in low f-number designs appear as a phase only aberration on the eyepiece. By inserting a phased array in place of the eyepiece these aberrations can be compensated and the desired result -- a compact system with magnification and good quality wide angle images -- is obtained.

Why has it taken so long for such a simple concept to surface? First, because it cannot be exploited at light wavelengths where equivalent phase control would entail using a different eyepiece lens for each angle of incidence. Second, recognition of the unique phase only nature of the scanning aberrations depends on accurate diffraction analyses of the inbound flow of energy. Opticians have used ray tracings for systems (scan angles) in which the energy can be brought

to a point of good focus; these are not adequate for situations involving substantial aberration. Antenna designers have relied on diffraction methods which apply to all conditions but are enormously expensive for large aperture systems.

NTL's examinations of three-element microwave telescopes have been based on efficient diffraction algorithms and have addressed systems with aperture extents ranging from several tens of wavelengths to several tens of thousands of wavelengths and have consumed hundreds of CPU hours on the CDC 7600. They have developed convincing evidence that the optics are frequency invariant: that amplitude/time delay distributions on the objective transform to amplitude/time delay distributions on the eyepiece, or phased array, which are equivalent except for scale magnification.

2.4 NTL'S MICROWAVE TELESCOPE

The previous descriptions were illustrated by systems employing lenses as optical elements for clarity. The recommended design (Figure 2-8) consists of two reflecting elements and a phased array.

FIGURE 2-8. MICROWAVE TELESCOPE

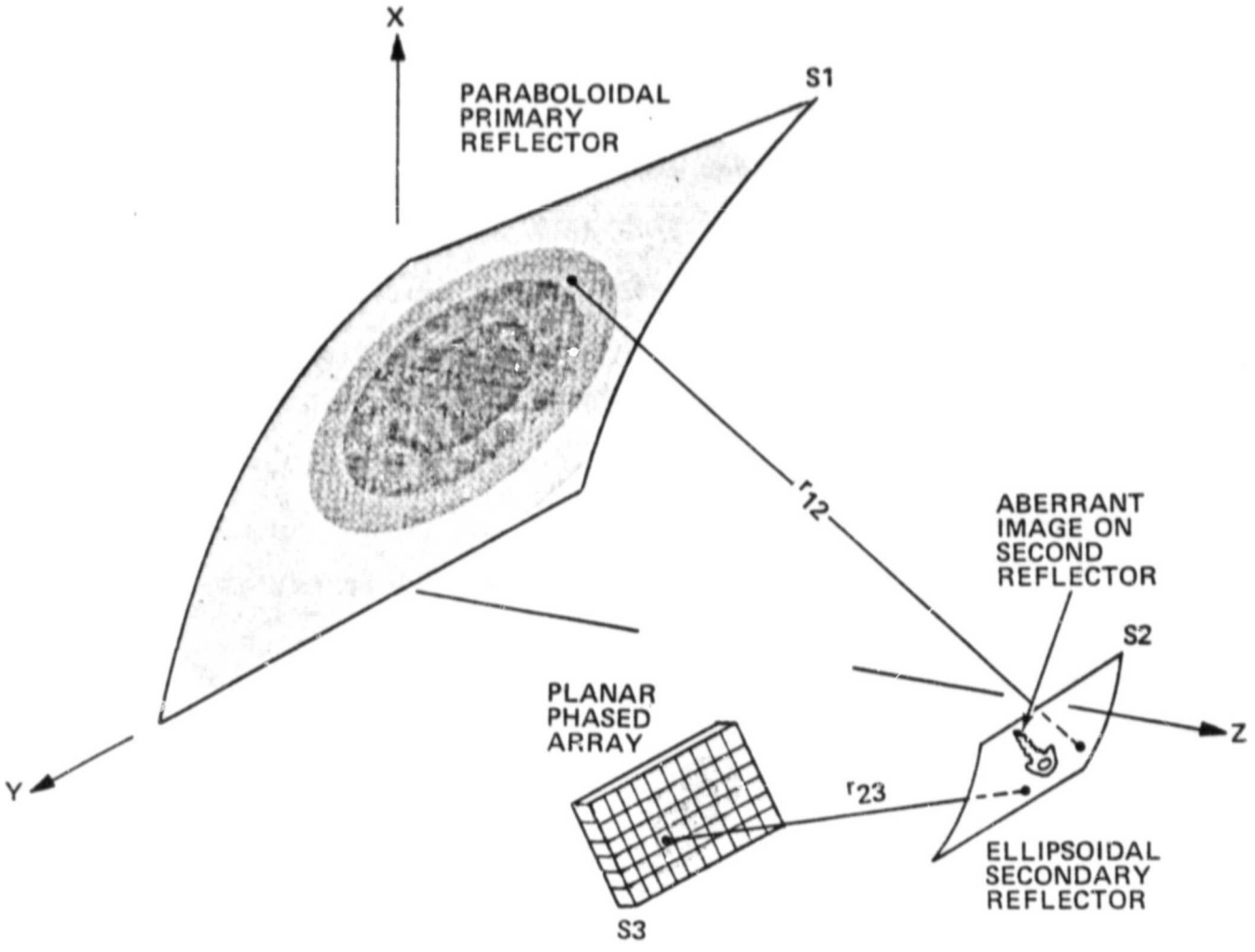

The primary reflector is a segment of a paraboloid of revolution. The field element is a segment of an ellipsoid of revolution with a surface which passes through the focus of the primary reflector. Its two foci are located near the primary aperture and the surface of the phased array.

The reflector configuration has an obvious blockage problem which is overcome by offset geometries. The blockage and offset parameters dominate the design of the antenna system.

3.0 COMPARISONS WITH SIMILAR SYSTEMS

A number of concepts have been proposed for providing electronic beam scanning over limited sectors (reference 1). NTL's microwave telescope is a marked improvement on them all. This section makes comparative examinations of the NTL antenna with other types of hybrid antenna which consists of an electronically scanned array combined with a radiating reflective aperture. Many of the underlying analytical methods are based on geometrical ray tracings which are not of sufficient accuracy to ensure very low sidelobe performance and the reported results reflect these limitations.

3.1 REFLECTOR WITH TRANSVERSE ARRAY FEED

The earliest of the limited scan electronic systems consisted of a transverse cluster feed for a reflector antenna (references 2 - 5, Figure 3-1). It was proposed as a technique for providing a few beamwidths of agile beam performance and as a mechanism for compensating reflector profile errors.

FIGURE 3-1. A CLUSTER FEED ANTENNA

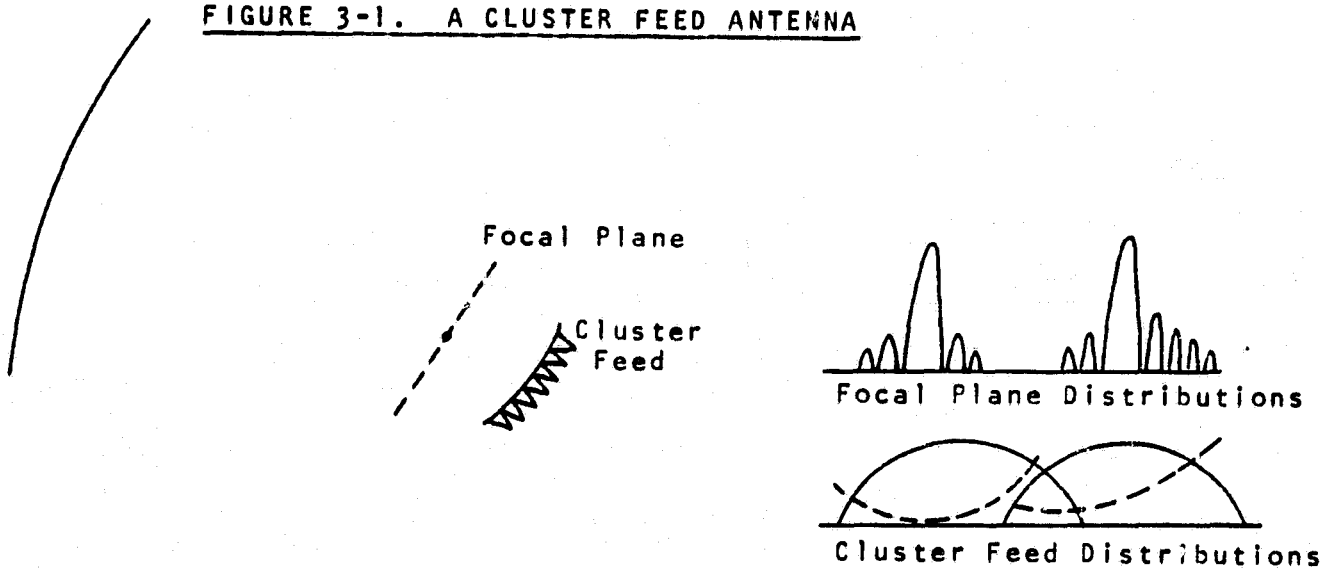

The essential feature is the displacement of the array away from the focus permitting the array excitation to vary slowly in both amplitude and phase for any angle of incidence, a requisite for avoiding disabling mutual coupling effects in the cluster feed. Early experimental models exhibited unprecedented sidelobe levels (-35 dB) and rapid performance deterioration with scan angle.

The scanning performance was limited by vignetting which can be overcome by requiring movement of the region of excitation on the cluster feed array. This requirement implies a need for amplitude as well as phase control and a substantial increase in the number of array elements to accomodate the spot motion.

The vignetting limitation can also be addressed using a fixed region of excitation on the array and movement of the illuminated portion of the reflector with scan angle. Aperture efficiency is limited using this approach and monopulse pattern performance has been demonstrated over extremely limited scan sectors.

3.2 TWO REFLECTORS WITH TRANSVERSE ARRAY FEED

NTL's microwave telescope employs a small second or sub-reflector to alliminate the vignetting over a limited scan sector and to permit efficient utilization of the surfaces of both the primary reflector and the phased array feed for all beam positions.

Earlier investigations recognized that this was an achievable performance goal and strove to achieve it, without success. In those days, our problem was not in techniques of analysis or modelling but in our persistent examinations of wrong configurations of reflector profiles.

An example which was pursued by several investigators is the confocal paraboloid geometry (Figure 3-2) which is an

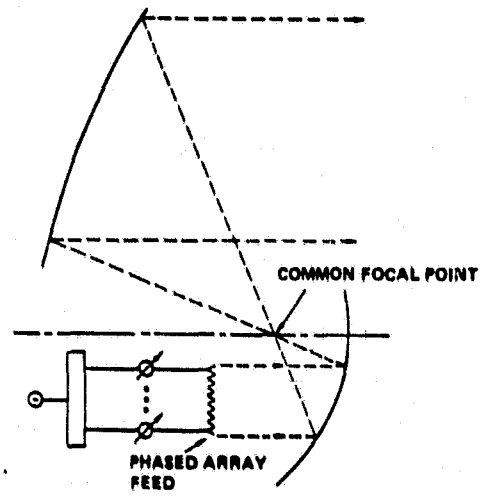

FIGURE 3-2
CONFOCAL PARABOLOID GEOMETRY

exact replication of a two element telescope in which the second reflector is the analog of the eyepiece and the phased array is the analog of the eye (references 6 and 7). These perform exactly as well as the equivalent telescopes and suffer their vignetting deficiencies. Experimental models demonstrated excellent performance -- provided that the phased array angle scanning was augmented by appropriate lateral displacements.

Other examples, of which the previous example is a limiting case, were based on the Cassegrain and Gregorian geometries illustrated in Figure 3-3. Energy intercepted by the parabolic reflector on the left is directed toward its focus F1. It can be intercepted by any one of a family of hyperbolic subreflectors and redirected toward a second focus F2 (cassegrain) or, after transiting the focus F1, it can be intercepted by any one of a family of elliptical subreflectors and redirected toward F2 (Gregorian). The selection of one of the families of surfaces determines the magnification of the system which is a measure of the angle subtended at F2 by the incident energy. A transverse array feed is inserted between F2 and the subreflector.

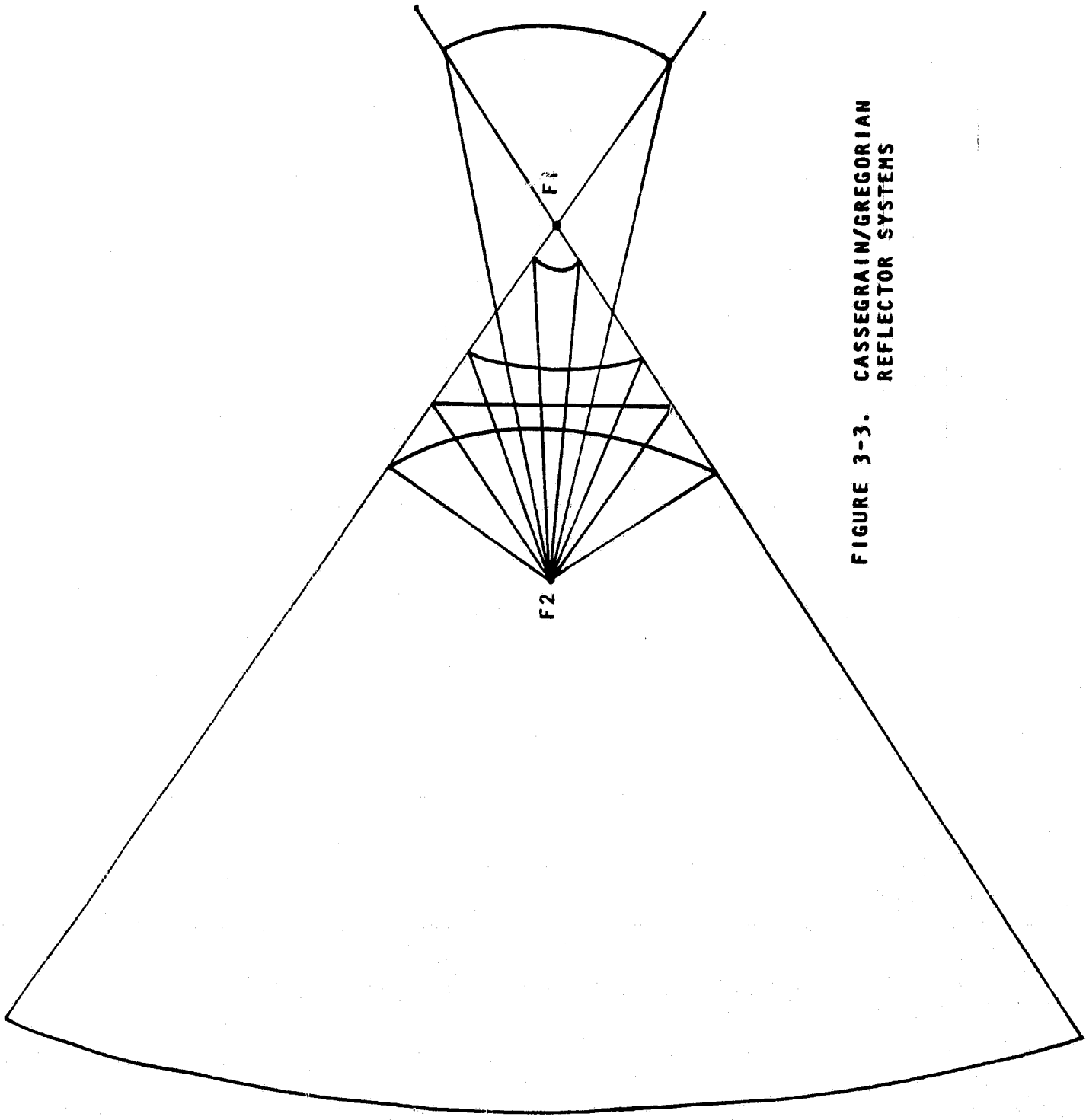

FIGURE 3-3. CASSEGRAIN/GREGORIAN REFLECTOR SYSTEMS

The scanning performance of these systems can be estimated by reviewing their lens analogs which eliminate the confusing propagation reversals of reflector systems. Figure 3-4 illustrates a lens analog with the two foci F1 and F2; the magnification is determined by the location of the smaller lens between F2 and F1 or between F1 and the objective.

A rotated angle of incidence causes the images at F1 and F2 to be displaced from the axis (Figure 3-4) and a vignetting loss to be experienced. Clearly the Cassegrain/ Gregorian systems are not able to eliminate the vignetting over any scanning sector even though they are able to offer a trade of the extent of the spot displacement as determined by the magnification and the size of the smaller lens.

A lens analog of the microwave telescope (Figure 3-5) illustrates how the introduction of a field element can eliminate the vignetting phenomenon. It does not offer any clear rationale for the localization of the other scanning aberrations in the phase distribution on the eyepiece.

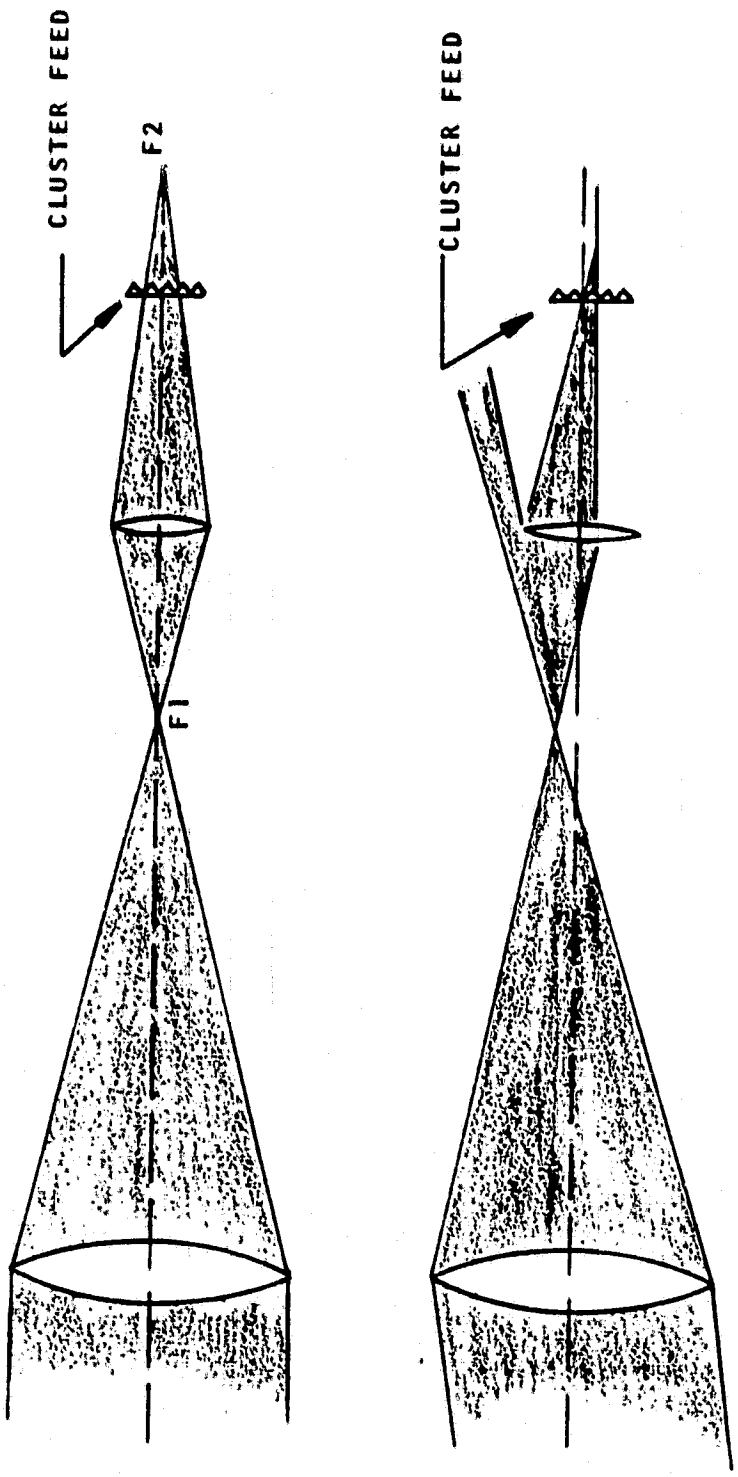

FIGURE 3-4. CASSEGRAIN/GREGORIAN ANALOGS

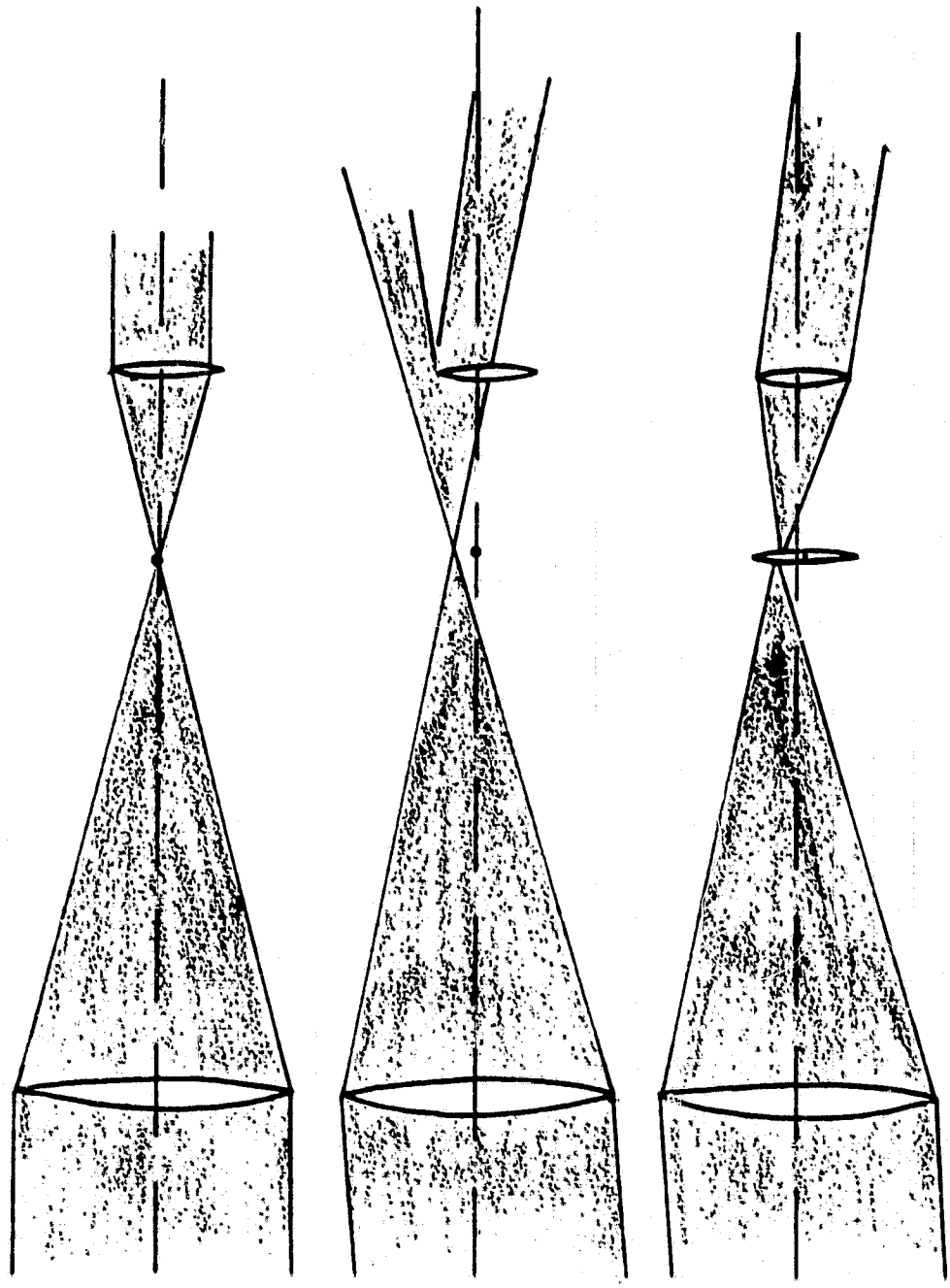

FIGURE 3-5. TELESCOPE SYSTEMS

3.3 SYSTEMS EMPLOYING MICROWAVE LENSES

The ordinary cluster feed system (Figure 3-1) can be configured to overcome the vignetting limitations by the use of various lens and array combinations. An active lens can provide a required phase distribution independently of the amplitude distribution determined by a phased array (Figure 3-6, reference 8). The field element of the NTL microwave telescope can be replaced with a microwave lens (Figure 3-7, reference 9). In either case, particularly the latter one, the mutual coupling effects will limit achievable sidelobe and scanning properties.

3.4 MATRIX FED SYSTEMS

Another way of providing separate control of the amplitude and phase on an oversized array feed employs the translation properties of the Butler matrix (Figure 3-8, reference 10) for movement of the illuminated region of the array and subsequent phase shifters for phase control. In the system illustrated the Butler matrix is sized to fit the illuminated region and the mapping to different parts of the feed array is accomplished by a simple switching matrix.

A simple translation results from linear control of the phasers on the mainfold side of the Butler matrix. Higher

FIGURE 3-6
ACTIVE LENS SYSTEM

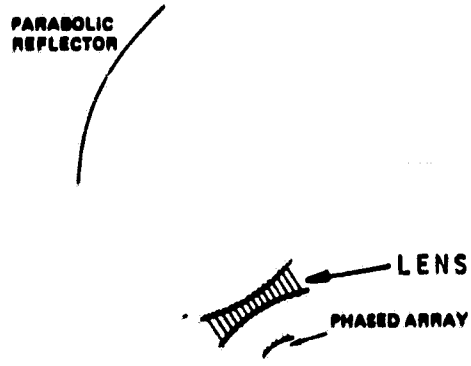

FIGURE 3-7
FIELD LENS SYSTEM

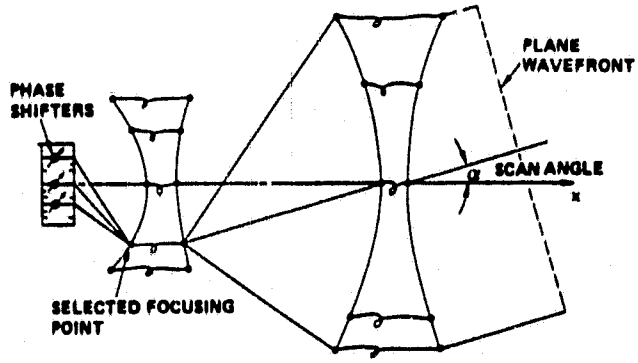

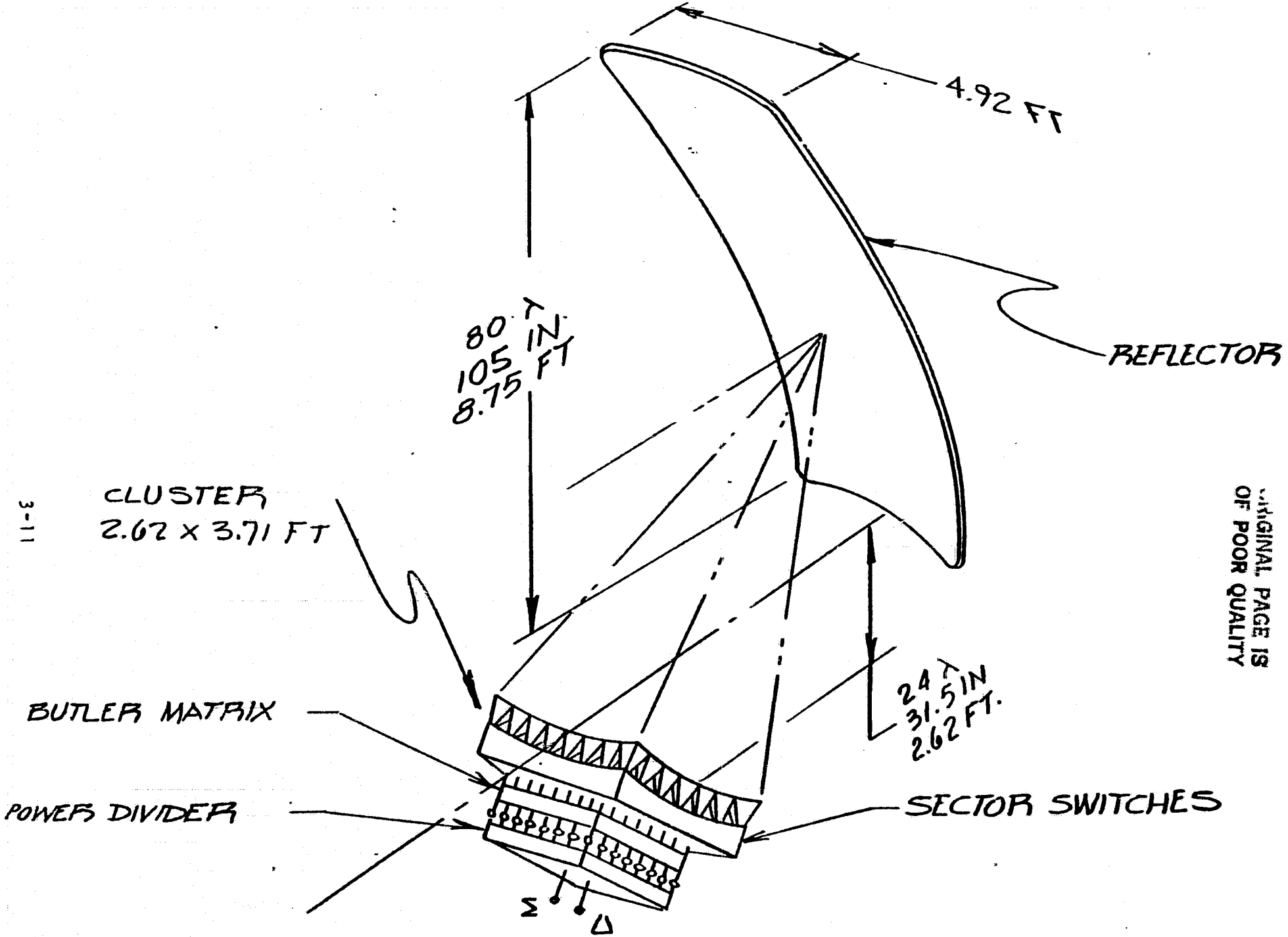

FIGURE 3-8. MATRIX FED SYSTEMS

order phaser control can be employed to diminish certain of the scanning aberrations. Tapering the spacing between array elements can extend the scanning sector. In certain situations a second set of phasers can be used for enhanced performance.

These matrix fed systems offer a viable and powerful alternative to the simple cluster feed designs and permit spot movement without requiring element-by-element amplitude control. It is important to locate the array carefully away from focal regions where the rapidly varying amplitude/phase structure of the diffraction images lead to severe degradations because of mutual coupling.

3.5 CONCLUSIONS

The NTL microwave telescope consists of an objective reflecting surface (paraboloid), a much smaller reflecting field element (ellipsoid), and an array feed employing control of only the phase. It offers:

- full use of the surface of the array over the scan sector.
- full use of the surface of the objective over the scan sector.
- angle limited (not beamwidth limited) scanning.
- infinite bandwidth optics (limited only by the array).
- finely structured diffraction images are isolated on the reflecting field element where mutual coupling is not a concern.
- dimished impact of phaser granularity and errors.

It is an improvement in every respect to previous limited field scanners. It is particularly well suited to 30/20 GHz SATCOM.

4.0 ANALYTICAL METHODS

NTL's analyses are based on diffraction methods in which the amplitude and phase distribution on one element of the system are used to generate the amplitude and phase distribution on the next (Figure 4-1).

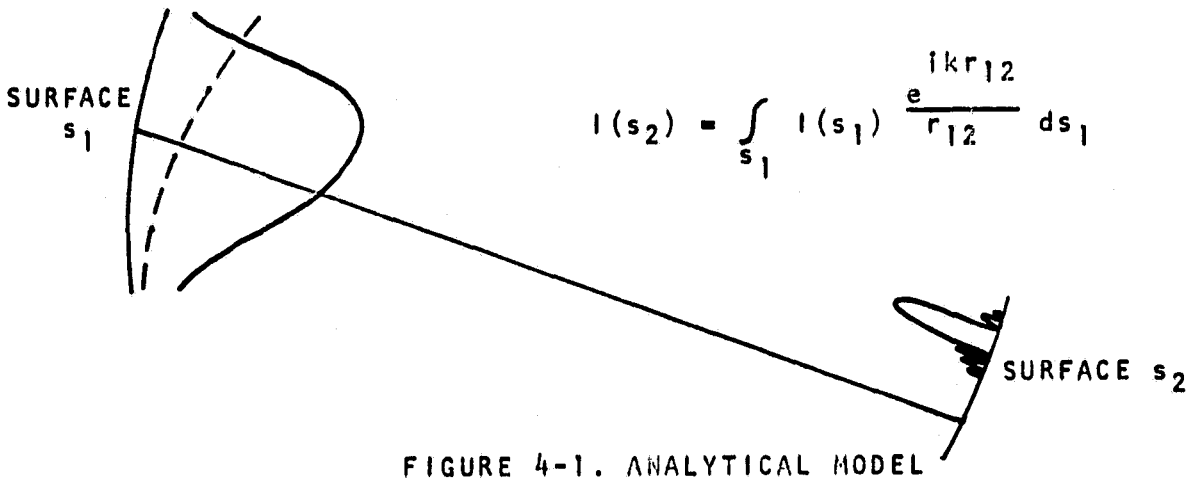

FIGURE 4-1. ANALYTICAL MODEL

For the telescope systems being examined (Figure 4-2) several analytical models can be utilized. An amplitude and phase distribution corresponding to a desired far field pattern

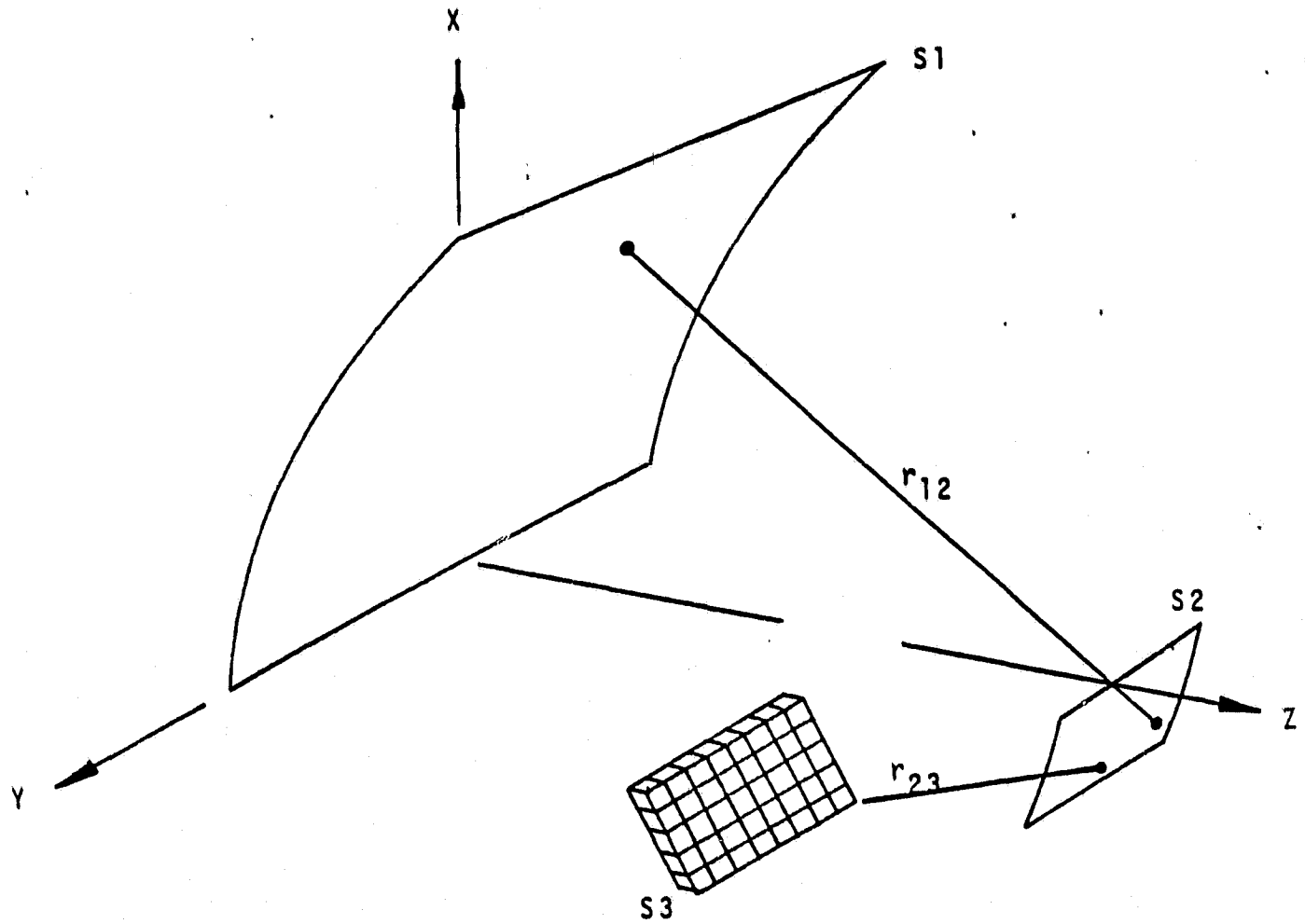

FIGURE 4-2. MICROWAVE TELESCOPE

can be postulated as incident on the surface of the objective and the resulting distributions on the surface of the field element and then on the surface of the array can be calculated.

An amplitude and phase distribution can be postulated as an excitation of the array and the resulting distributions on the surface of the field element, and then on the surface of the objective, and then on the far field can be calculated.

When the surfaces are of adequate size and oriented to intercept the large majority of the energy flow, then we can postulate an inbound distribution, perform the inbound diffraction calculations to obtain the array illumination, impose the retrodirective or conjugate phase condition to establish an appropriate array excitation, perform the outbound diffraction calculations to obtain a nearly perfect (conjugate) replica of the postulated inbound distribution and the desired far field pattern.

For systems employing amplitude as well as phase control of the elements of the array we can examine the scanning performance of a configuration by successive executions of inbound-outbound calculations for a range of incident angles.

For systems employing only phase control of the elements of the array scanning performance is examined by fixing an amplitude excitation obtained from an inbound calculation for a central angle of incidence and then trying a number of phase excitations obtained from inbound calculations for a range of incident angles.

In practice the analysis consists of many inbound calculations in which the configurational parameters of element size, location and orientation are related to the issues of size of the field, blockage, array phase gradients and, most importantly, vignetting. For the 30/20 SATCOM the design goal is to eliminate both blockage and vignetting over a field of ± 4 degrees east-west by ± 2 degrees north-south.

Once a configuration is selected it is straightforward, although expensive, to run through its performance variations with scan angle (Section 5).

During the performance of this contract for NASA Lewis Research Center, NTL's analysis package was improved to permit introduction of phase granularity, phaser errors and array profile errors (Section 5).

4.1 TWO DIMENSIONAL MODELS

The analyses used in developing the data in this report were developed using two dimensional diffraction models. Compatible offset and symmetrical configurations (Figure 4-3) were examined for their scanning capabilities and the performance of a three dimensional composite was inferred from the results.

Even though these models suffer from obvious deficiencies in their ability to characterize the performance of a three dimensional system, they have been used by a number of investigators and have proven successful at predicting the wide angle performance of array fed reflector systems (references 1 - 10).

Attempts to apply these models rigorously to specific planar or conical cuts through a pair of three dimensional elements have not been fruitful in establishing the exact design parameters or the accurate amplitude/phase requirements of a three dimensional geometry. These require the more elaborate three dimensional diffraction algorithms described in Section 4.2.

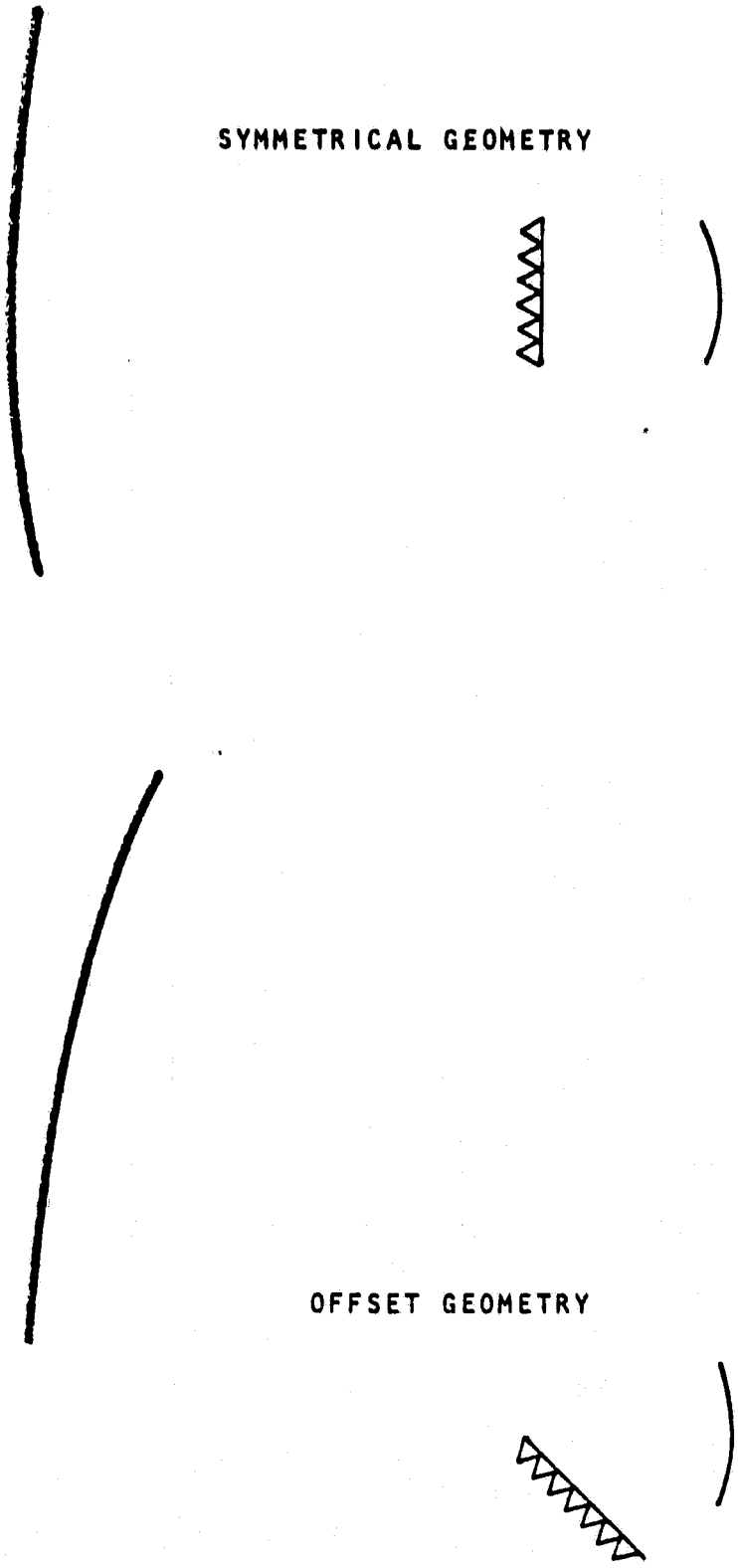

FIGURE 4-3. TWO DIMENSIONAL ANALYSIS MODELS

Our experience indicates that performance predictions based on the two dimensional analysis models are more faithful to actual three dimensional system performance when a divergence or space loss of $1/\sqrt{r}$ is used in place of $1/r$ (Figure 4-1).

4.2 THREE DIMENSIONAL MODELS

An accurate three dimensional analysis of these types of optical systems would include evaluations of the three dimensional diffraction integrals, provision for examination of polarization conversions, and evaluations of edge effects. Any of these contributions can be handled in straightforward fashion although the amount of calculation required can be extremely high.

So far NTL has relied on scalar diffraction models in its examinations of three dimensional systems. Our failure to examine the other issues has been based on using highly tapered, low sidelobe illuminations in which edge effects are small, on examining systems which are long enough to minimize polarization conversion, on using array elements which exhibit the polarization properties of an electromagnetic dipole rather than those of an electric dipole, and on the fact that the "simple" scalar diffraction model has been overwhelming in its consumption of computer resources for apertures of hundreds,

thousands, and tens of thousands of wavelengths. Our resources have been focussed on extending and streamlining the scalar diffraction analyses so they can be applied to optical systems with apertures of millions of wavelengths.

We believe that NTL's scalar diffraction methods use the most efficient and most accurate models available in the world today.

They have been used to generate some interesting and unique focal region images. For example, Figure 4-4 illustrates the amplitude distribution in the focal plane for a 300 wavelength objective with f-number of unity for an incident angle of 9 degrees. The focal image for the same conditions except for frequency scaling of 50 (aperture = 15,000 wavelengths) is illustrated in Figure 4-5. The strange looking distributed image of Figure 4-6 was obtained near the focal region of an elliptical torus reflector with aperture of 30 x 30 meters, f-number = 2.33, wavelength = 3mm.

To date these models have been limited to the problem of the performance of single element systems with array feeds (Figure 4-7).

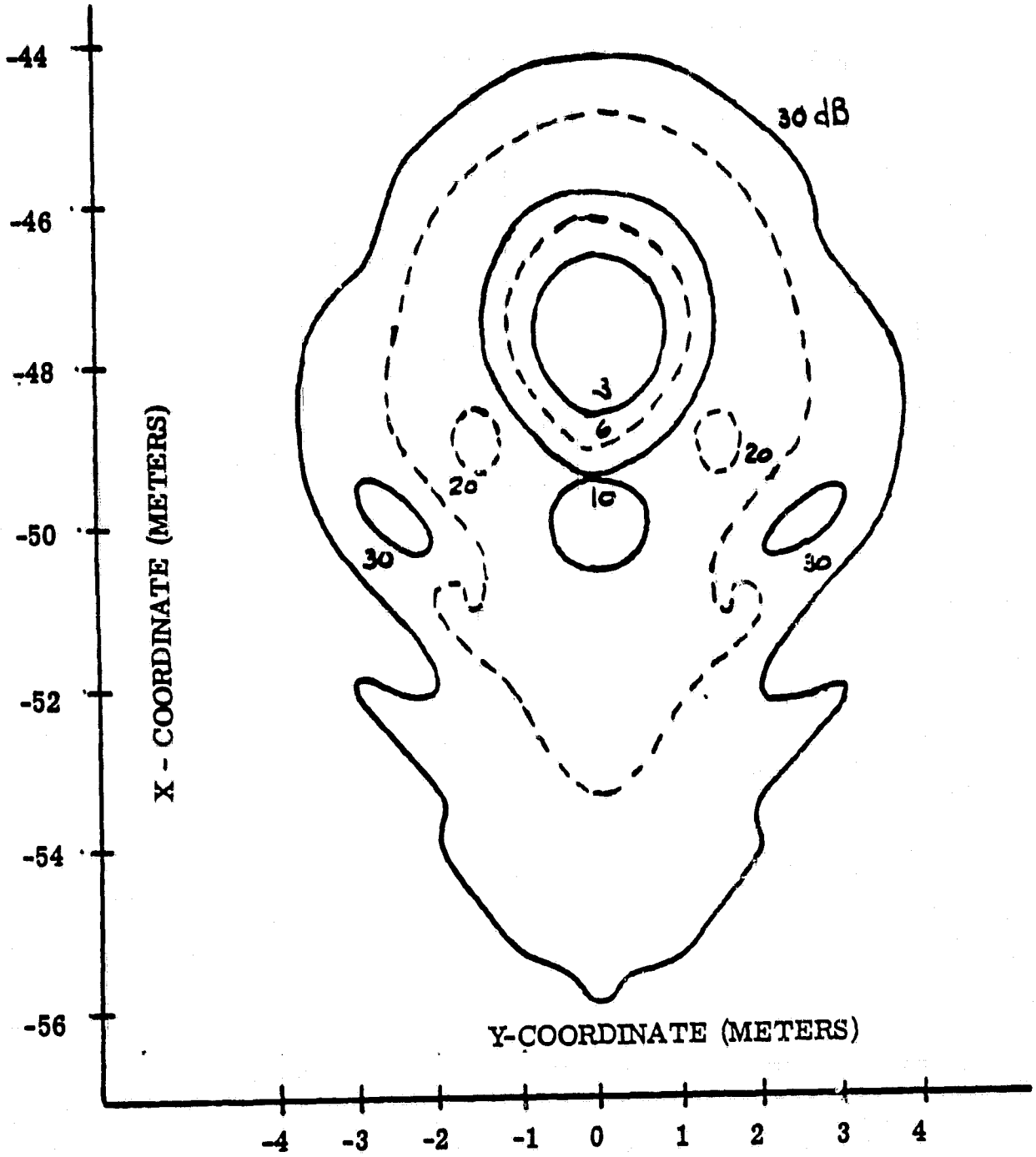

FIGURE 4-4

FOCAL REGION AMPLITUDE DISTRIBUTION, F = D = 300 METERS, λ = 1 METER, SCAN = 9 DEGREES

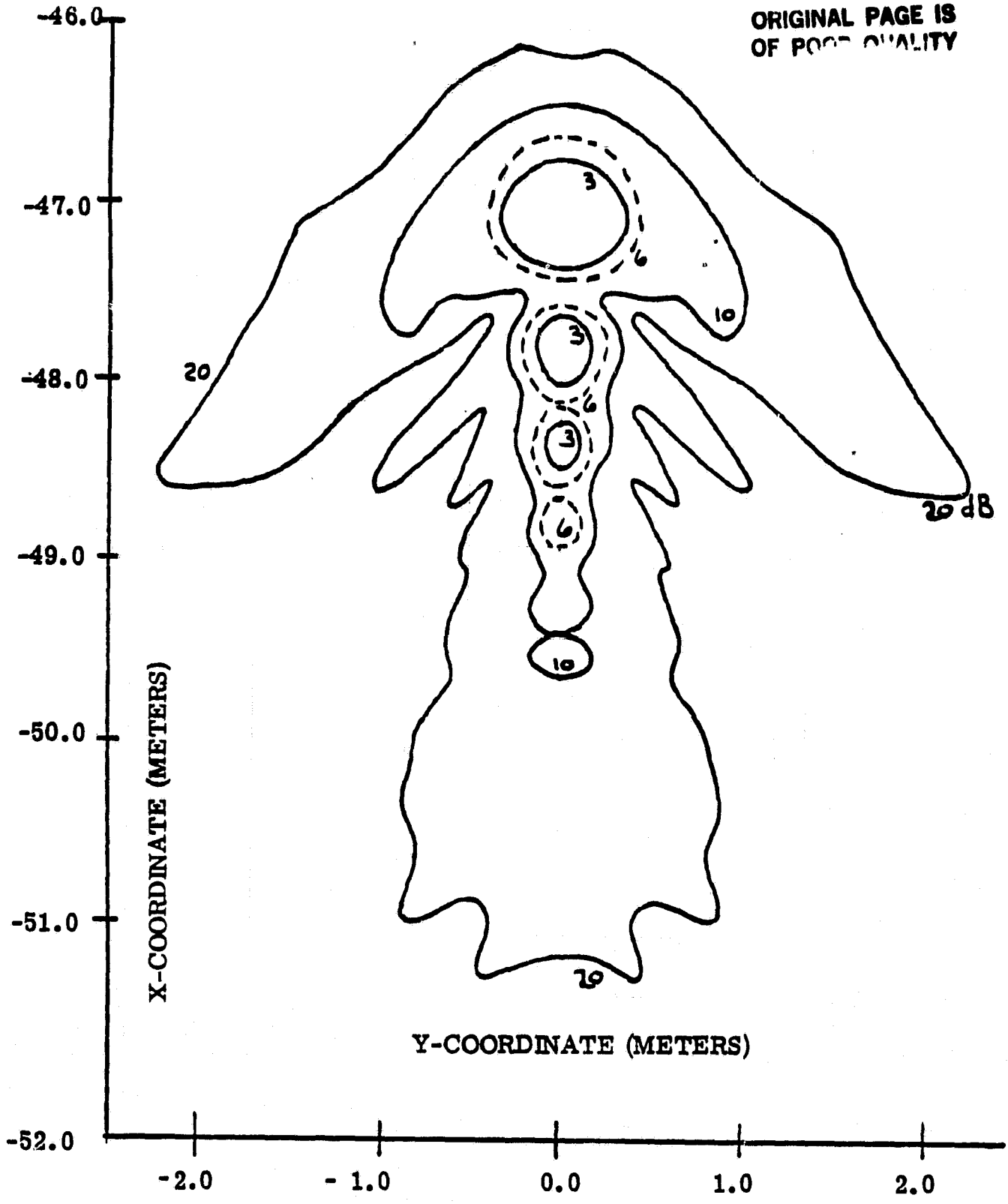

FIGURE 4-5

FOCAL REGION AMPLITUDE DISTRIBUTIONS, F = D = 300 METERS
λ = 0.02 METERS, SCAN = 9 DEGREES

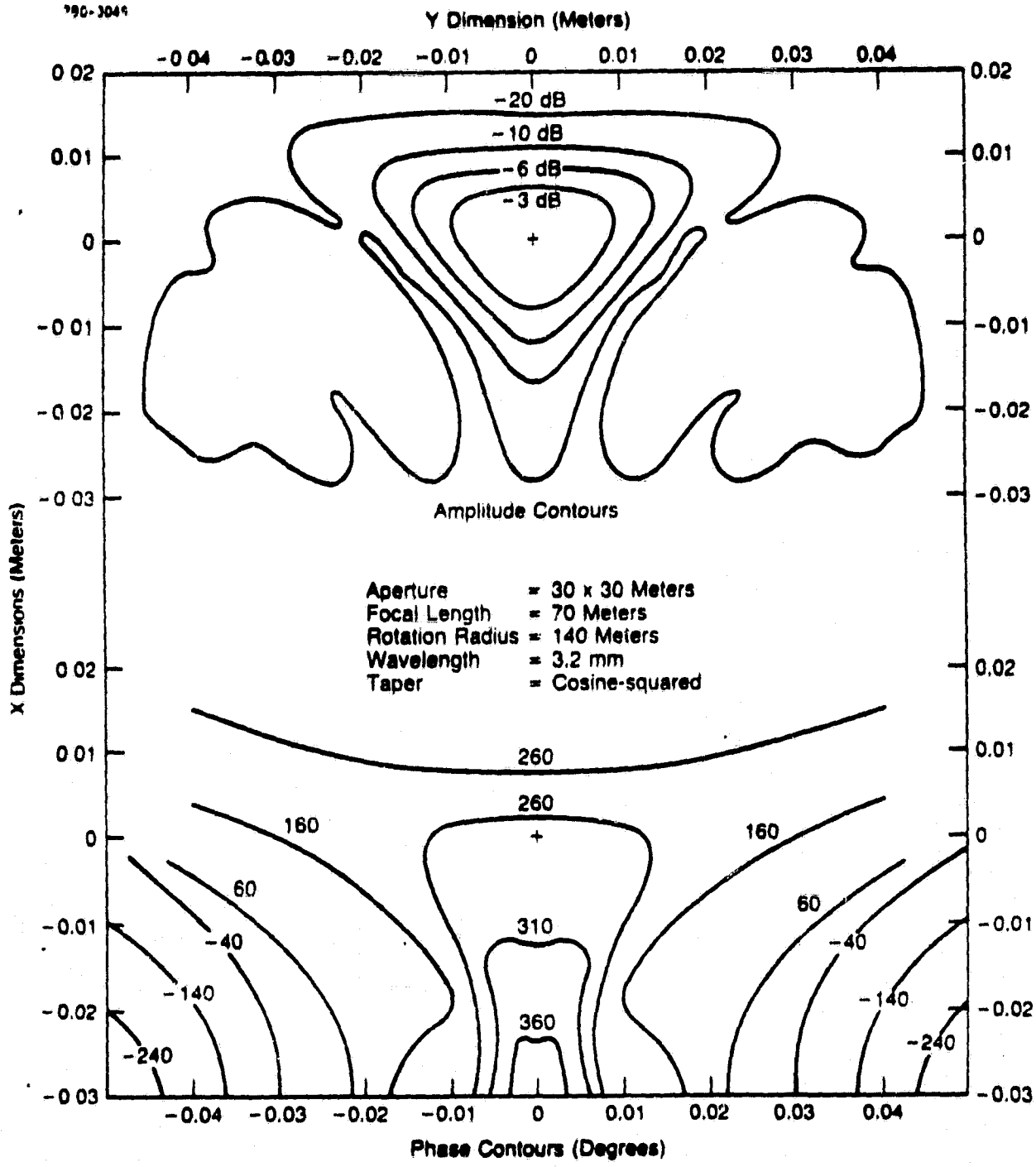

Figure 4-6. Amplitude/Phase Contours

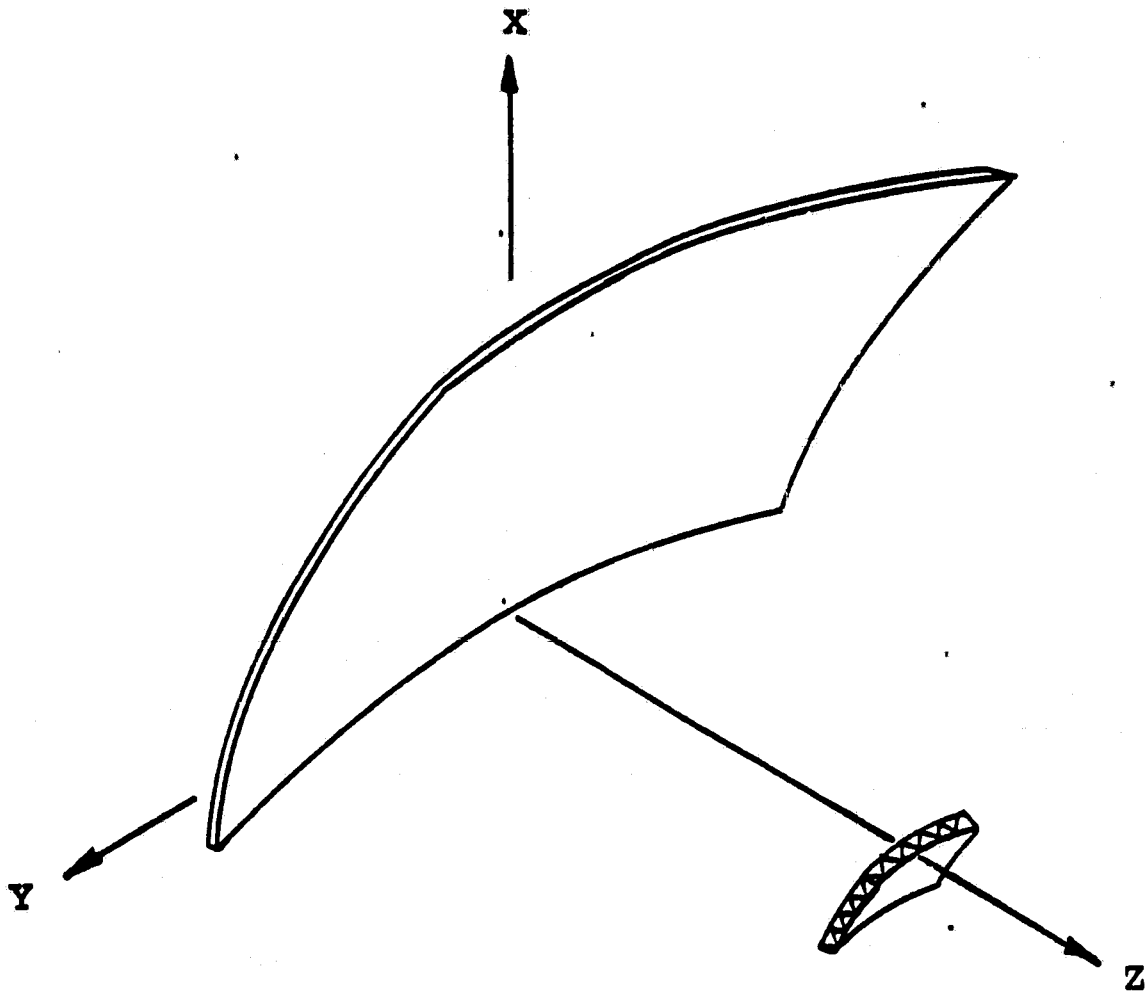

FIGURE 4-7

PARABOLOIDAL REFLECTOR WITH CLUSTER FEED

Multiple reflector systems can be examined by successive executions of existing models. However, automatic procedures for characterizing the performance of multiple reflector systems need to be developed.

NTL's models are brutally straightforward, the result of decades of investigation and years of fruitlessly searching for the subtle technique of accurate and efficient diffraction calculation. They are based on exact calculation of the contribution to every field point of a number of widely separated differential surface areas on the reflector; the contributions of the rest of the reflecting surface are estimated by interpolation techniques. The models are self-calibrating in the sense that an inadequate formulation leads to identifiable distortions.

4.3 OPTICAL ANALYSIS METHODS

An essential element in the design of an optical system which dynamically compensates for aberration is a method for accurately characterizing the energy flow. The common optical analytical models permit accurate determination of the electromagnetic field in limiting cases or in local regions but they cannot generate the accurate phase information needed to design the compensating device -- a phased array or a deformable surface.

Diffraction methods for calculating the amplitude/phase distribtions over arbitrary regions of space are needed. Ray tracings are not adequate for design purposes although they can confirm the validity of designs based on the diffraction studies. Ray tracings are normally used to confirm that a good image can be formed at a point and the correct diffraction pattern is then inferred from our knowledge of the behavior of electromagnetic radiation at or near a focal point.

Because of the staggering amount of calculations required to characterize the energy flow in large aperture systems, designs are usually based on ray tracing methods which restrict us to systems in which the energy is, or can be, brought to a clear focus. The NTL telescope uses the control of phase at the array surface to eliminate scanning aberrations which would otherwise be crippling. Without diffraction methods for determining the correct phase settings, the system could not be designed.

Consider the problem of characterizing the field of a monochromatic plane wave after it has been intercepted and reradiated by a paraboloid. For the case of axial incidence a perfect image is obtained at the focus and the nearby field is of known character.
If we require information about the transverse field far

from the focus, or if we need to examine the axial field far from the focus, or if we rotate the angle of incidence, or if we want to explore the impact of profile errors, or if the source approaches the paraboloid, then we can call on special analysis models which have been developed to handle these special situations. So long as conditions do not deviate too far from the ideal and do not occur in unmanageable combinations, we can use these special analyses to characterize the field without recourse to large volume calculations.

When conditions deviate far from that of the good image -- and they must if we hope to achieve or even examine wide angle scanning with short focus systems -- we need a generally applicable diffraction analysis. This will require that we perform an integration over the entire surface of the reflector for every point of interest.

5.0 PERFORMANCE OF SELECTED SYSTEM WITH DISCUSSION OF RESULTS

5.1 THE SELECTED CONFIGURATION

The configuration selected for examination for 20/30 GHz SATCOM consisted of a paraboloid, an ellipsoid and a phased array (Figure 5-1). Three dimensional performance was derived from analyses of compatible offset and symmetrical geometries (Figures 5-2 and 5-3). The configurational parameters (f-number = 1.5, magnification = 5) were obtained as the result of a converging process which involved adjustment of the placements and orientations of the two smaller elements and the offset parameters of all three surfaces.

The performance of the selected configuration was examined for error free deployments and excitations for scanning of 0 $\pm$4 degrees in the symmetry plane (Section 5.2.1) and for scanning of +1 $\pm$2 degrees in the offset plane (Section 5.2.2).

The impact of phaser granularity and of phase errors in the excitation of the array elements was explored (Section 5.3.1) as was the impact of several types of errors in the profile of the array surface (Section 5.3.2).

Performance as a function of frequency was examined (Section 5.4).

FIGURE 5-1. MICROWAVE TELESCOPE

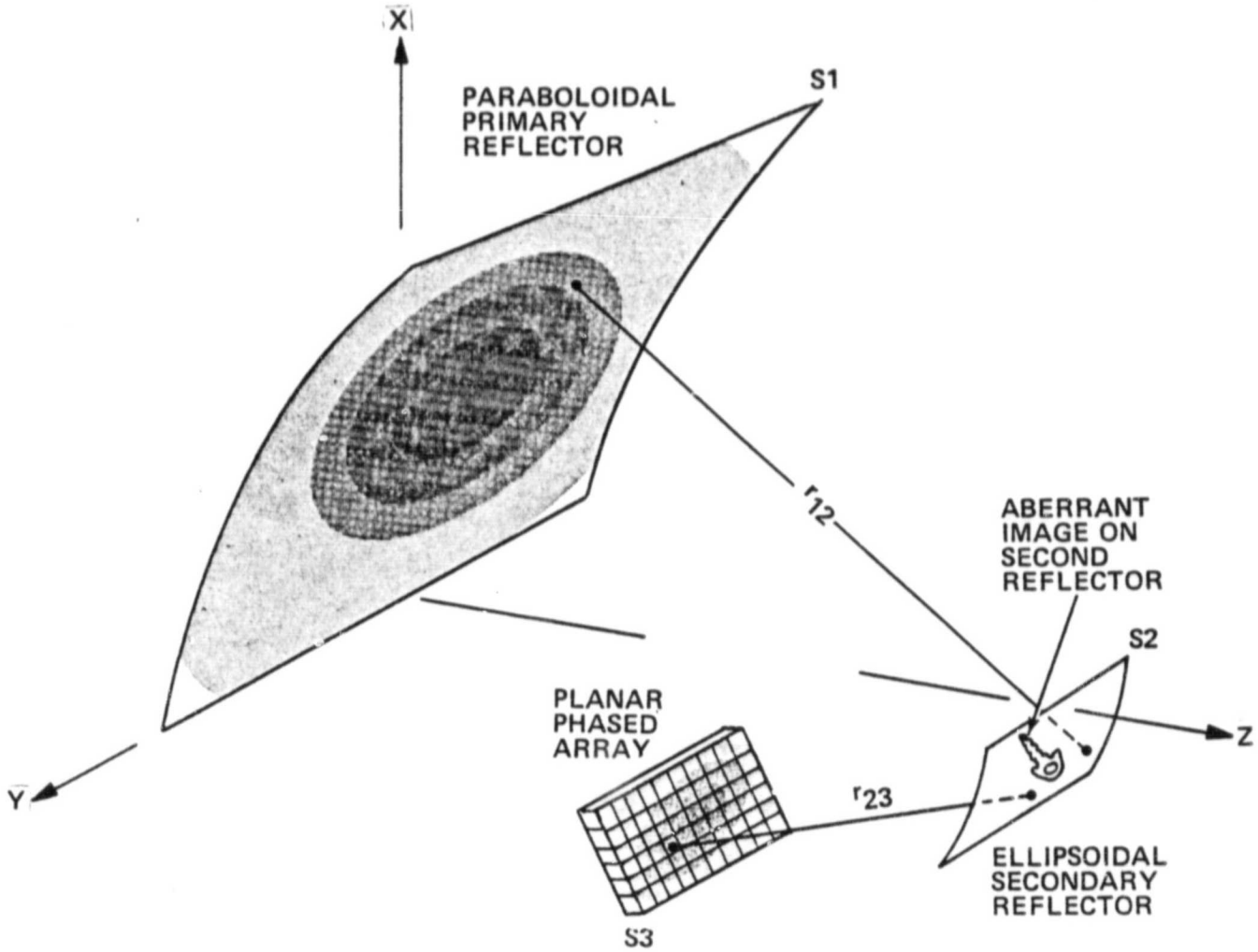

DATE: 01/21/82 TIME: 19.09.24.

ANTENNA GEOMETRY

FIGURE 5-2. SYMMETRICAL CONFIGURATION

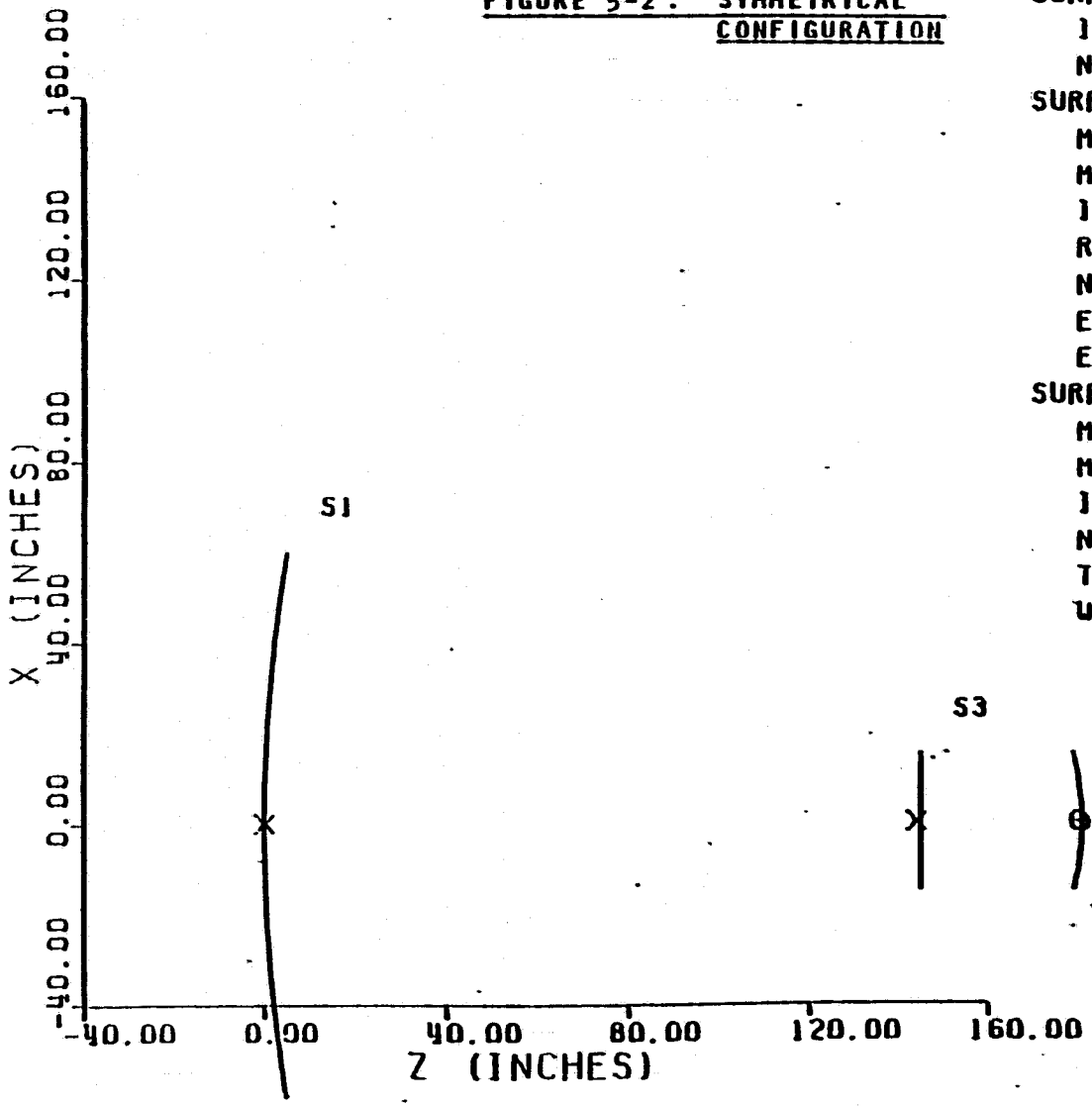

GEOMETRIC DATA

SURFACE ONE:

INTERVAL	1.000	INCHES
NO. OF PTS	121	

SURFACE TWO:

MINIMUM X	15.000	INCHES
MINIMUM Z	178.500	INCHES
INTERVAL	-.200	INCHES
ROT. INT.	-.200	INCHES
NO. OF PTS	151	
ELL. AXIS	108.374	INCHES
ECCENTRIC.	.664	

SURFACE THREE:

MINIMUM X'	15.000	INCHES
MINIMUM Z	145.000	INCHES
INTERVAL	-.200	INCHES
NO. OF PTS	151	
TILT ANGLE	0.000	DEGREES
WAVELENGTH	.394	INCHES

DATE: 01/22/82 TIME: 20.05.11.

ANTENNA GEOMETRY

FIGURE 5-3 . OFFSET CONFIGURATION

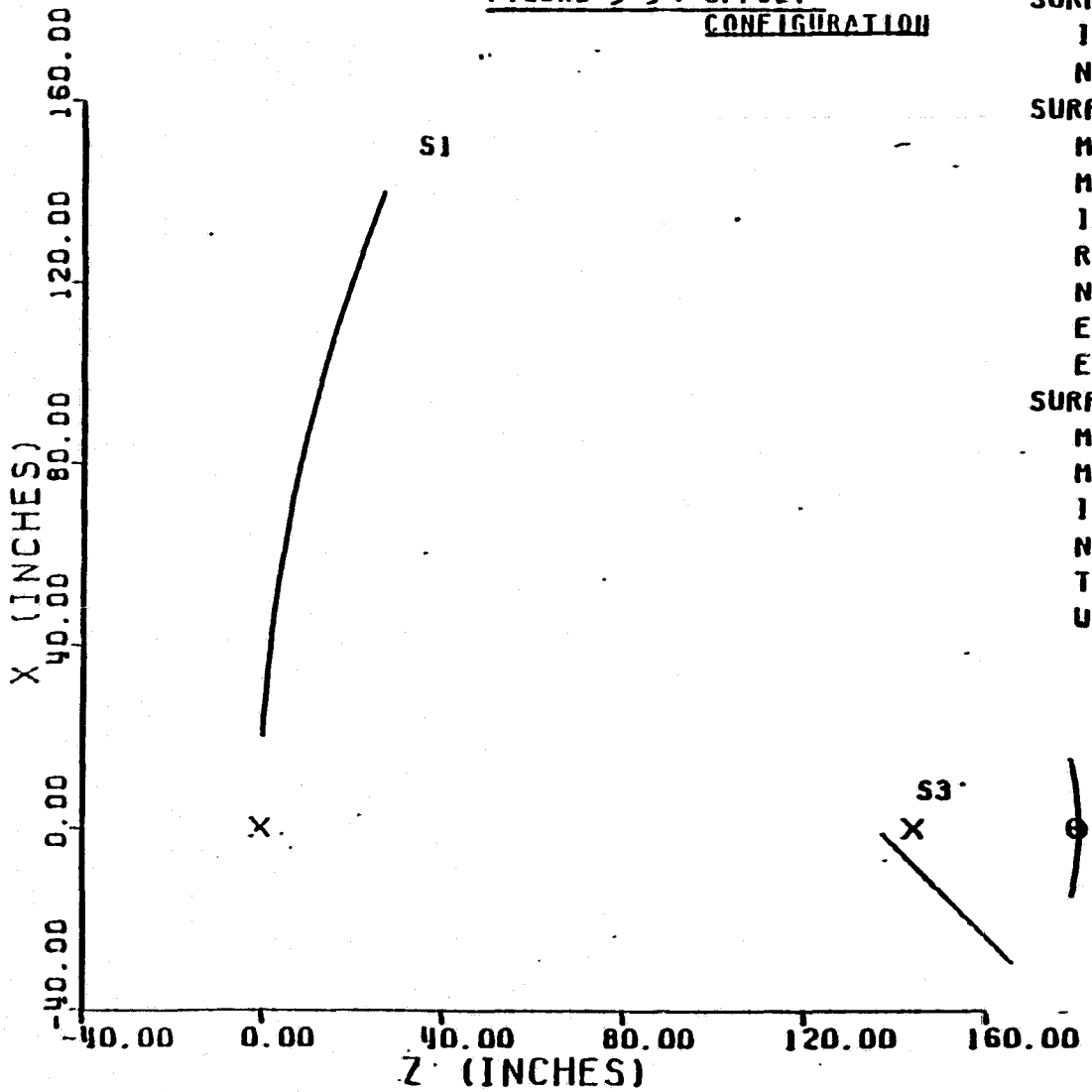

GEOMETRIC DATA

SURFACE ONE:

INTERVAL	1.000	INCHES
NO. OF PTS	121	

SURFACE TWO:

MINIMUM X	15.000	INCHES
MINIMUM Z	178.500	INCHES
INTERVAL	-.200	INCHES
ROT. INT.	-.200	INCHES
NO. OF PTS	151	
ELL. AXIS	108.374	INCHES
ECCENTRIC.	.664	

SURFACE THREE:

MINIMUM X	-1.414	INCHES
MINIMUM Z	137.586	INCHES
INTERVAL	-.200	INCHES
NO. OF PTS	201	
TILT ANGLE	-45.000	DEGREES
WAVELENGTH	.394	INCHES

The offset geometry was configured for zero blockage of all energy flow.

In the scale for the phase of the radiation patterns the symbol TW stands for 2π.

5.2 ERROR FREE CONFIGURATIONS

The configuration examined employed an aperture extent, in both planes, of 120 inches with a focal length of 180 inches and a magnification (ratio of primary to phased array aperture) of 5. Except for the frequency studies described in Section 5.4 all results are presented at a wavelength of 0.3934 inches (30 GHz). For these studies an illumination taper of the form 1 + 4 (cosine-squared) was postulated on the surface of the primary reflector. The antenna pattern for this illumination function exhibits diffraction sidelobe levels below -30 dB relative to the main lobe (Figure 5-4).

5.2.1 SYMMETRICAL GEOMETRY

An example of a complete analysis is illustrated in Figures 5-5 through 5-9, which depict, for the symmetrical geometry and boresight incidence onto the primary reflector, the resulting distributions:

- on the second reflector (Figure 5-5)
- on the phased array (Figure 5-6), and

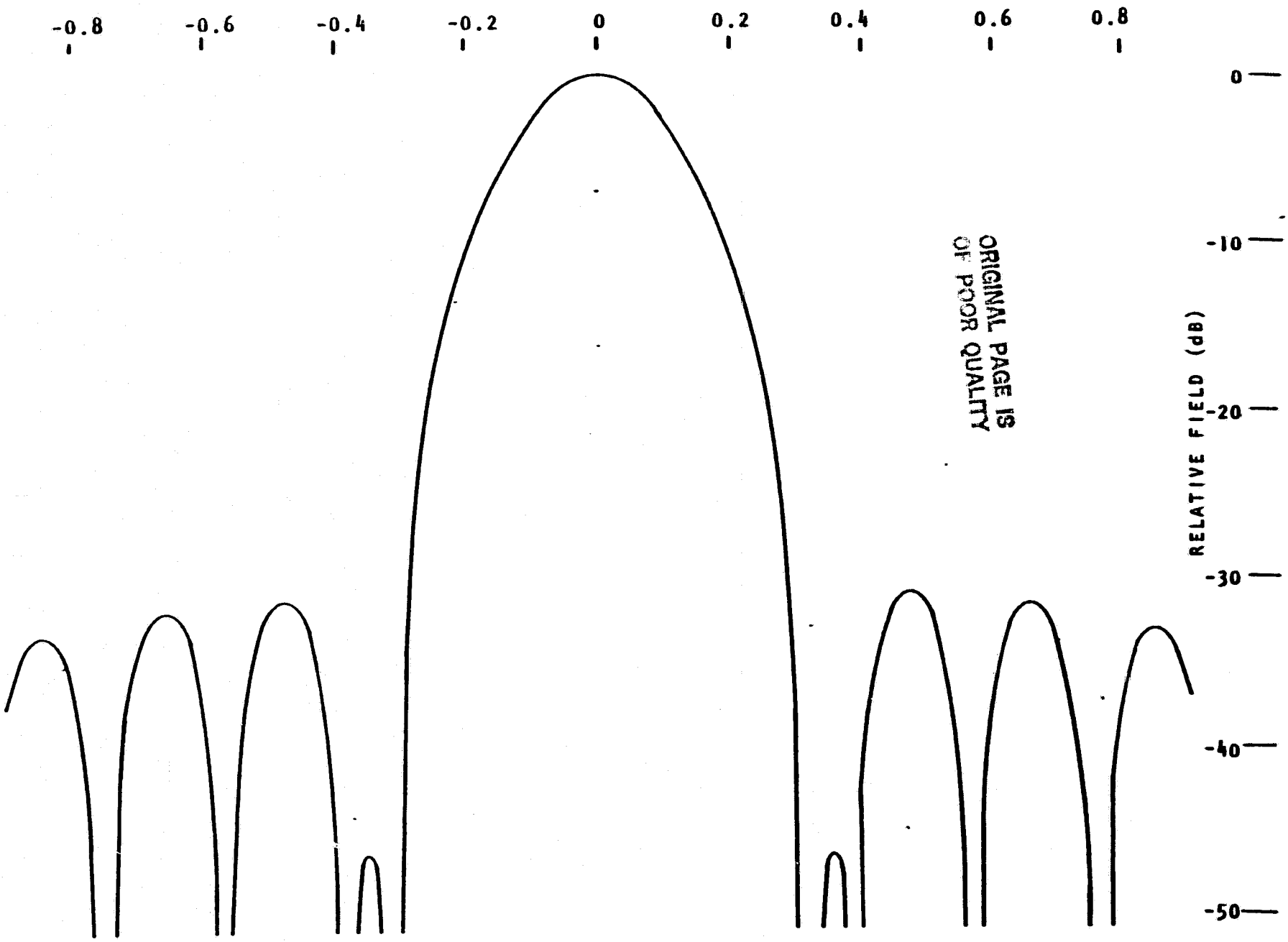

FIGURE 5-4. IDEAL PATTERN

DATE: 01/18/82 TIME: 19.12.15.

AMP TAPER
20.00 0.00 80.00
PHASE FUNC
0.00 0.00 0.00

SECOND SURFACE - AMPLITUDE AND PHASE - INBOUND

FIGURE 5-5. SECOND SURFACE INBOUND DISTRIBUTIONS FOR SYMMETRICAL GEOMETRY, SCAN = 0

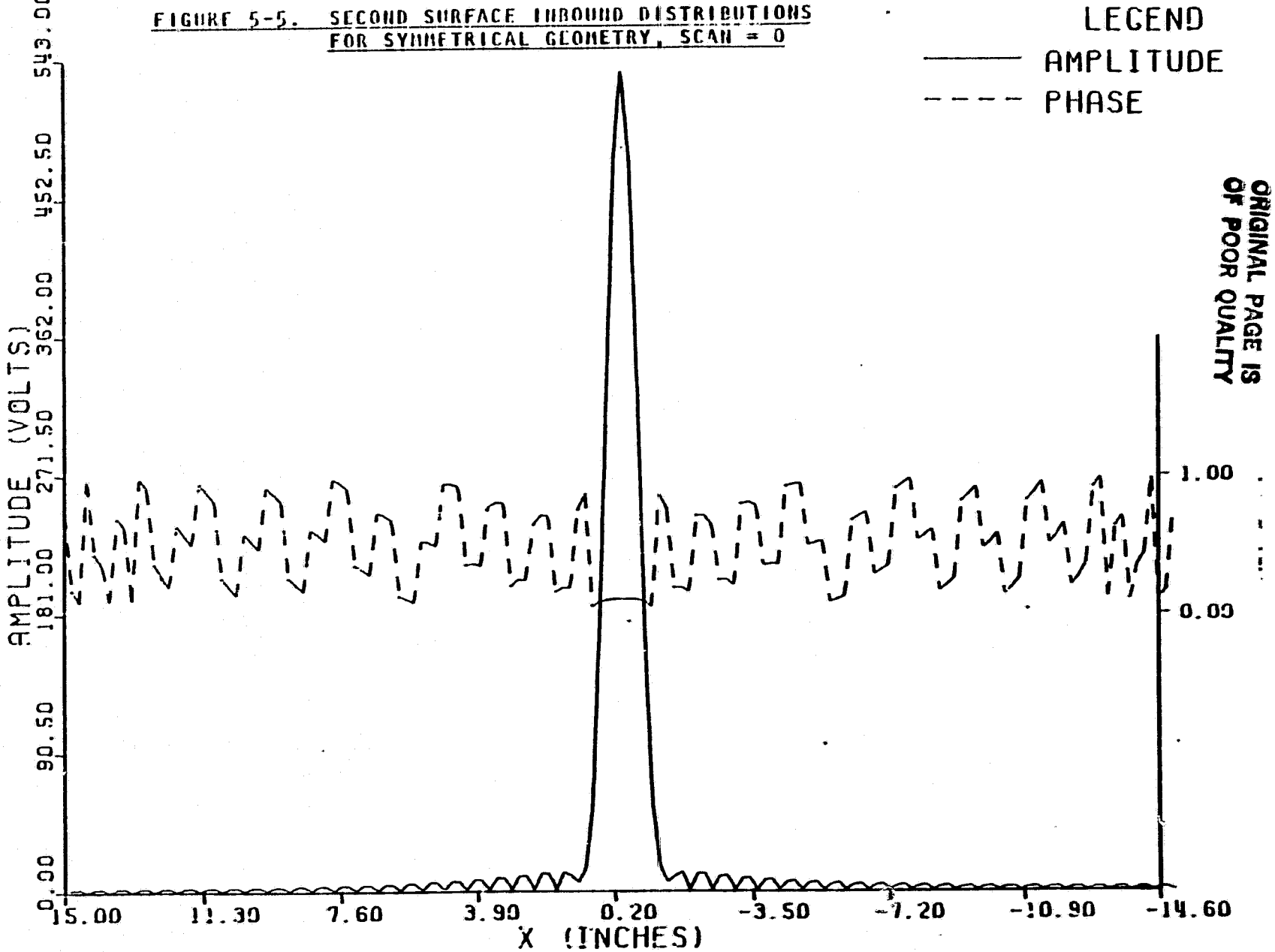

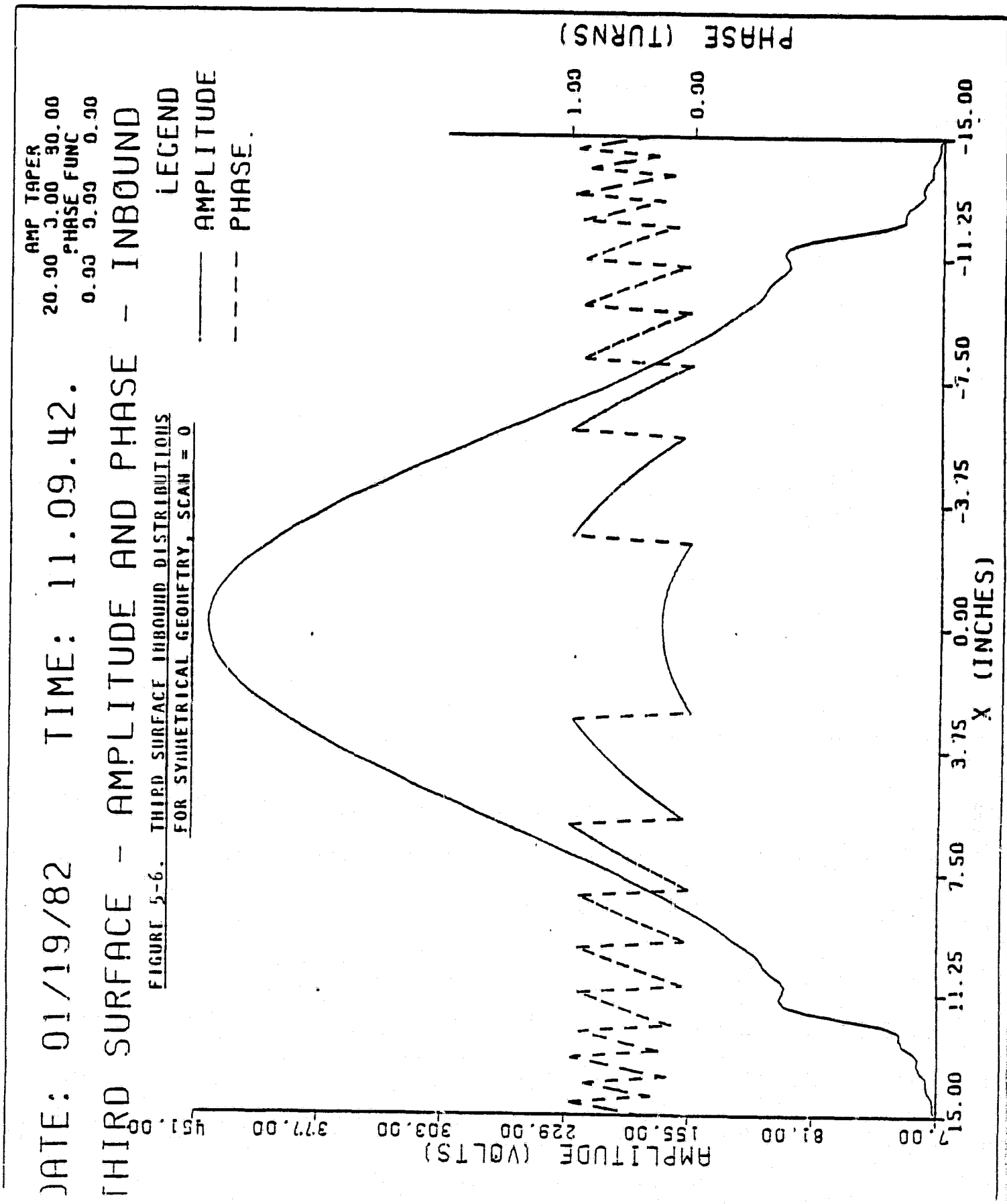

FIGURE 5-6. THIRD SURFACE INBOUND DISTRIBUTIONS FOR SYMMETRICAL GEOMETRY, SCAN = 0

for a conjugate phase (retrodirective) excitation of the phased array, the resulting distributions:

- on the second reflector (Figure 5-7),
- on the first reflector (Figure 5-8), and
- in the far field (Figure 5-9).

The success of the design -- for this incident angle -- is measured by how well the inbound/outbound energy distributions replicate one another on the reflectors and how well the calculated far field pattern (Figure 5-9) matches the ideal pattern (Figure 5-4).

The far field patterns based on this model for scan angles of ± 4 degrees are illustrated in Figures 5-10 and 5-11. The scanning performance is very close to the ideal in this instance because we are using the exact conjugate phase excitation of the array, allowing the amplitude as well as the phase of each active element to vary with scan angle.

A system not employing amplitude control was examined by freezing the phased array amplitude distribution to that obtained for the central scan angle (zero) and using the phase distributions obtained from the inbound calculations for the range of scan angles between ± 4 degrees. The results are excellent (Figures 5-12, 5-13, 5-14 and also Figure 1-2), although not quite as good as

DATE: 01/21/82 TIME: 19.21.41.

AMP TAPER
20.00 0.00 80.00
PHASE FUNC
0.00 0.00 0.00

SECOND SURFACE - AMPLITUDE AND PHASE - OUTBOUND

FIGURE 5-7. SECOND SURFACE OUTBOUND DISTRIBUTIONS FOR SYMMETRICAL GEOMETRY, THIRD SURFACE AMPLITUDE FOR SCAN = 0, THIRD SURFACE PHASE FOR SCAN = 0

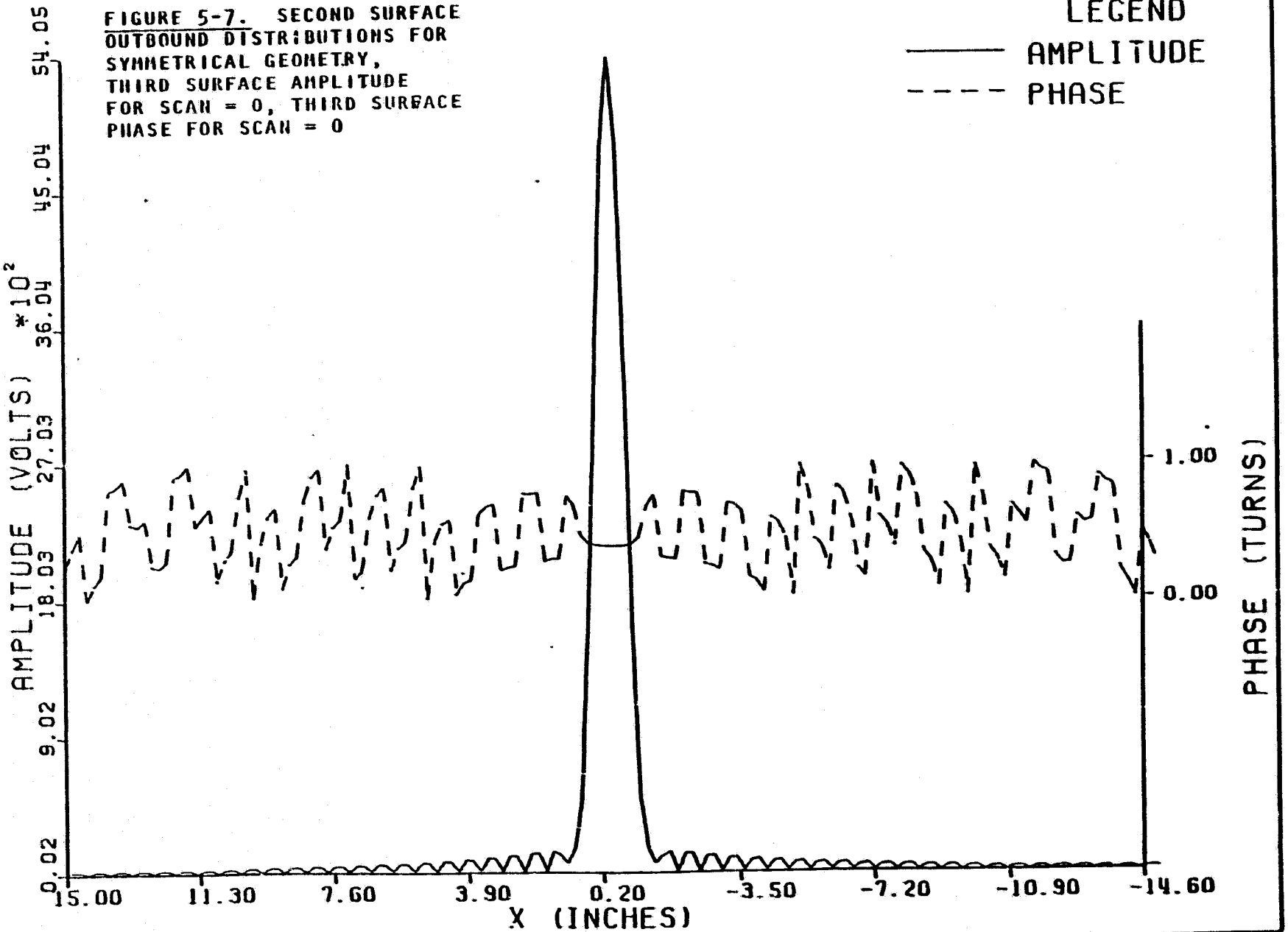

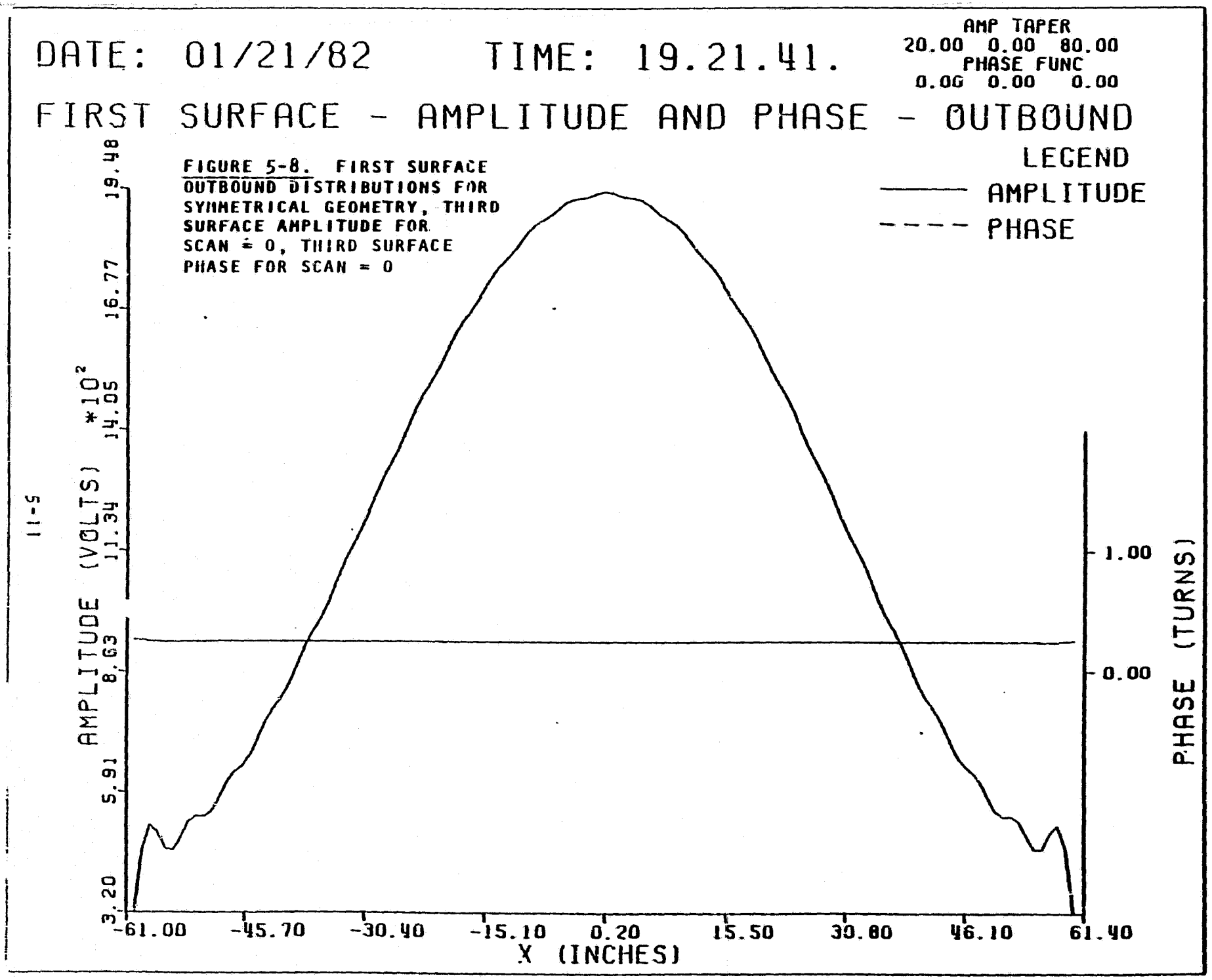

DATE: 01/21/82 TIME: 19.21.41.

AMP TAPER
20.00 0.00 80.00
PHASE FUNC
0.00 0.00 0.00

FAR FIELD AMPLITUDE AND PHASE PATTERN

FIGURE 5-9

FAR FIELD PATTERN FOR SYMMETRICAL GEOMETRY, THIRD SURFACE AMPLITUDE FOR SCAN = 0, THIRD SURFACE PHASE FOR SCAN = 0

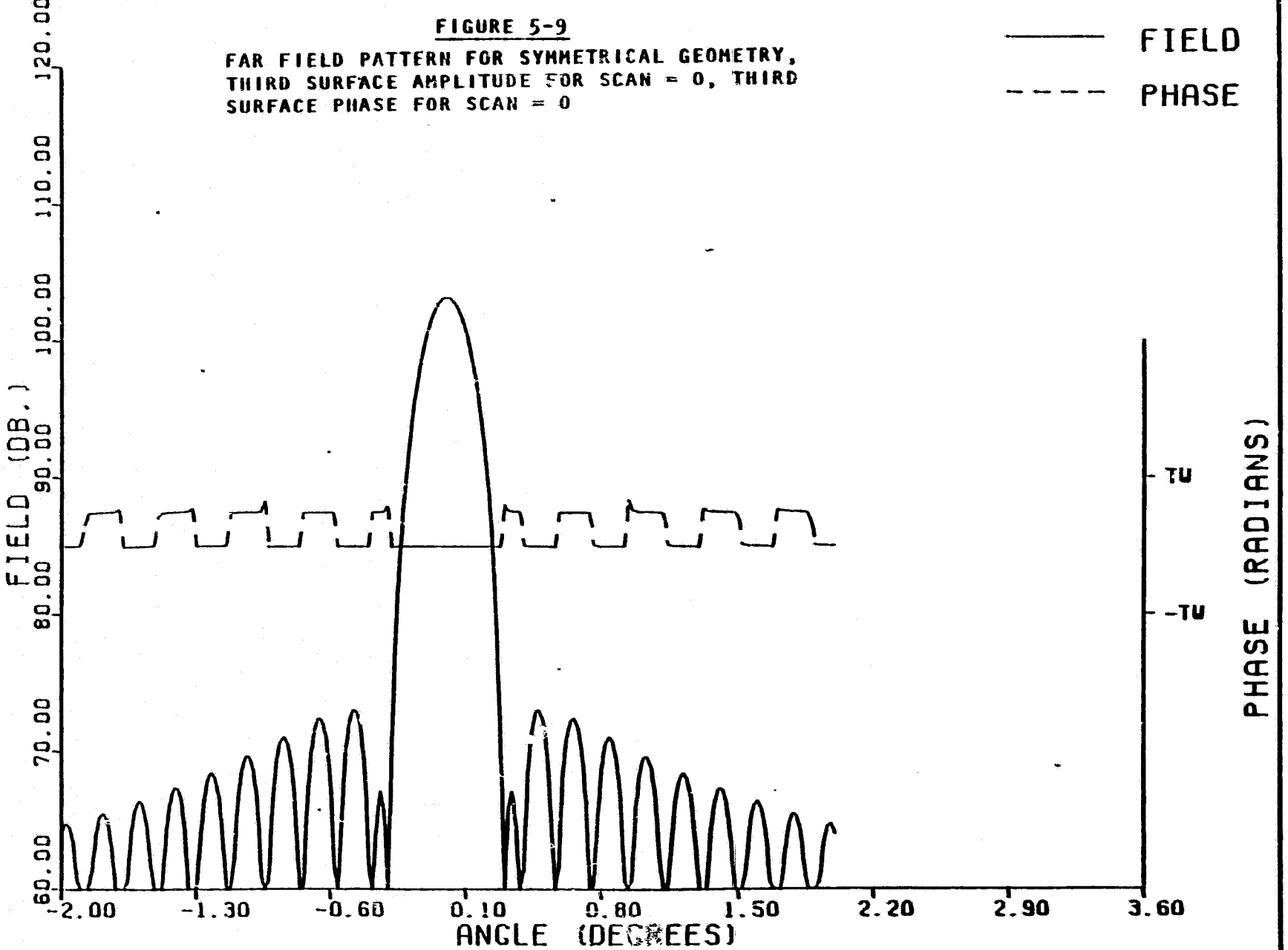

DATE: 01/21/82 TIME: 19.20.24.

AMP TAPER
20.00 0.00 80.00
PHASE FUNC
-8.37 0.00 0.00

FAR FIELD AMPLITUDE AND PHASE PATTERN

FIGURE 5-10

FAR FIELD PATTERNS FOR SYMMETRICAL GEOMETRY, THIRD SURFACE AMPLIUTDE FOR SCAN = -4 DEGREES, THIRD SURFACE PHASE FOR SCAN = -4 DEGREES

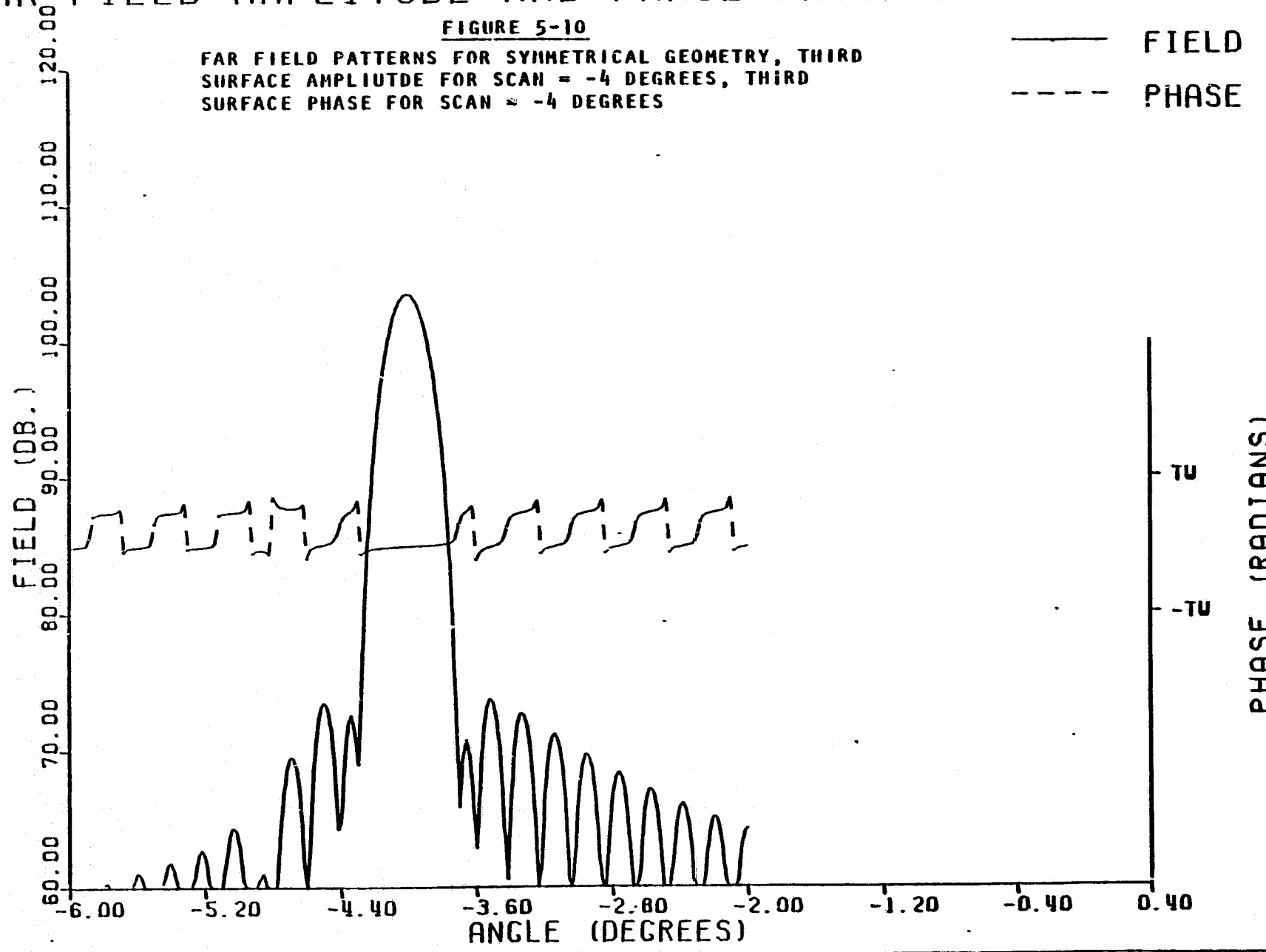

DATE: 01/21/82 TIME: 19.22.59.

AMP TAPER
20.00 0.00 80.00
PHASE FUNC
8.37 0.00 0.00

FAR FIELD AMPLITUDE AND PHASE PATTERN

FIGURE 5-11

FAR FIELD PATTERNS FOR SYMMETRICAL GEOMETRY, THIRD SURFACE AMPLITUDE FOR SCAN = +4 DEGREES, THIRD SURFACE PHASE FOR SCAN = +4 DEGREES

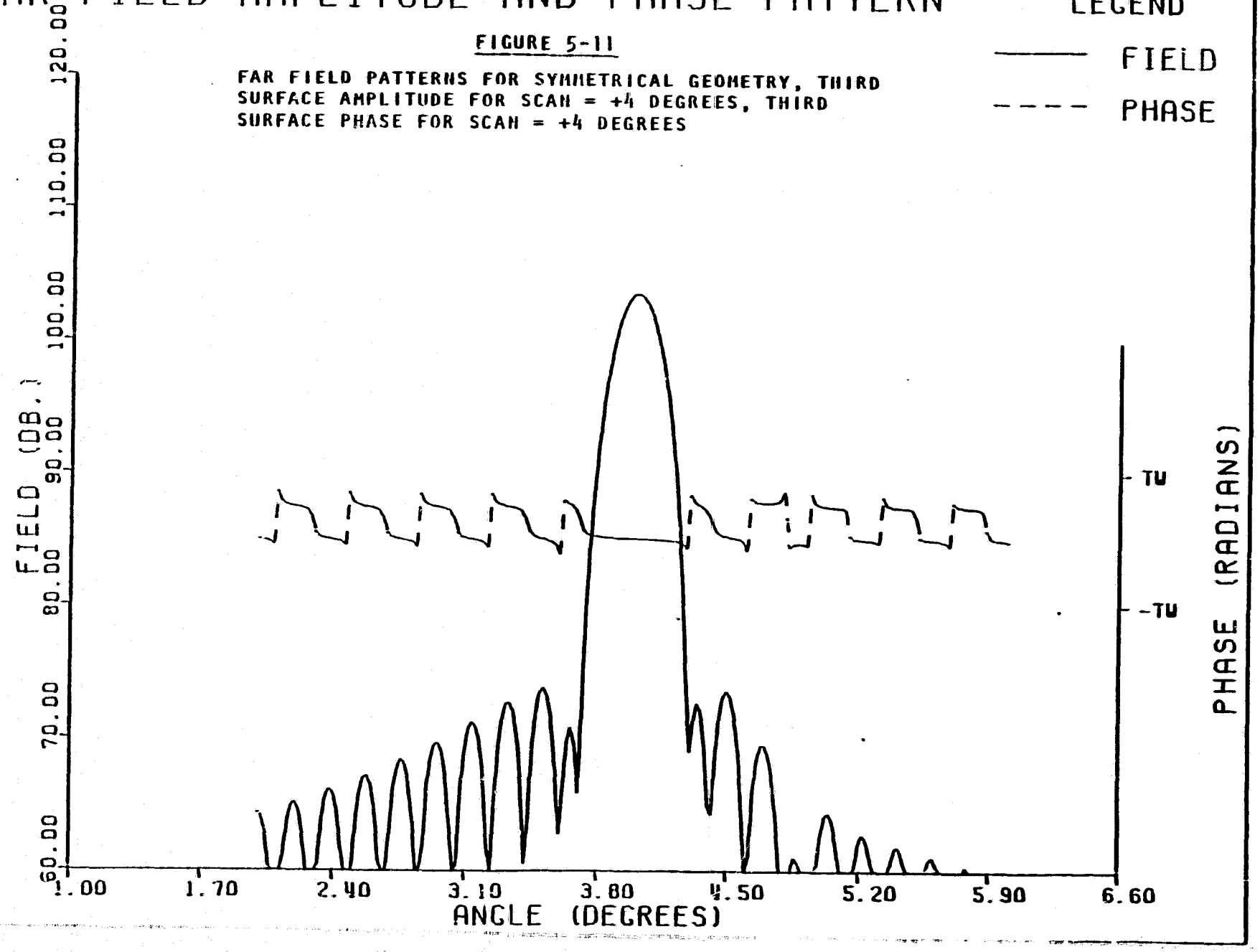

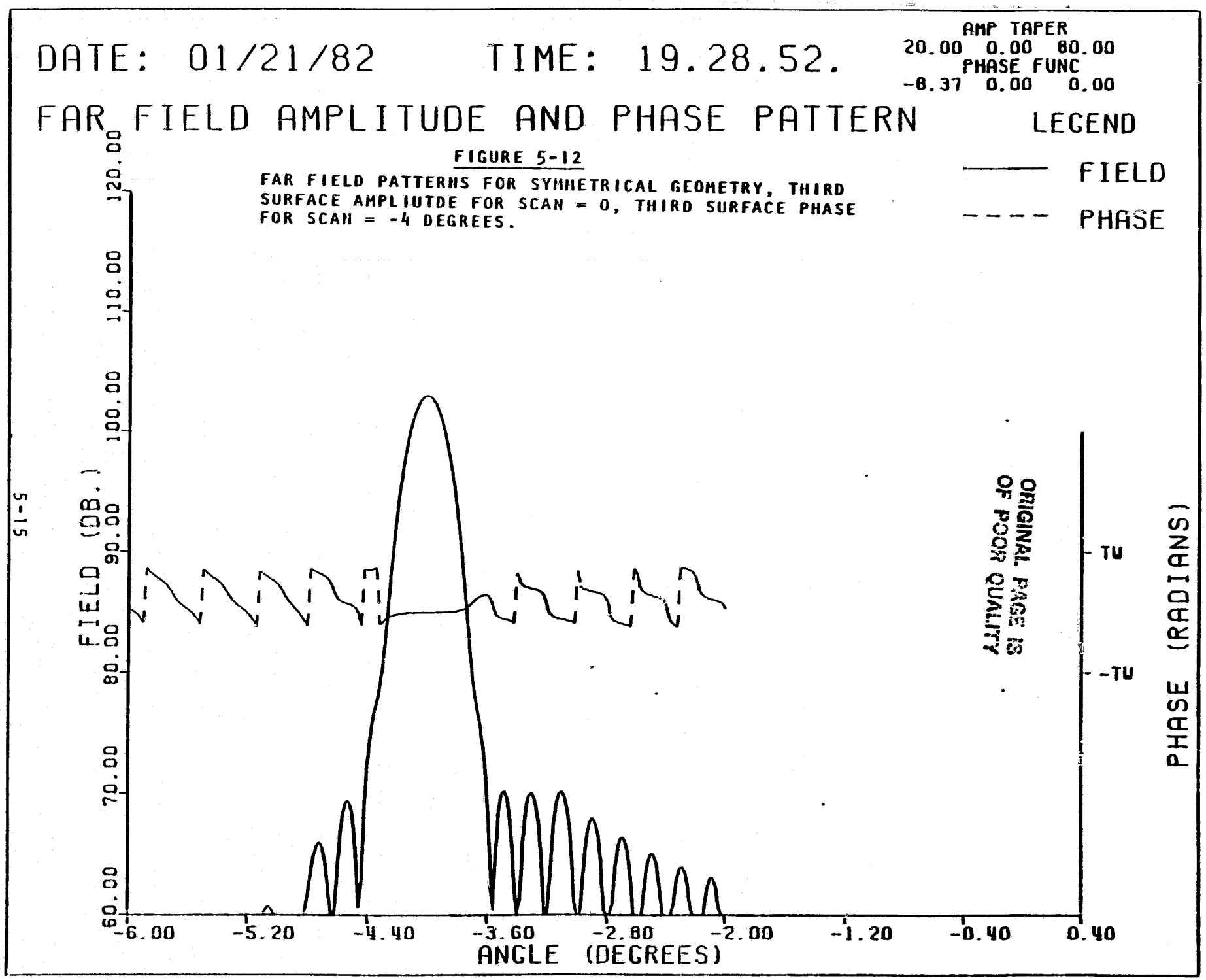
DATE: 01/21/82
TIME: 19.28.52.
AMP TAPER
20.00 0.00 80.00
PHASE FUNC
-8.37 0.00 0.00
FAR FIELD AMPLITUDE AND PHASE PATTERN
LEGEND
FIELD
PHASE
FIGURE 5-12
FAR FIELD PATTERNS FOR SYMMETRICAL GEOMETRY, THIRD SURFACE AMPLIUTDE FOR SCAN = 0, THIRD SURFACE PHASE FOR SCAN = -4 DEGREES.
FIELD (DB.)
120.00
110.00
100.00
90.00
80.00
70.00
60.00
TU
-TU
PHASE (RADIANS)
-6.00
-5.20
-4.40
-3.60
-2.80
-2.00
-1.20
-0.40
0.40
ANGLE (DEGREES)
ORIGINAL PAGE IS OF POOR QUALITY

DATE: 01/21/82 TIME: 19.21.41.

AMP TAPER
20.00 0.00 80.00
PHASE FUNC
0.00 0.00 0.00

FAR FIELD AMPLITUDE AND PHASE PATTERN

LEGEND
——— FIELD
- - - - PHASE

FIGURE 5-13

FAR FIELD PATTERNS FOR SYMMETRICAL GEOMETRY, THIRD SURFACE AMPLITUDE FOR SCAN = 0 DEGREE, THIRD SURFACE PHASE FOR SCAN = 0 DEGREE

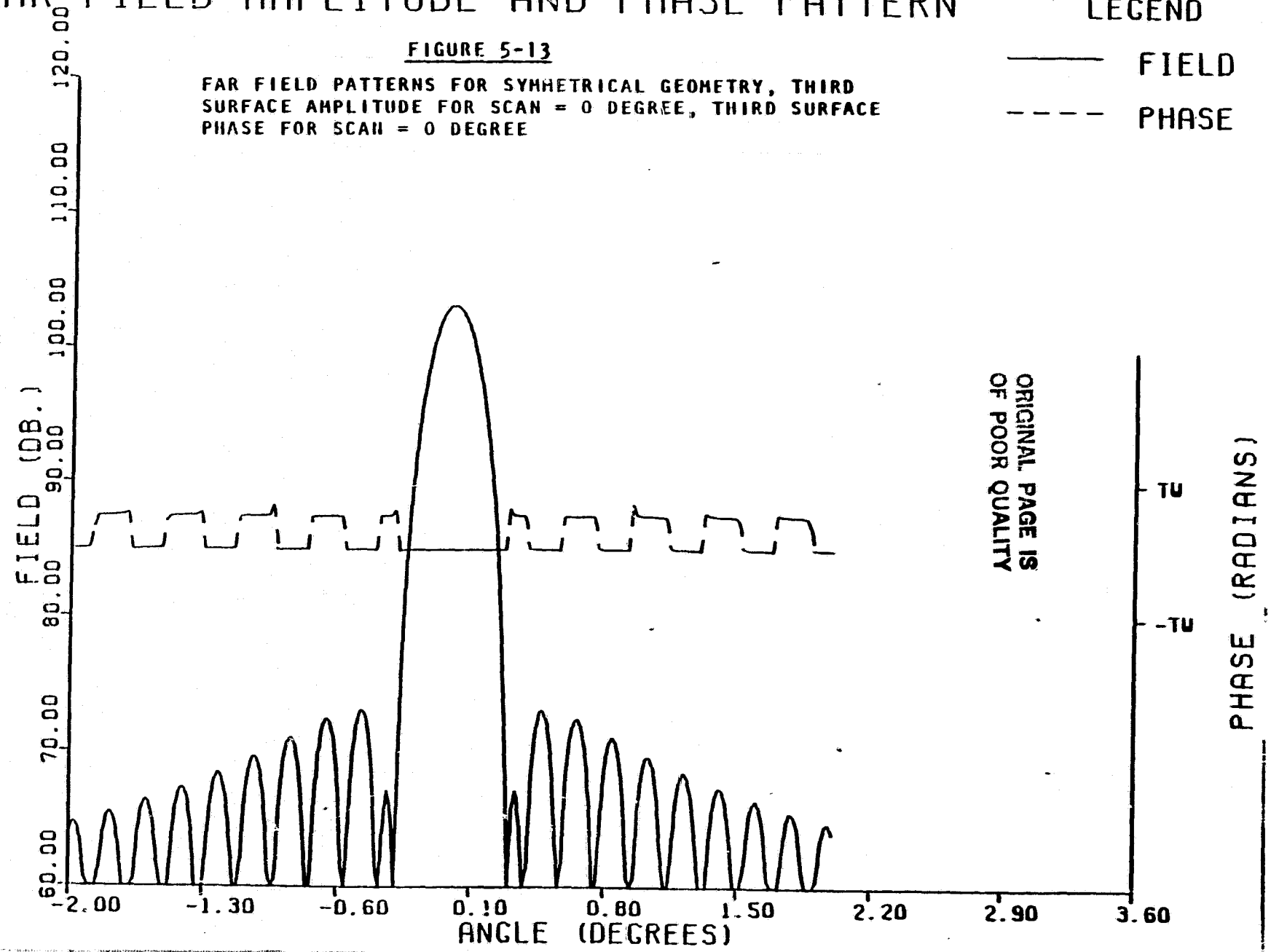

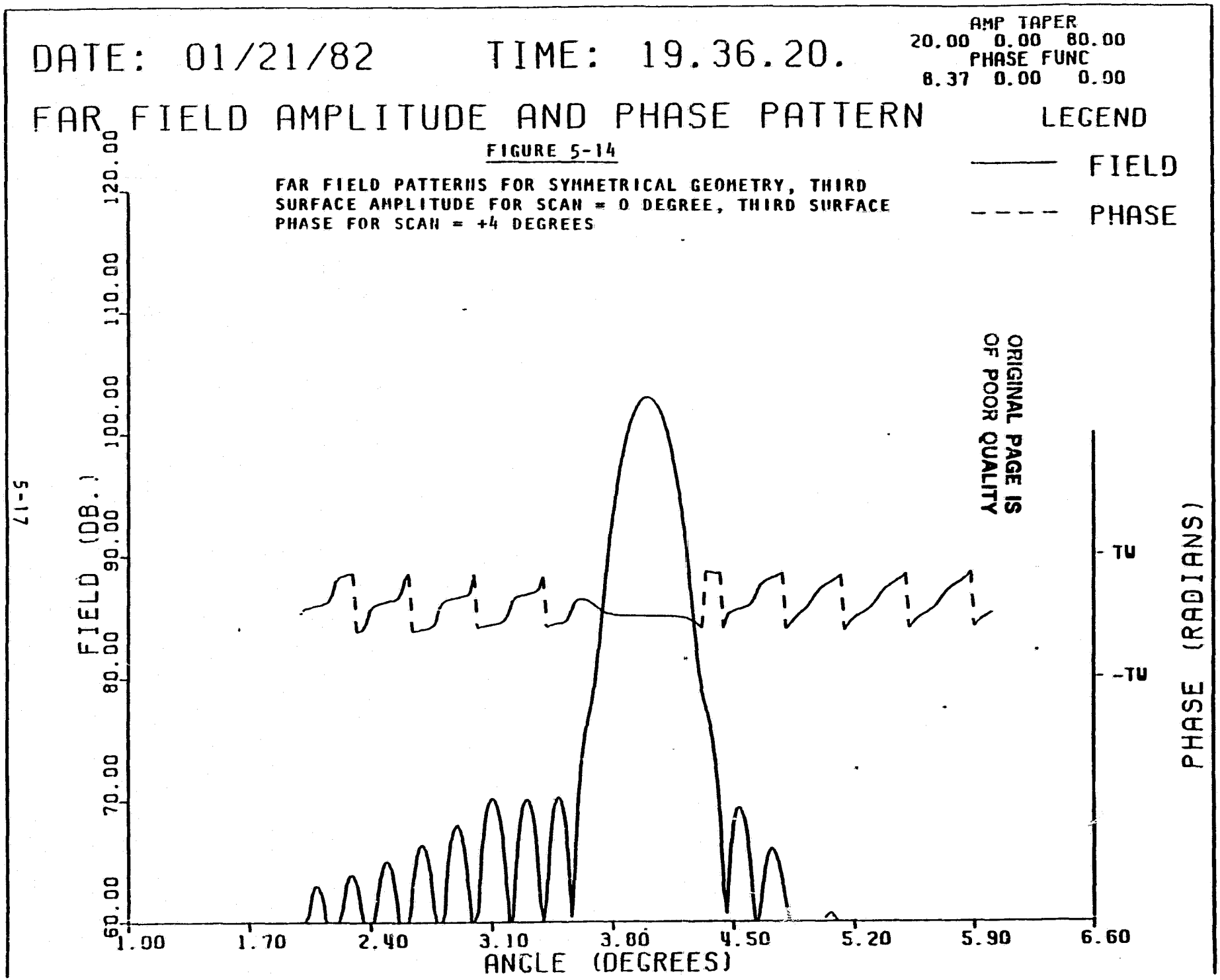
DATE: 01/21/82
TIME: 19.36.20.
AMP TAPER
20.00 0.00 80.00
PHASE FUNC
8.37 0.00 0.00
FAR FIELD AMPLITUDE AND PHASE PATTERN
LEGEND
FIELD
PHASE
FIGURE 5-14
FAR FIELD PATTERNS FOR SYMMETRICAL GEOMETRY, THIRD SURFACE AMPLITUDE FOR SCAN = 0 DEGREE, THIRD SURFACE PHASE FOR SCAN = +4 DEGREES
ORIGINAL PAGE IS OF POOR QUALITY
FIELD (DB.)
120.00
110.00
100.00
90.00
80.00
70.00
60.00
TU
-TU
PHASE (RADIANS)
1.00
1.70
2.40
3.10
3.80
4.50
5.20
5.90
6.60
ANGLE (DEGREES)

those obtained using both amplitude and phase control. The small first lobe of the central pattern has blended into the main beam as a result of a modest phase error near the edge of the primary aperture.

5.2.2 OFFSET GEOMETRY

Patterns obtained for the selected offset geometry are shown for a range of scan angles from -1 to +3 degrees for the conditions of:

- amplitude plus phase control of the phased array (Figures 5-15, 5-16, and 5-17),
- phase control only with the amplitude chosen for a scan of zero (Figures 5-18, 5-19 and 5-20) and
- phase control only with the amplitude chosen for a scan of +1 degree (Figures 5-21, 5-22 and 5-23).

5.3 ERROR AND GRANULARITY STUDIES

5.3.1 PHASER ERRORS AND GRANULARITY

Phaser granularity was examined for the offset configuration at a scan of +3 degrees with the baseline amplitude and phase both optimized for 3 degree performance. The degradations in aperture distributions and far field patterns as the phasers vary from perfect devices to 4-bit, 3-bit and then 2-bit devices (Figures 5-24 through 5-31) are rather unusual. The aperture errors appear to have been transformed into the amplitude function and the impact on the far field patterns are diminished.

DATE: 01/22/82 TIME: 20.16.51.

AMP TAPER
20.00 0.00 80.00
PHASE FUNC
-2.09 0.00 0.00

FAR FIELD AMPLITUDE AND PHASE PATTERN

LEGEND
——— FIELD
- - - - PHASE

FIGURE 5-15

FAR FIELD PATTERNS FOR OFFSET GEOMETRY, THIRD SURFACE AMPLITUDE FOR SCAN = -1 DEGREE, THIRD SURFACE PHASE FOR SCAN = -1 DEGREE

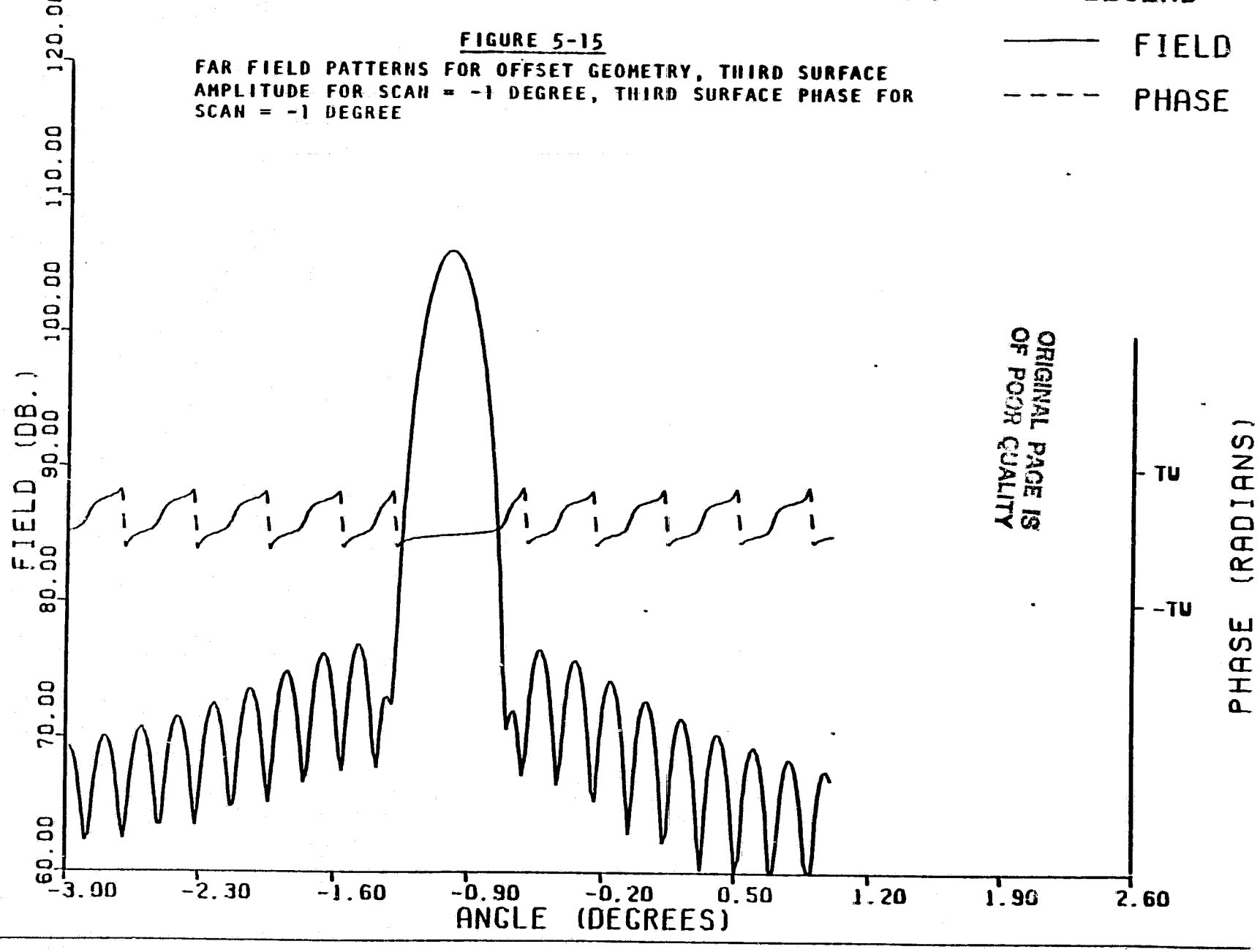

DATE: 01/22/82 TIME: 20.29.08.

AMP TAPER
20.00 0.00 80.00
PHASE FUNC
2.09 0.30 0.90

FAR FIELD AMPLITUDE AND PHASE PATTERN

LEGEND
FIELD
PHASE

FIGURE 5-16

FAR FIELD PATTERNS FOR OFFSET GEOMETRY, THIRD SURFACE
AMPLITUDE FOR SCAN = +1 DEGREE, THIRD SURFACE
PHASE FOR SCAN = +1 DEGREE

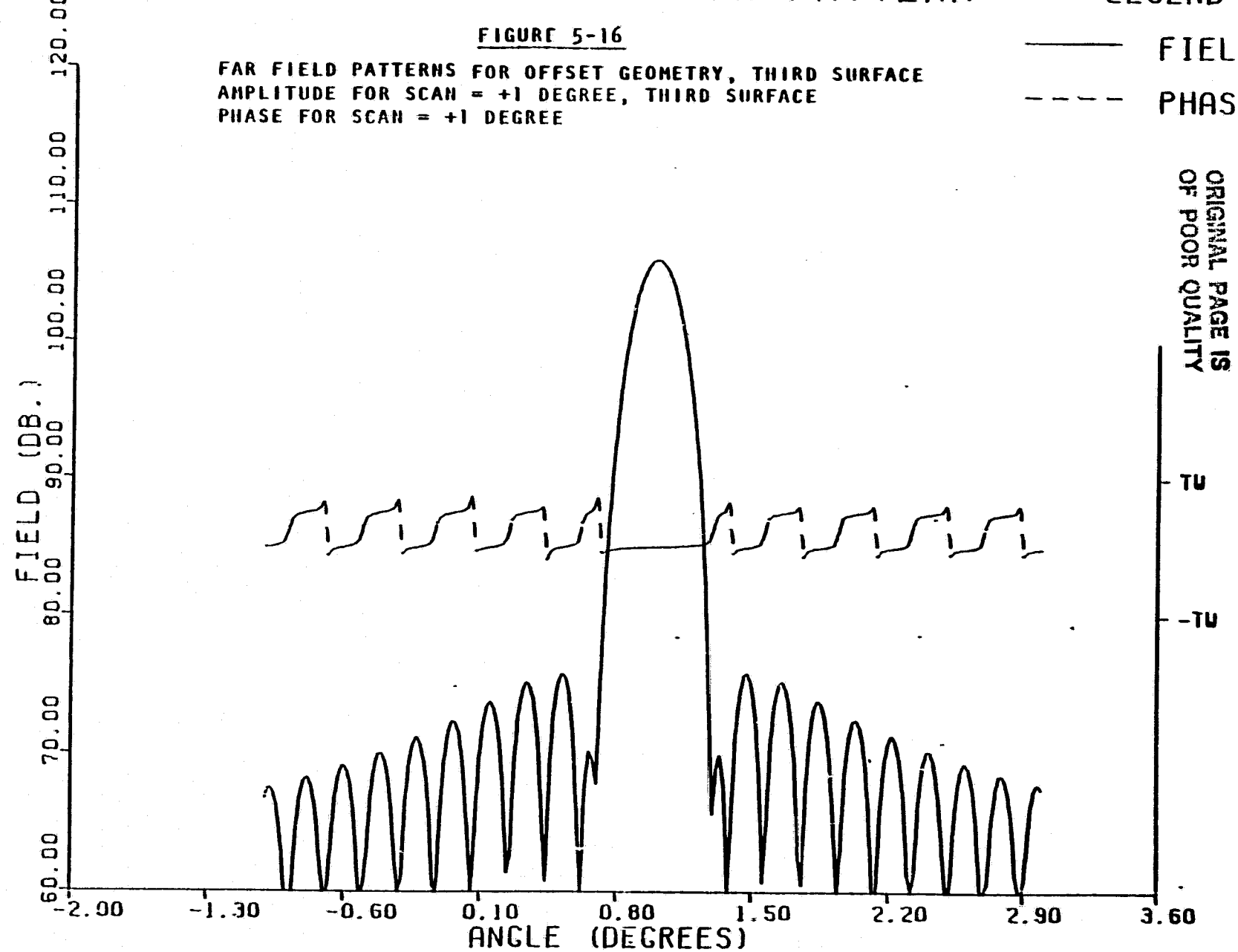

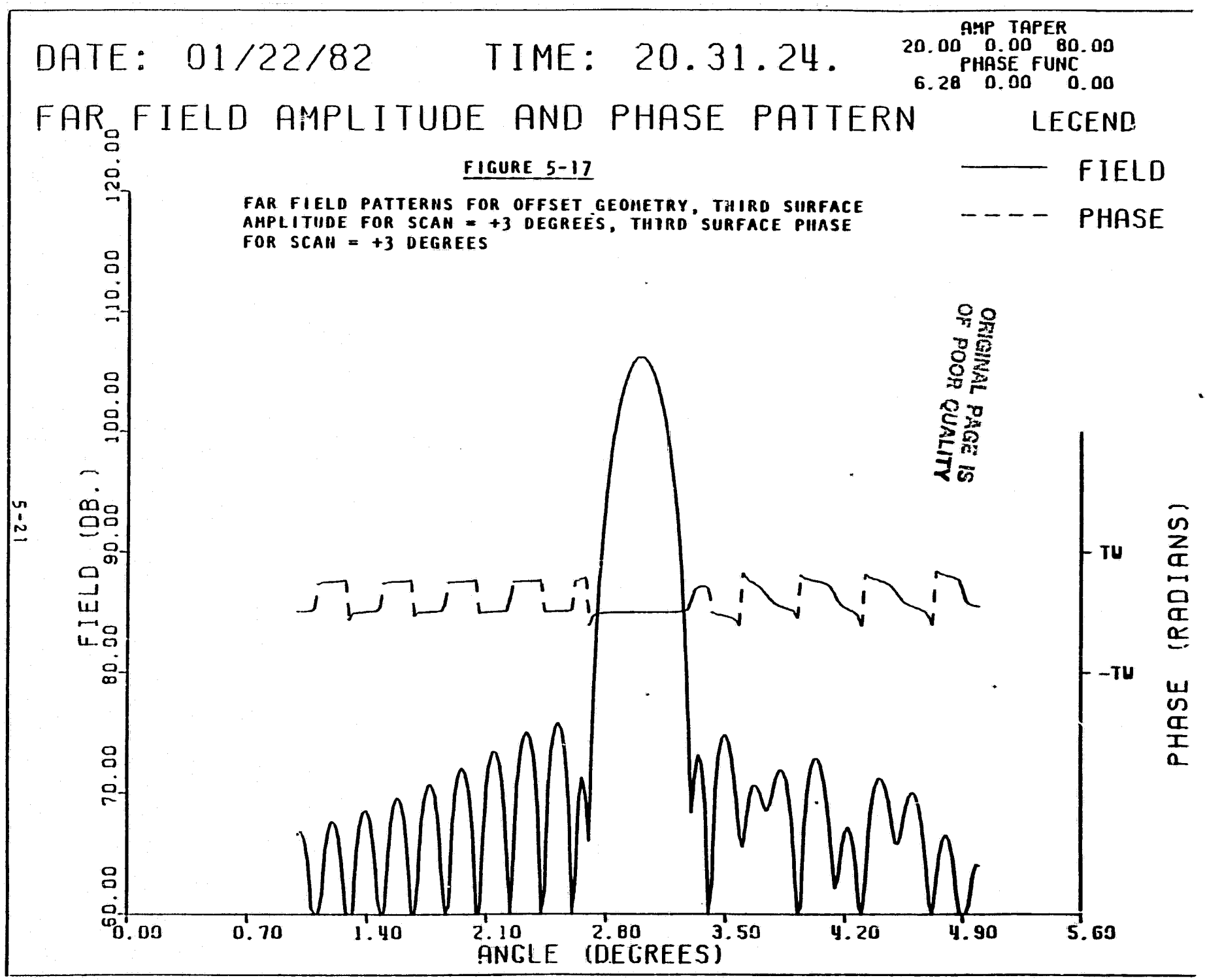
DATE: 01/22/82
TIME: 20.31.24.
AMP TAPER
20.00 0.00 80.00
PHASE FUNC
6.28 0.00 0.00
FAR FIELD AMPLITUDE AND PHASE PATTERN
LEGEND
FIELD
PHASE
FIGURE 5-17
FAR FIELD PATTERNS FOR OFFSET GEOMETRY, THIRD SURFACE AMPLITUDE FOR SCAN = +3 DEGREES, THIRD SURFACE PHASE FOR SCAN = +3 DEGREES
ORIGINAL PAGE IS OF POOR QUALITY
FIELD (DB.)
120.00
110.00
100.00
90.00
80.00
70.00
60.00
TU
-TU
PHASE (RADIANS)
0.00
0.70
1.40
2.10
2.80
3.50
4.20
4.90
5.69
ANGLE (DEGREES)

DATE: 01/22/82 TIME: 20.33.45.

AMP TAPER
20.00 0.00 80.00
PHASE FUNC
-2.09 0.00 0.00

FAR FIELD AMPLITUDE AND PHASE PATTERN

LEGEND
——— FIELD
- - - - PHASE

FIGURE 5-18

FAR FIELD PATTERNS FOR OFFSET GEOMETRY, THIRD SURFACE AMPLITUDE FOR SCAN = 0, THIRD SURFACE PHASE FOR SCAN = -1 DEGREE

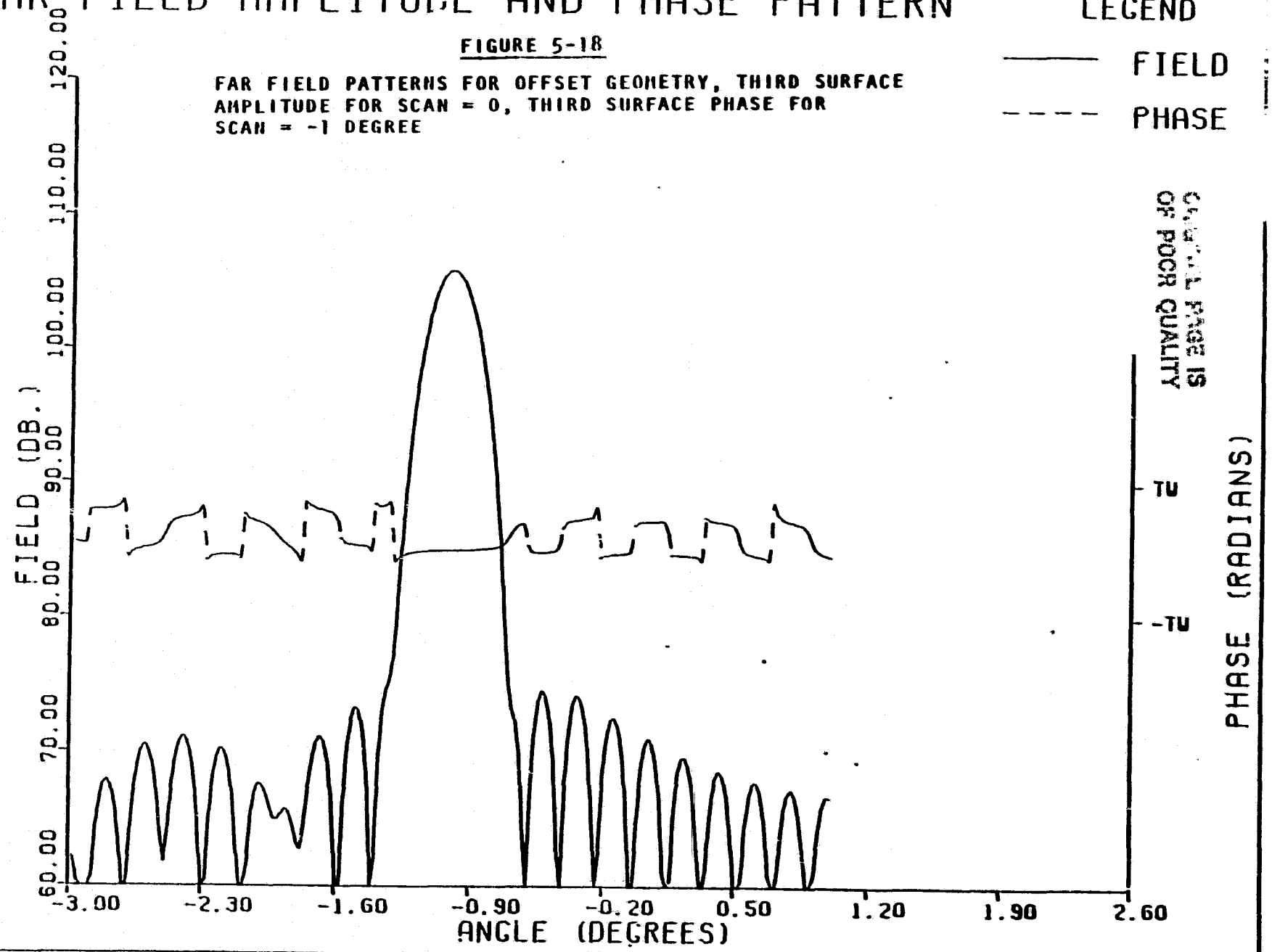

DATE: 01/22/82 TIME: 20.37.30.

AMP TAPER
20.00 0.00 80.00
PHASE FUNC
2.09 0.00 0.00

FAR FIELD AMPLITUDE AND PHASE PATTERN

LEGEND
——— FIELD
- - - - PHASE

FIGURE 5-19

FAR FIELD PATTERNS FOR OFFSET GEOMETRY, THIRD SURFACE AMPLITUDE FOR SCAN = 0, THIRD SURFACE PHASE FOR SCAN = +1 DEGREE

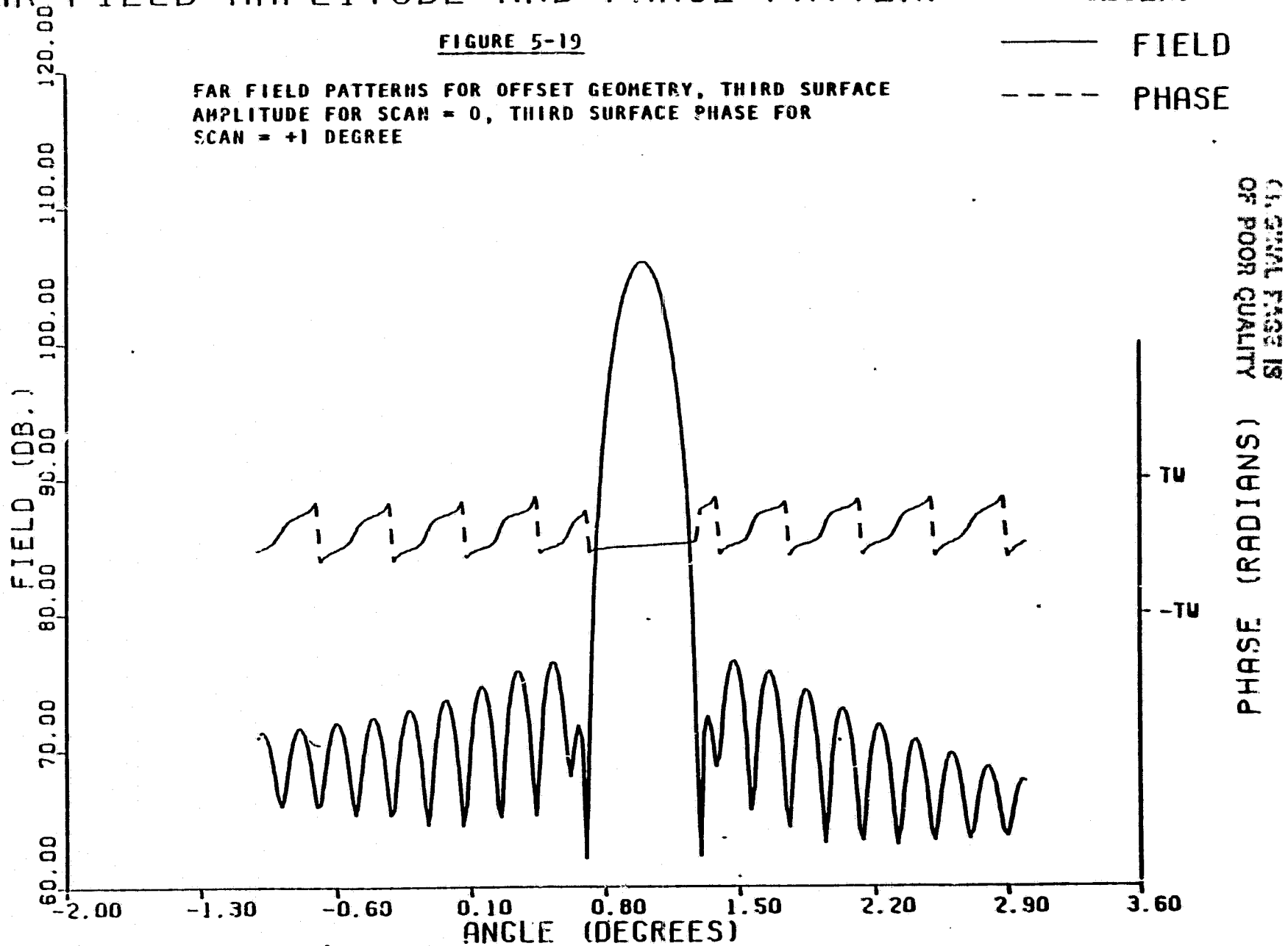

DATE: 01/22/82 TIME: 20.41.36.

AMP TAPER
20.00 0.00 80.00
PHASE FUNC
6.28 0.00 0.00

FAR FIELD AMPLITUDE AND PHASE PATTERN

FIGURE 5-20

FAR FIELD PATTERNS FOR OFFSET GEOMETRY, THIRD SURFACE
AMPLITUDE FOR SCAN = 0, THIRD SURFACE
PHASE FOR SCAN = +3 DEGREES

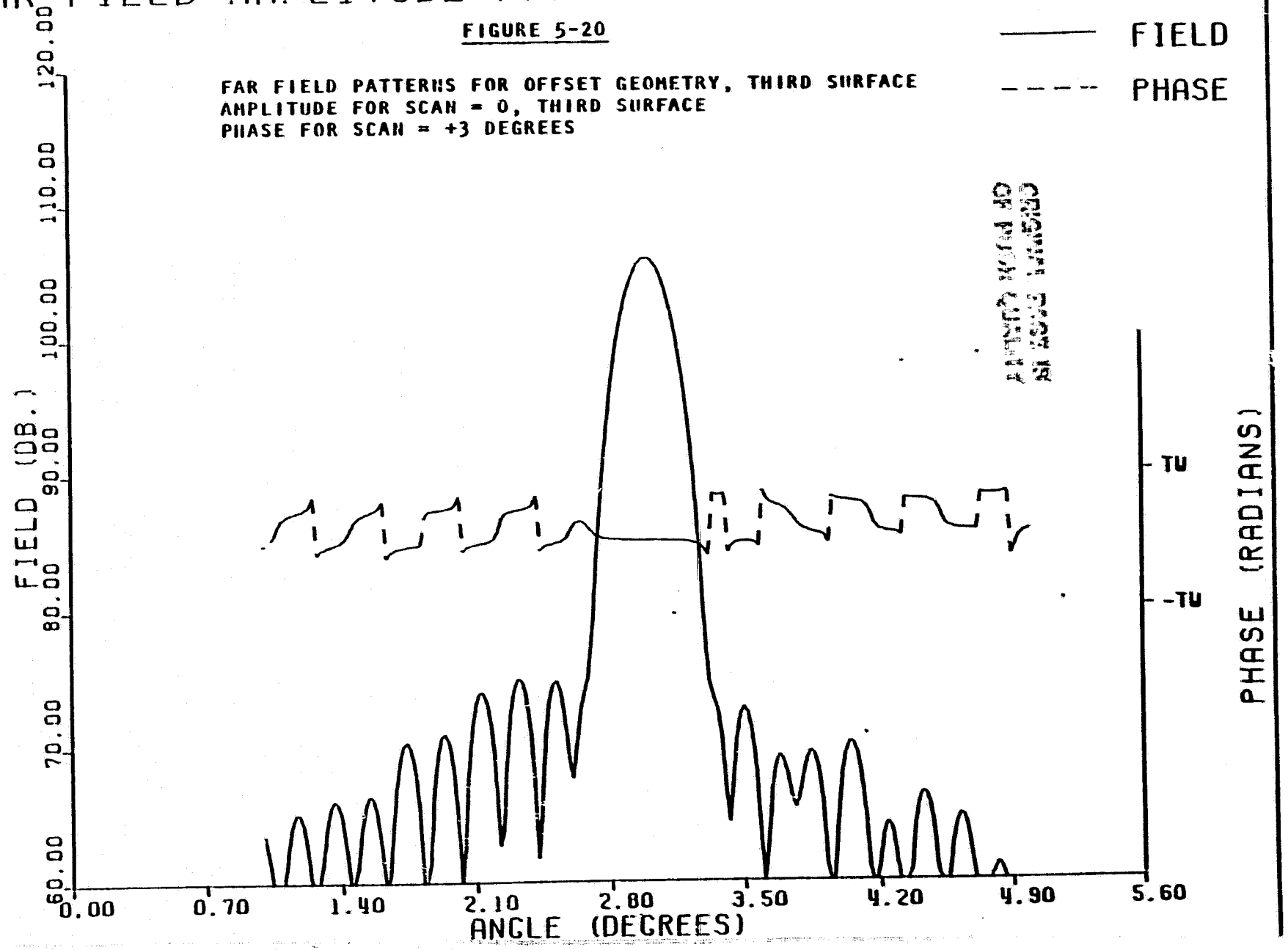

DATE: 01/22/82 TIME: 20.44.30.

AMP TAPER
20.00 0.00 80.00
PHASE FUNC
-2.09 0.00 0.00

FAR FIELD AMPLITUDE AND PHASE PATTERN

FIGURE 5-21

FAR FIELD PATTERNS FOR OFFSET GEOMETRY, THIRD SURFACE AMPLITUDE FOR SCAN = +1 DEGREE, THIRD SURFACE PHASE FOR SCAN = -1 DEGREE

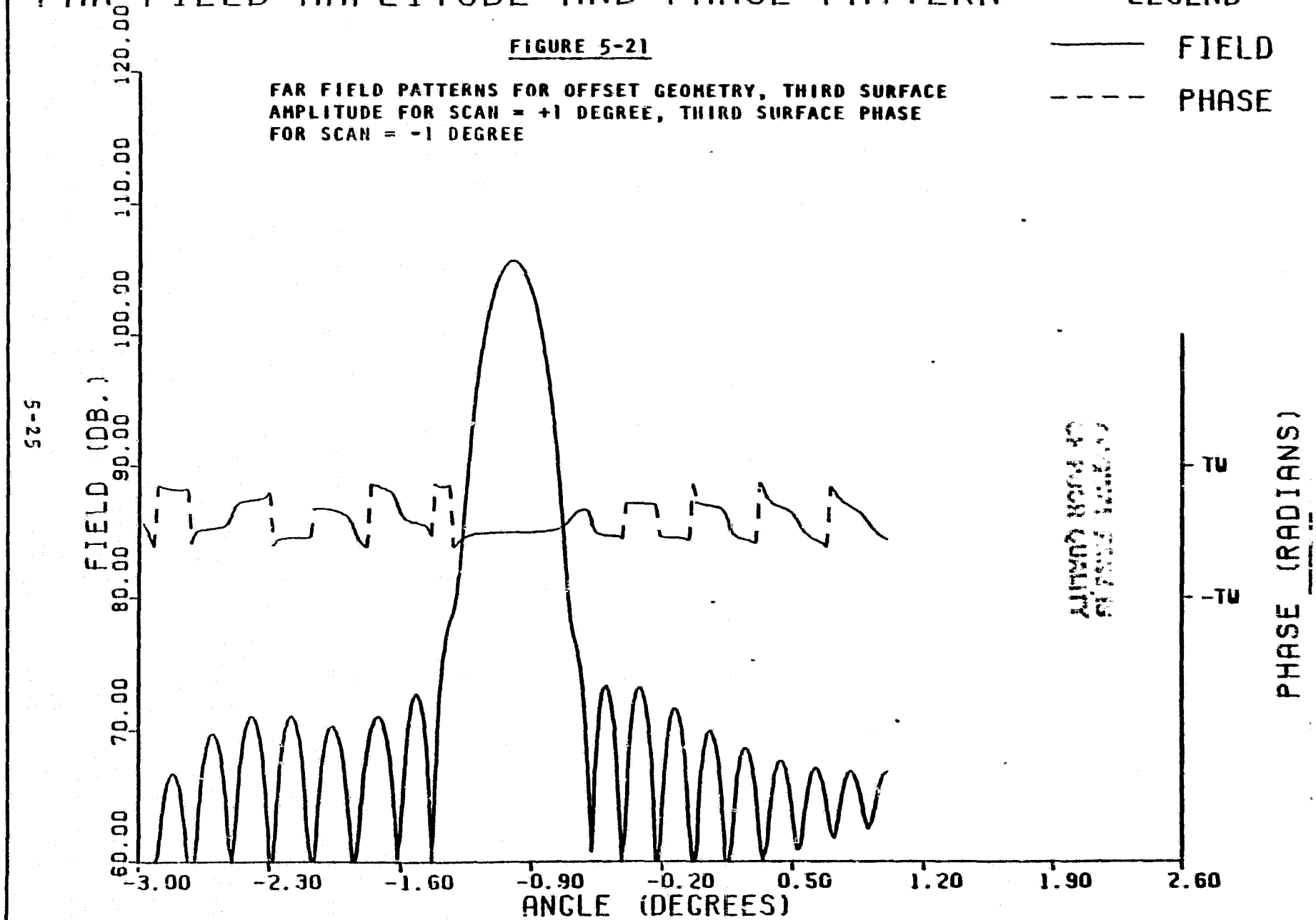

DATE: 01/22/82 TIME: 20.29.08.

AMP TAPER
20.00 0.00 80.00
PHASE FUNC
2.09 0.00 0.00

FAR FIELD AMPLITUDE AND PHASE PATTERN

LEGEND
——— FIELD
- - - - PHASE

FIGURE 5-22

FAR FIELD PATTERNS FOR OFFSET GEOMETRY, THIRD SURFACE AMPLITUDE FOR SCAN = +1 DEGREE, THIRD SURFACE PHASE FOR SCAN = +1 DEGREE

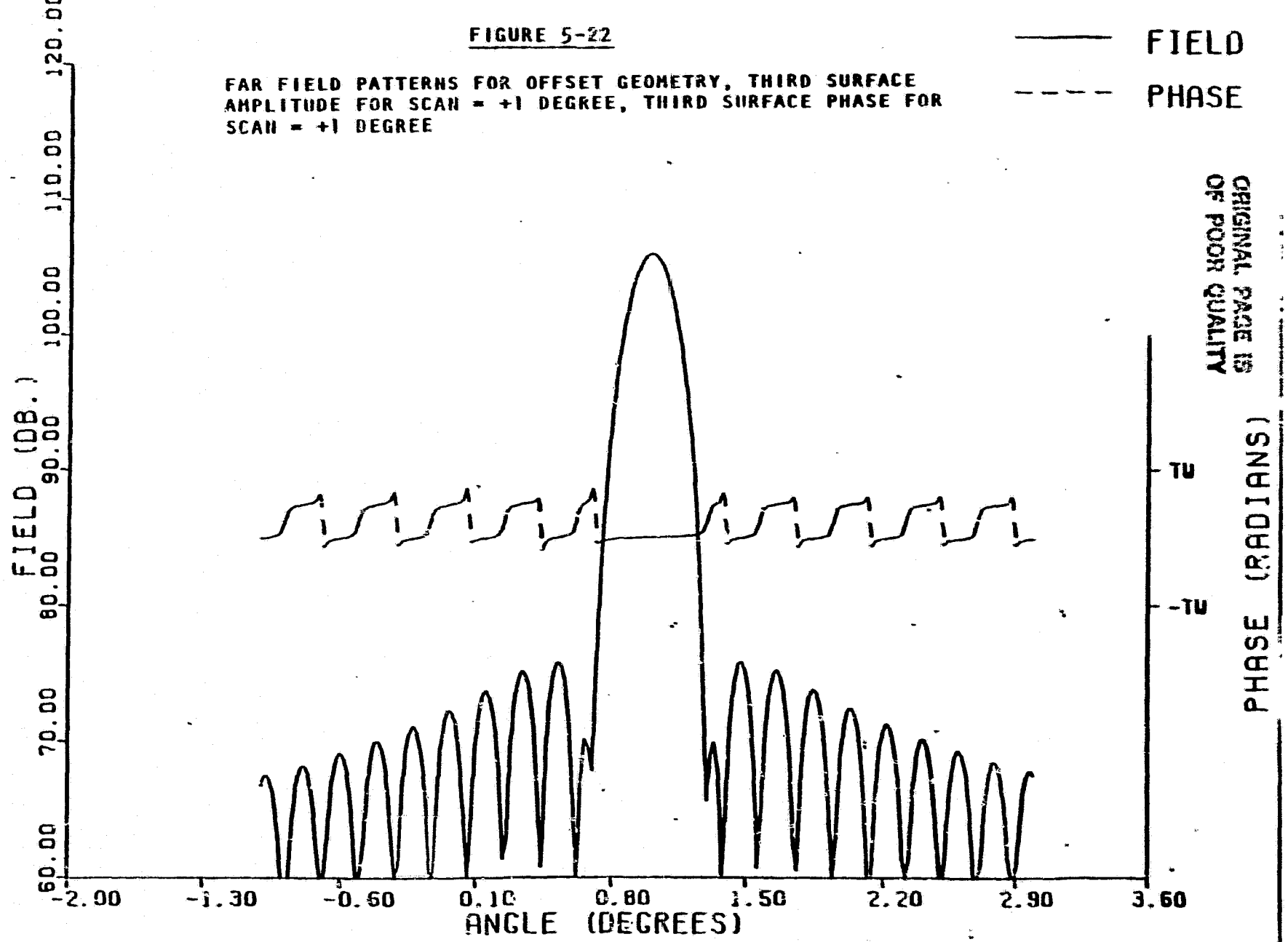

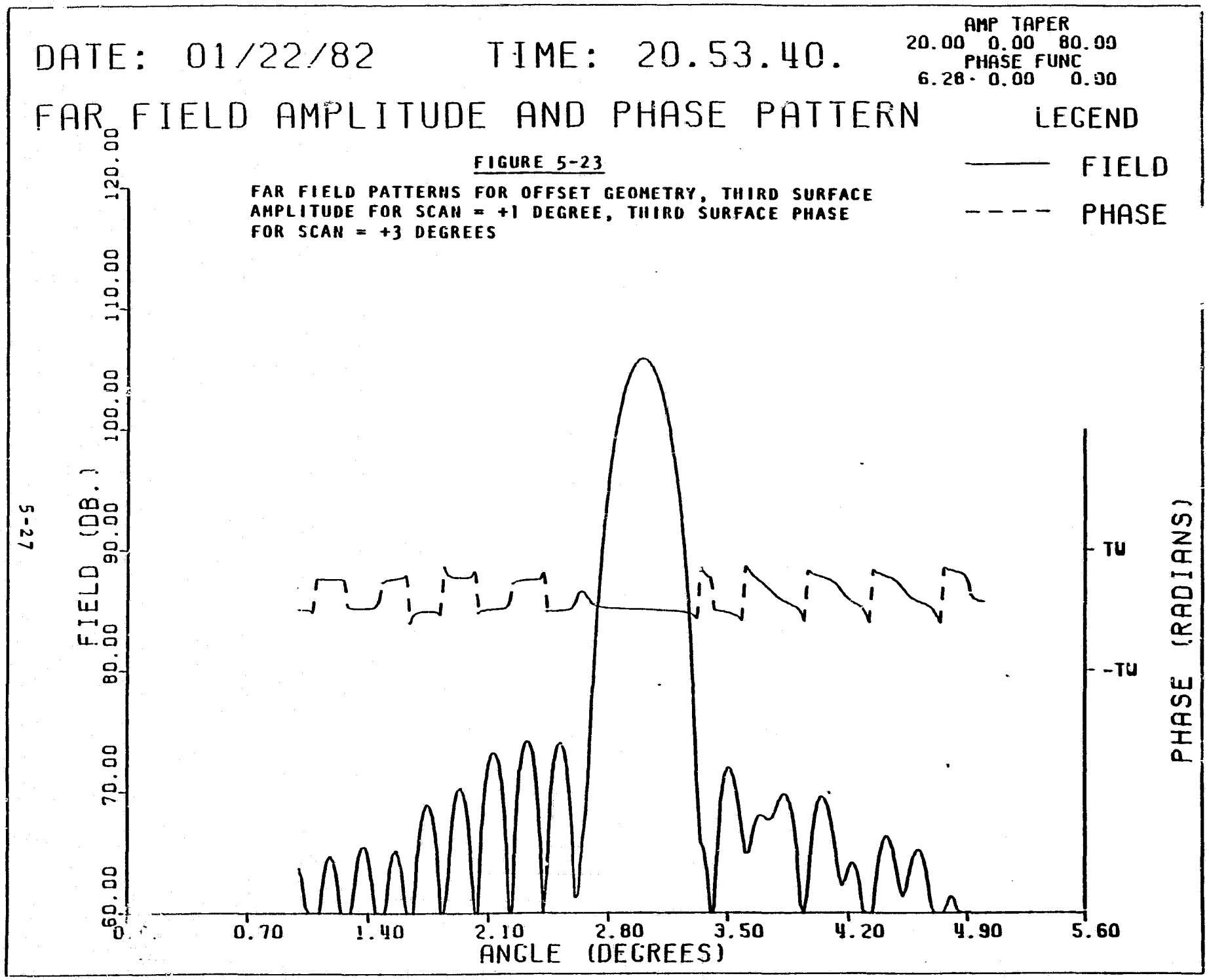
DATE: 01/22/82
TIME: 20.53.40.
AMP TAPER
20.00 0.00 80.00
PHASE FUNC
6.28 0.00 0.00
FAR FIELD AMPLITUDE AND PHASE PATTERN
LEGEND
FIELD
PHASE
FIGURE 5-23
FAR FIELD PATTERNS FOR OFFSET GEOMETRY, THIRD SURFACE
AMPLITUDE FOR SCAN = +1 DEGREE, THIRD SURFACE PHASE
FOR SCAN = +3 DEGREES
FIELD (DB.)
120.00
110.00
100.00
90.00
80.00
70.00
60.00
TU
-TU
PHASE (RADIANS)
0.
0.70
1.40
2.10
2.80
3.50
4.20
4.90
5.60
ANGLE (DEGREES)

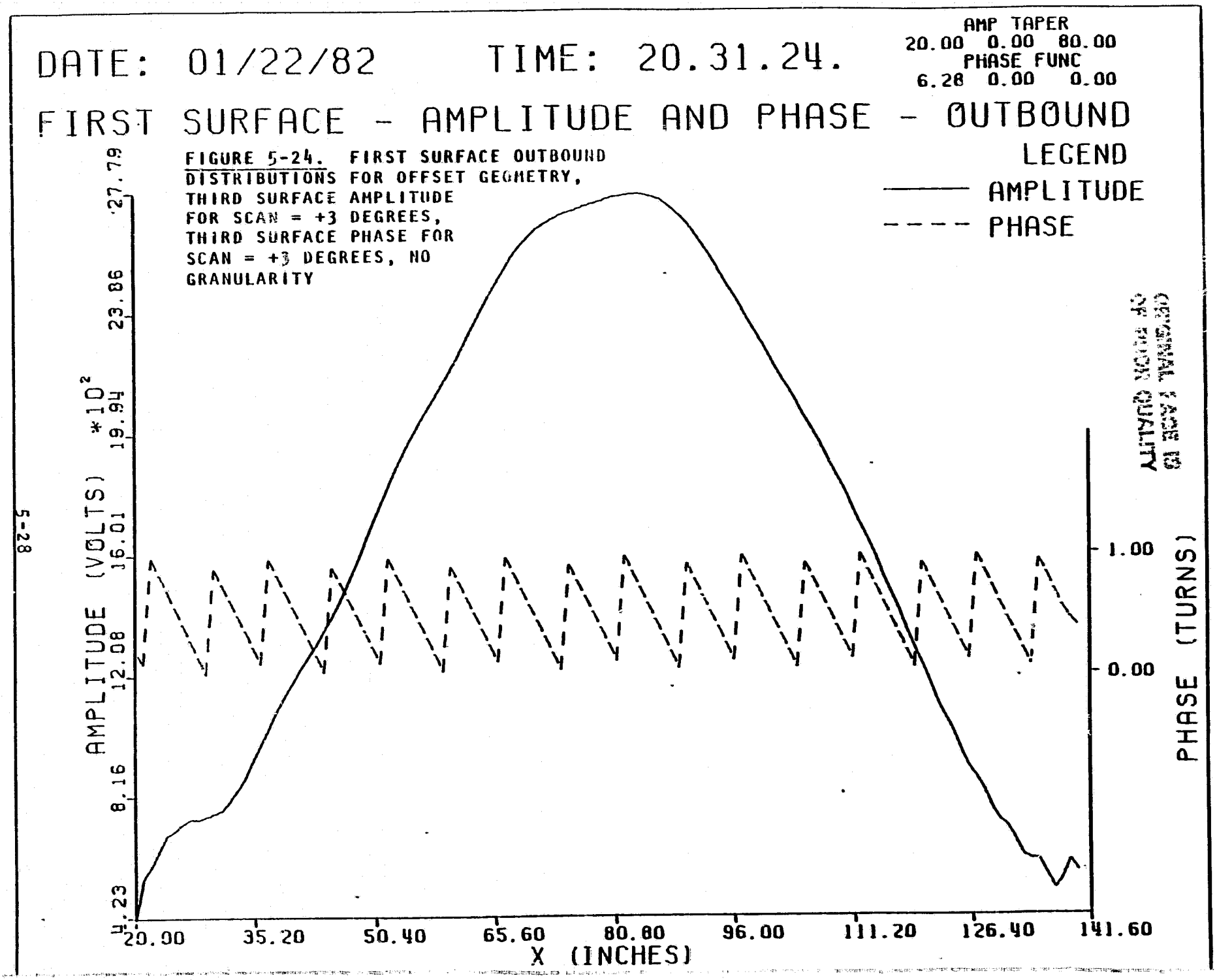

FIGURE 5-24. FIRST SURFACE OUTBOUND DISTRIBUTIONS FOR OFFSET GEOMETRY, THIRD SURFACE AMPLITUDE FOR SCAN = +3 DEGREES, THIRD SURFACE PHASE FOR SCAN = +3 DEGREES, NO GRANULARITY

DATE: 01/22/82 TIME: 20.31.24.

AMP TAPER
20.00 0.00 80.00
PHASE FUNC
6.28 0.00 0.00

FAR FIELD AMPLITUDE AND PHASE PATTERN

FIGURE 5-25

FAR FIELD PATTERNS FOR OFFSET GEOMETRY, THIRD SURFACE AMPLITUDE FOR SCAN = +3 DEGREES, THIRD SURFACE PHASE FOR SCAN = +3 DEGREES, NO GRANULARITY

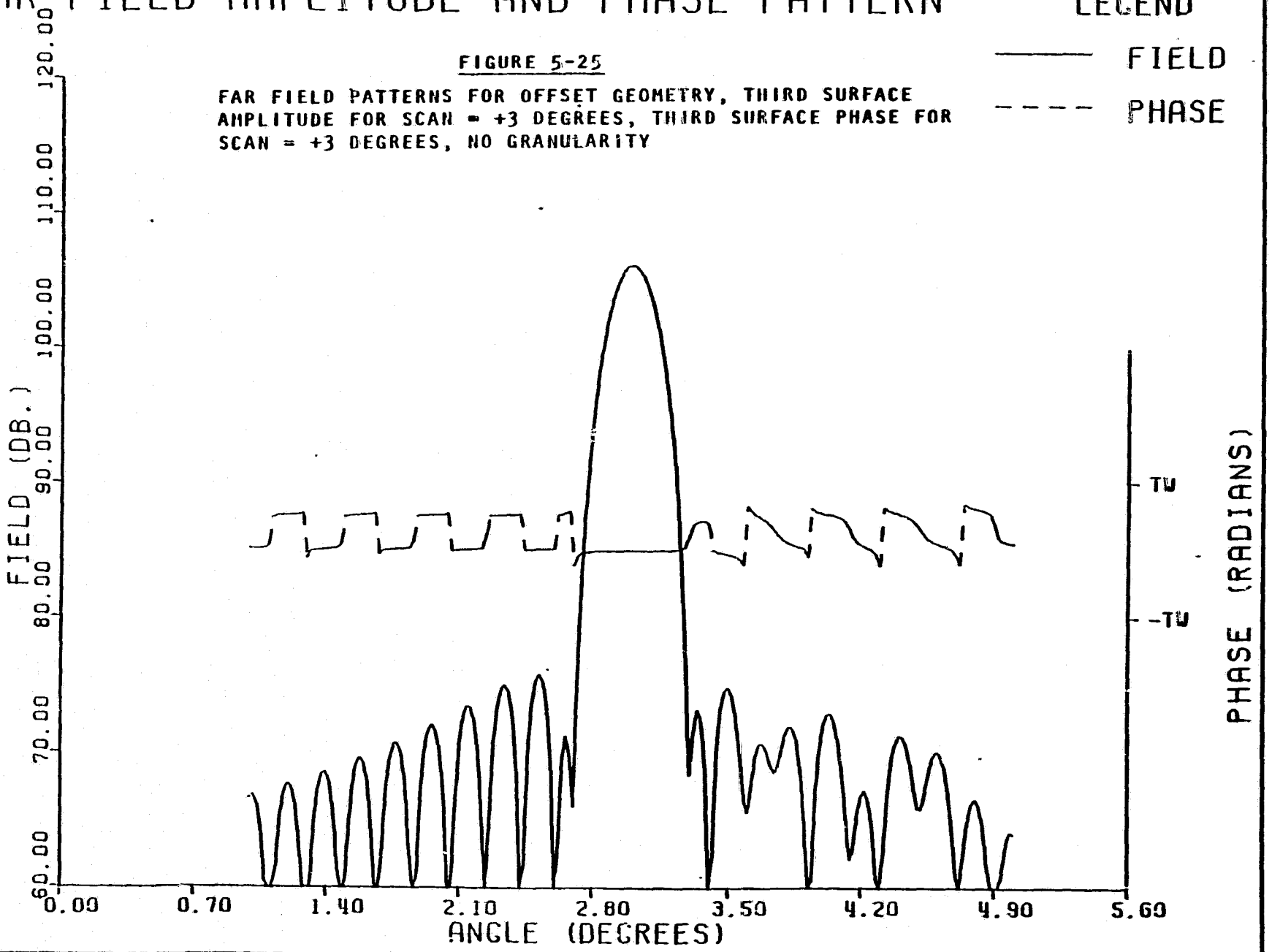

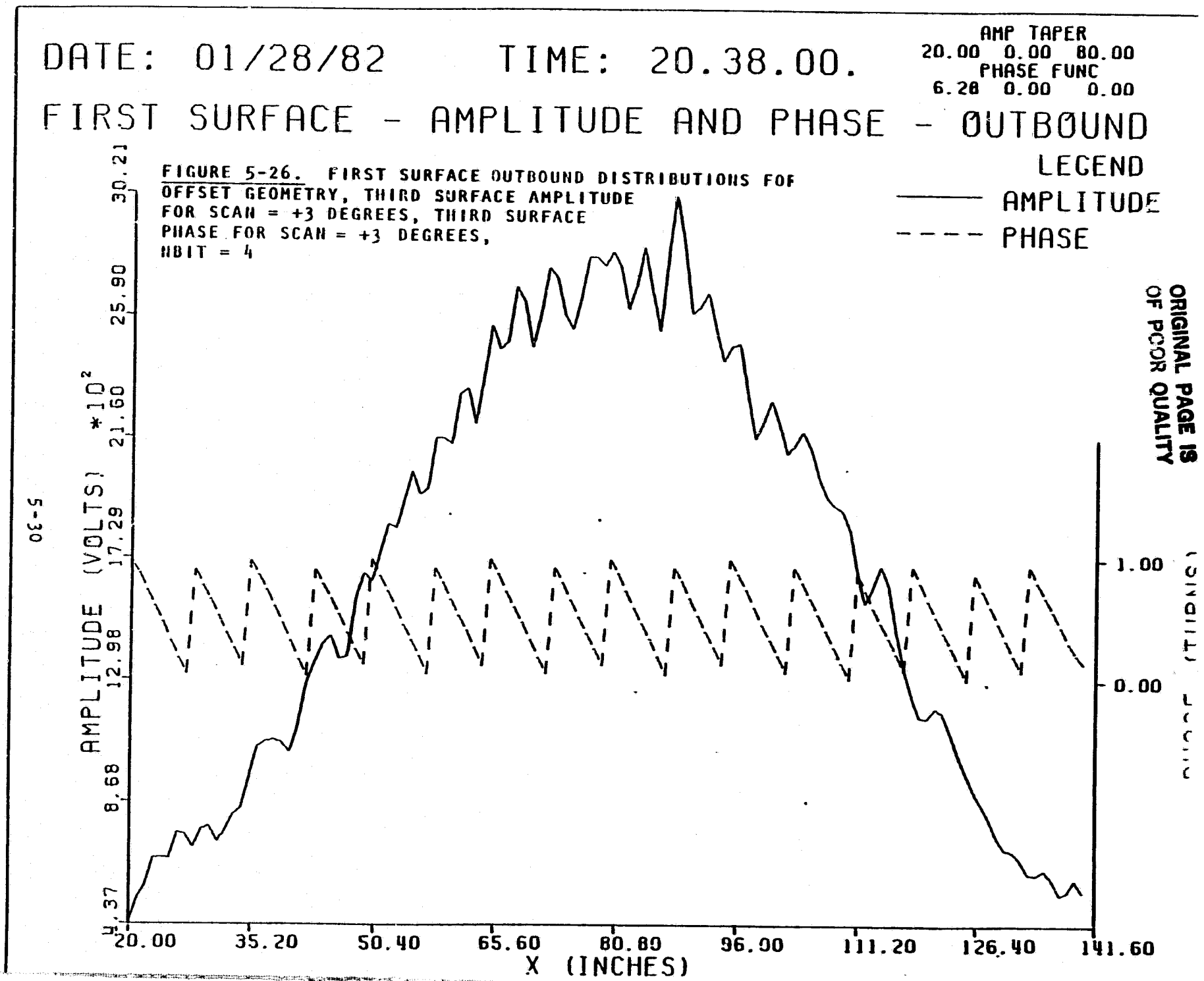
DATE: 01/28/82
TIME: 20.38.00.
AMP TAPER
20.00 0.00 80.00
PHASE FUNC
6.28 0.00 0.00
FIRST SURFACE - AMPLITUDE AND PHASE - OUTBOUND
FIGURE 5-26. FIRST SURFACE OUTBOUND DISTRIBUTIONS FOR OFFSET GEOMETRY, THIRD SURFACE AMPLITUDE FOR SCAN = +3 DEGREES, THIRD SURFACE PHASE FOR SCAN = +3 DEGREES, NBIT = 4
LEGEND
AMPLITUDE
PHASE
AMPLITUDE (VOLTS) *10²
30.21
25.90
21.60
17.29
12.98
8.68
4.37
1.00
0.00
20.00
35.20
50.40
65.60
80.80
96.00
111.20
126.40
141.60
X (INCHES)
5-30
ORIGINAL PAGE IS OF POOR QUALITY

DATE: 01/28/82 TIME: 20.38.00.

20.00 0.00 80.00
PHASE FUNC
6.28 0.00 0.00

FAR FIELD AMPLITUDE AND PHASE PATTERN

LEGEND
——— FIELD
- - - - PHASE

FIGURE 5-27
FAR FIELD PATTERNS FOR OFFSET GEOMFTRY, THIRD SURFACE AMPLITUDE FOR SCAN = +3 DEGREES, THIRD SURFACE PHASE FOR SCAN = +4 DEGREES, NBIT = 4

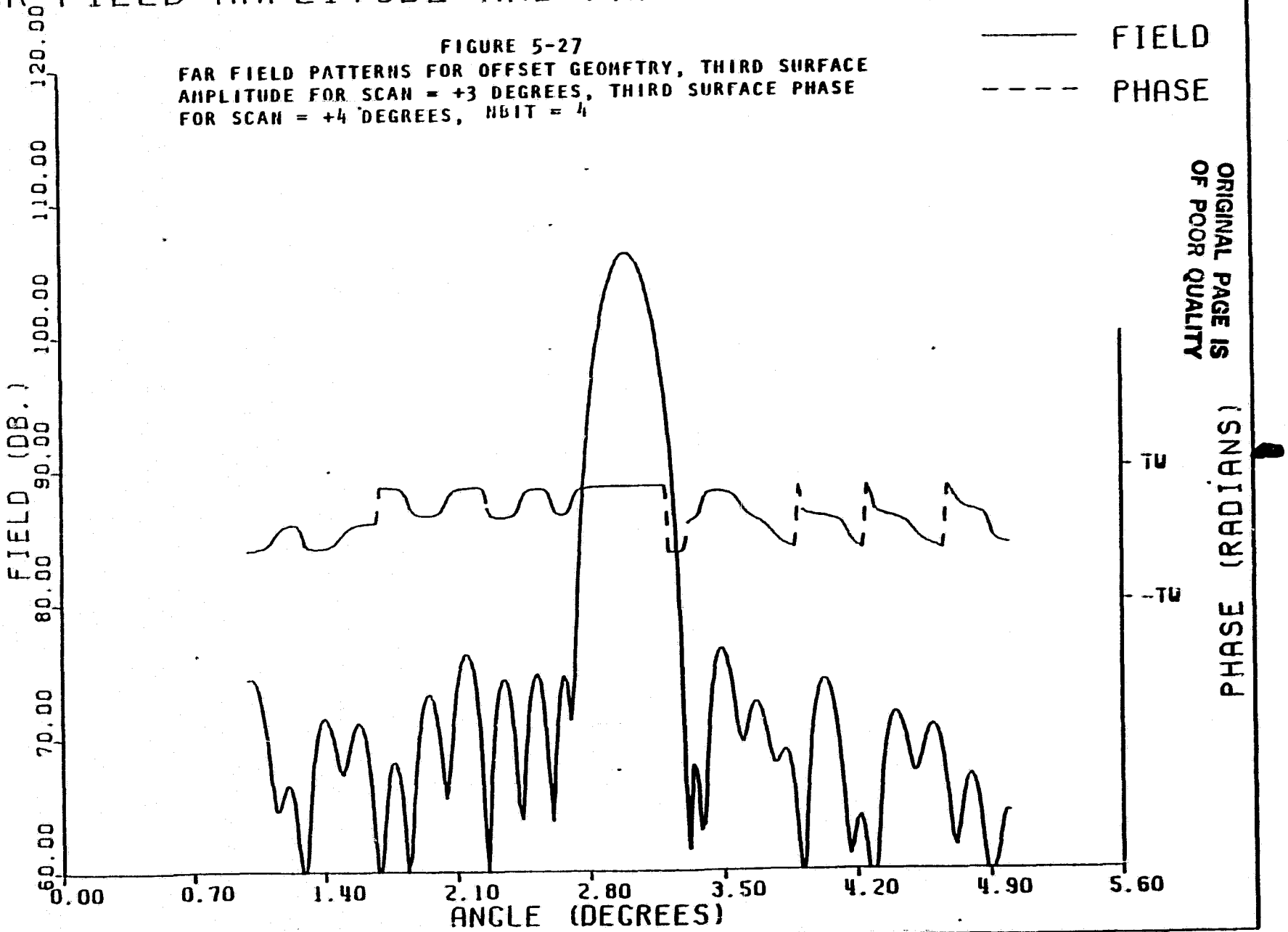

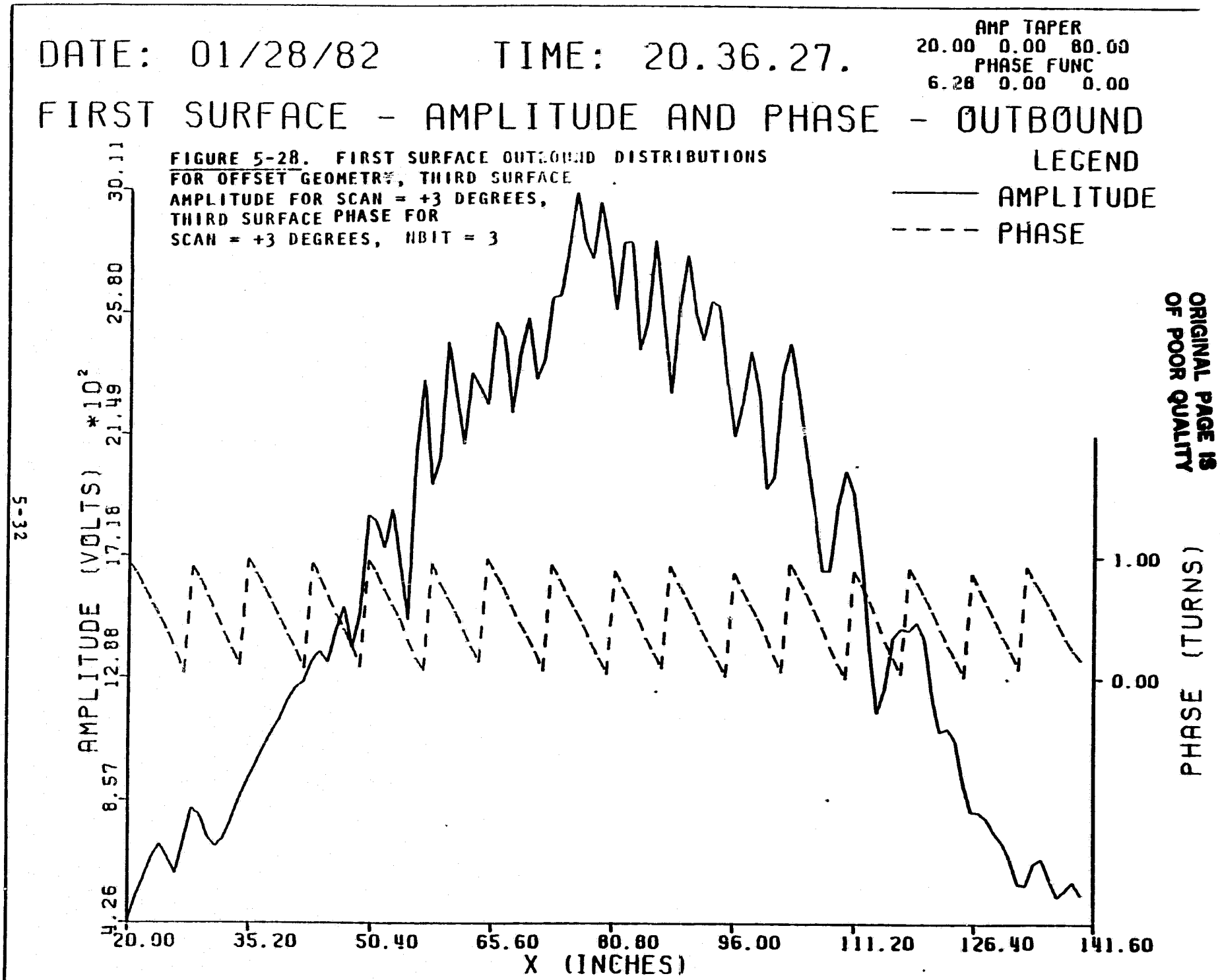
DATE: 01/28/82
TIME: 20.36.27.
AMP TAPER
20.00 0.00 80.00
PHASE FUNC
6.28 0.00 0.00
FIRST SURFACE - AMPLITUDE AND PHASE - OUTBOUND
FIGURE 5-28. FIRST SURFACE OUTBOUND DISTRIBUTIONS FOR OFFSET GEOMETRY, THIRD SURFACE AMPLITUDE FOR SCAN = +3 DEGREES, THIRD SURFACE PHASE FOR SCAN = +3 DEGREES, NBIT = 3
LEGEND
AMPLITUDE
PHASE
AMPLITUDE (VOLTS) *10²
30.11
25.80
21.49
17.18
12.88
8.57
4.26
PHASE (TURNS)
1.00
0.00
20.00
35.20
50.40
65.60
80.80
96.00
111.20
126.40
141.60
X (INCHES)
ORIGINAL PAGE IS OF POOR QUALITY

DATE: 01/28/82 TIME: 20.36.27.

AMP TAPER
20.00 0.00 80.00
PHASE FUNC
6.28 0.00 0.00

FAR FIELD AMPLITUDE AND PHASE PATTERN

FIGURE 5-29

FAR FIELD PATTERNS FOR OFFSET GEOMETRY, THIRD SURFACE AMPLITUDE FOR SCAN = +3 DEGREES, THIRD SURFACE PHASE FOR SCAN = +3 DEGREES, NBIT = 3

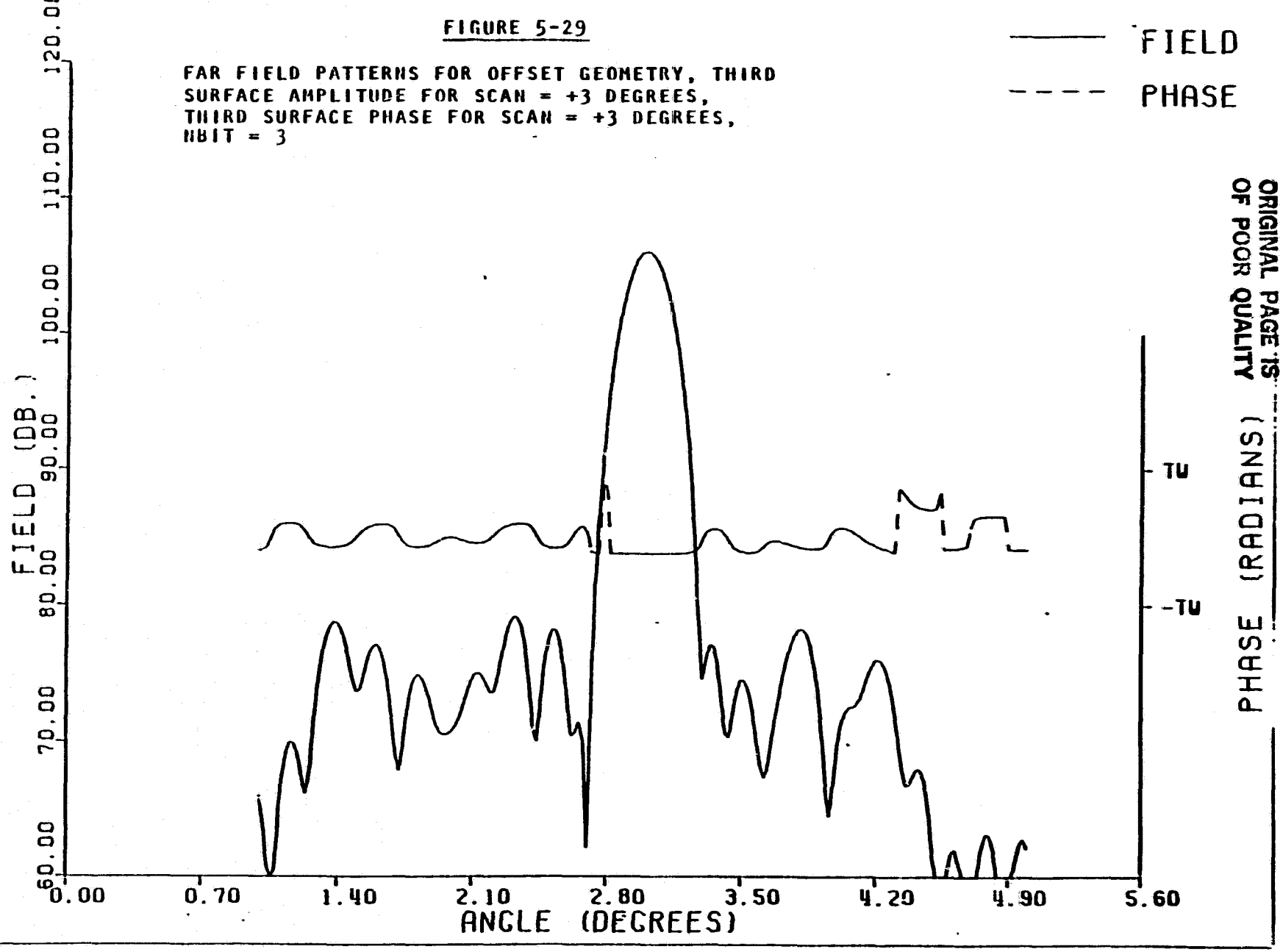

DATE: 01/28/82 TIME: 20.34.23.

AMP TAPER
20.00 0.00 80.00
PHASE FUNC
6.28 0.00 0.00

FIRST SURFACE - AMPLITUDE AND PHASE - OUTBOUND

FIGURE 5-30. FIRST SURFACE OUTBOUND DISTRIBUTIONS FOR OFFSET GEOMETRY, THIRD SURFACE AMPLITUDE FOR SCAN = +3 DEGREES, THIRD SURFACE PHASE FOR SCAN = +3 DEGREES, NBIT = 2

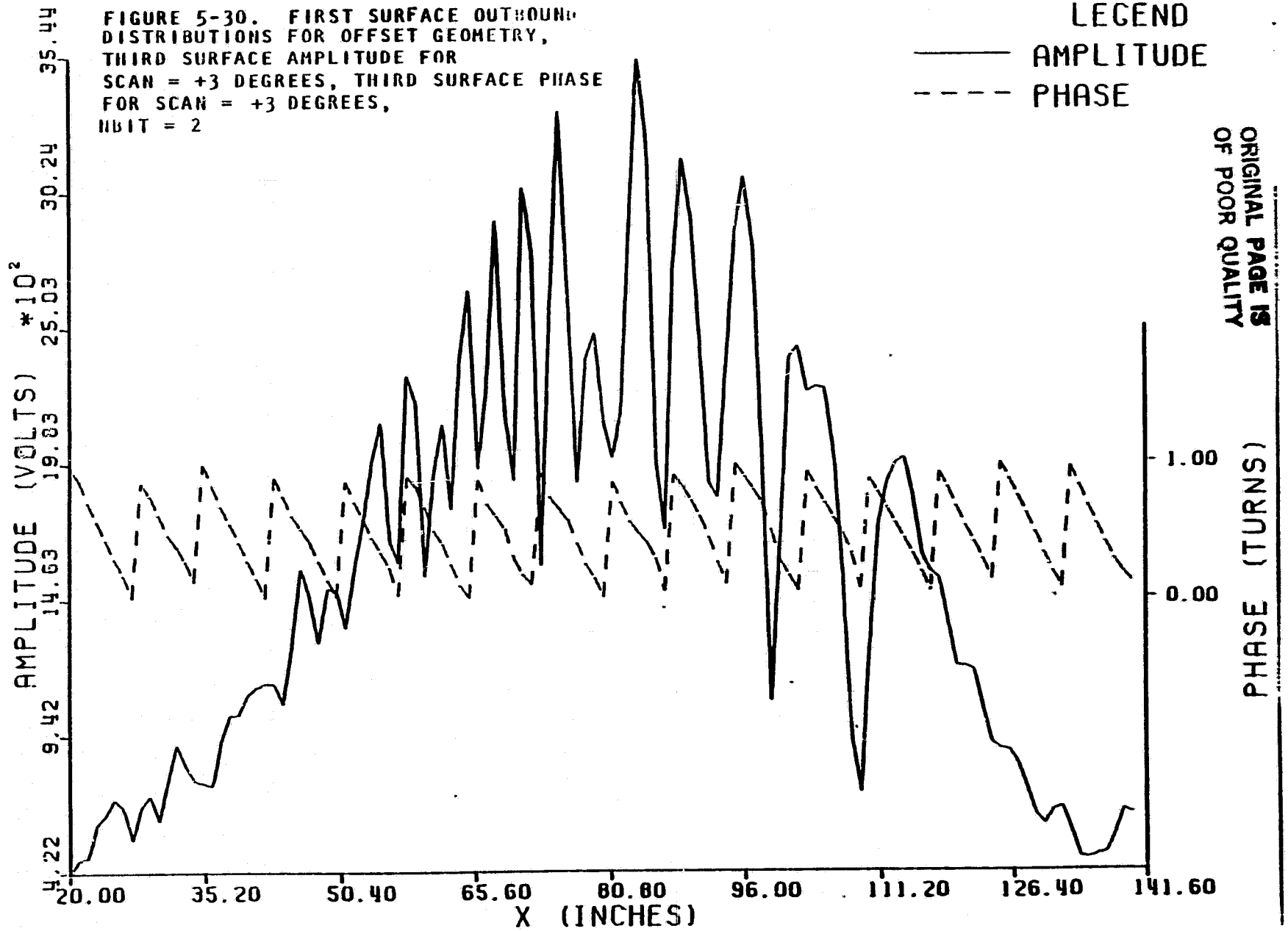

DATE: 01/28/82 TIME: 20.34.23.

AMP TAPER
20.00 0.00 80.00
PHASE FUNC
6.28 0.00 0.00

FAR FIELD AMPLITUDE AND PHASE PATTERN

FIGURE 5-31

FAR FIELD PATTERNS FOR OFFSET GEOMETRY, THIRD SURFACE AMPLITUDE FOR SCAN = +3 DEGREES, THIRD SURFACE PHASE FOR SCAN = 3 DEGREES, NBIT = 2

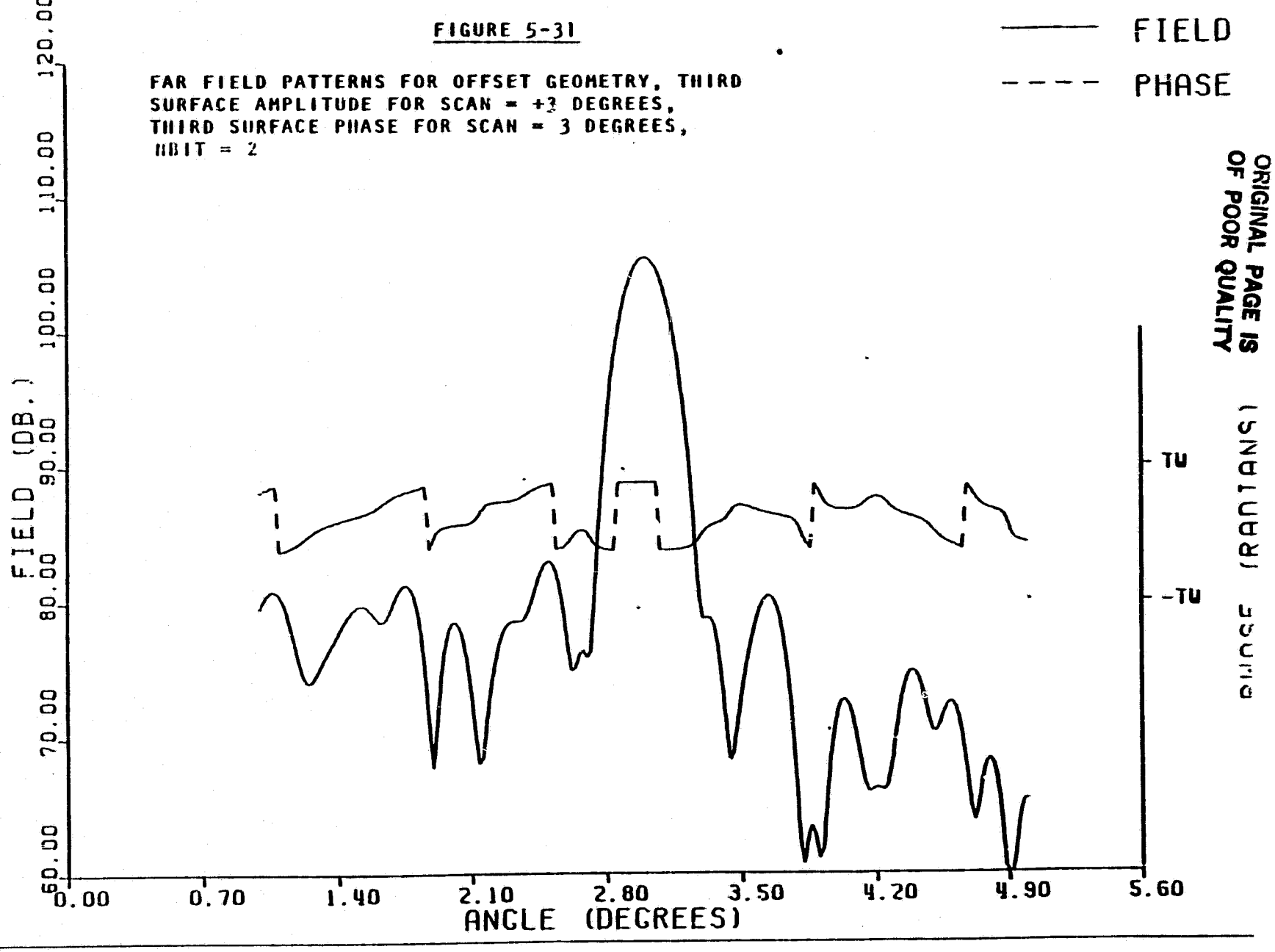

Similarly, when a random phase error (uniformly distributed over ±0.12 wavelengths) was imposed on the array elements, the error in the aperture appeared primarily in the amplitude term, diminishing the impact on the far-field pattern. Direct application of the Ruze formula would lead us to expect a gain loss of 3.3 dB for this case. We actually experience a loss of only 1.5 dB (Figures 5-32 and 5-33).

5.3.2 PROFILE ERRORS

Slowly varying profile errors were imposed on the surface of the array and the results were very similar to those that would be obtained had they been imposed directly to the primary aperture as indicated in Figure 1-4. Patterns exhibiting the results of focus, coma, and harmonic distributions are illustrated in Figures 5-34, 5-35, 5-36 and 5-37.

5.4 BANDWIDTH

Convincing evidence has been developed that the bandwidth of the NTL microwave telescope is infinite -- that an amplitude/time delay distribution imposed on the third surface transforms without frequency variation to an amplitude/time delay distribution on the first surface. This means that a combined 20/30 GHz design is limited only by the bandwidth capability of the array, not at all by the optics.

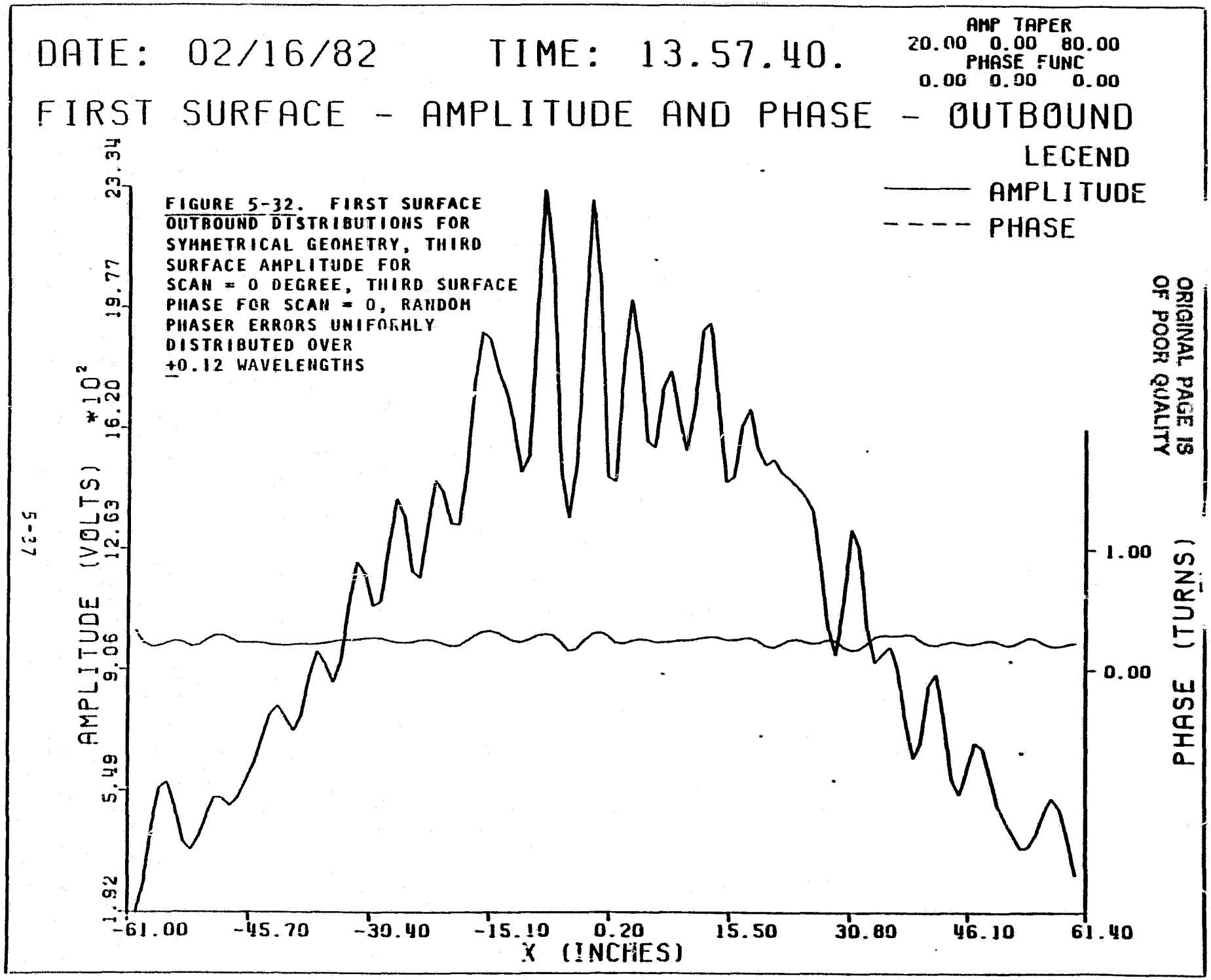
DATE: 02/16/82 TIME: 13.57.40.
AMP TAPER
20.00 0.00 80.00
PHASE FUNC
0.00 0.00 0.00
FIRST SURFACE - AMPLITUDE AND PHASE - OUTBOUND
LEGEND
AMPLITUDE
PHASE
FIGURE 5-32. FIRST SURFACE OUTBOUND DISTRIBUTIONS FOR SYMMETRICAL GEOMETRY, THIRD SURFACE AMPLITUDE FOR SCAN = 0 DEGREE, THIRD SURFACE PHASE FOR SCAN = 0, RANDOM PHASER ERRORS UNIFORMLY DISTRIBUTED OVER ±0.12 WAVELENGTHS
AMPLITUDE (VOLTS) *10²
23.34
19.77
16.20
12.63
9.06
5.49
1.92
PHASE (TURNS)
1.00
0.00
-61.00
-45.70
-30.40
-15.10
0.20
15.50
30.80
46.10
61.40
X (INCHES)
ORIGINAL PAGE IS OF POOR QUALITY
5-37

DATE: 02/16/82 TIME: 13.57.40.

AMP TAPER
20.00 0.00 80.00
PHASE FUNC
0.00 0.00 0.00

FAR FIELD AMPLITUDE AND PHASE PATTERN

LEGEND
——— FIELD
- - - - PHASE

FIGURE 5-33

FAR FIELD PATTERNS FOR SYMMETRICAL GEOMETRY, THIRD SURFACE AMPLITUDE FOR SCAN = 0, THIRD SURFACE PHASE FOR SCAN = 0, RANDOM PHASER ERRORS UNIFORMLY DISTRIBUTED OVER ±0.12 WAVELENGTHS

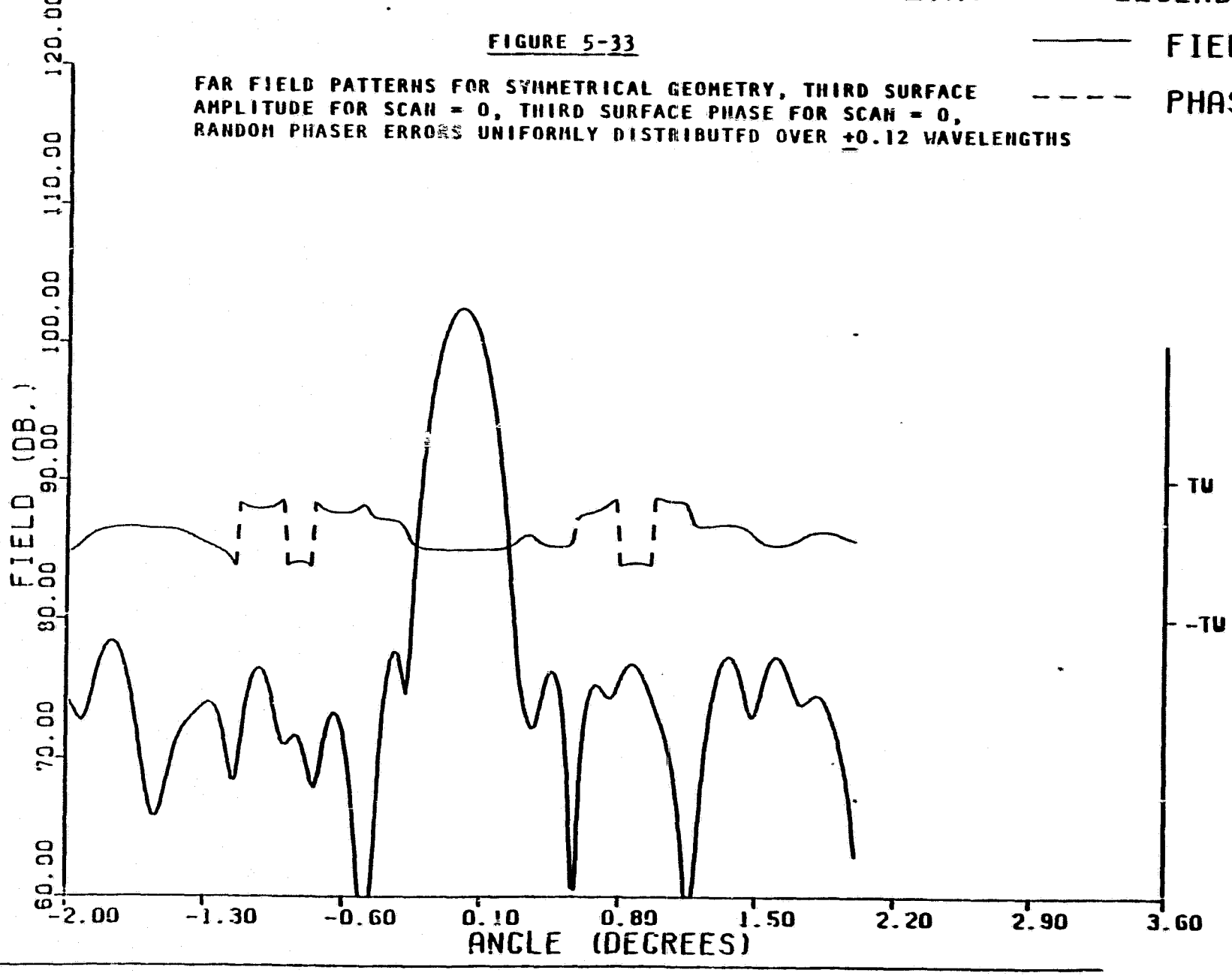

DATE: 01/28/82 TIME: 21.07.51.

AMP TAPER
20.00 0.00 60.00
PHASE FUNC
0.00 0.00 0.00

FAR FIELD AMPLITUDE AND PHASE PATTERN

FIGURE 5-34

FAR FIELD PATTERNS FOR SYMMETRICAL GEOMETRY, THIRD SURFACE AMPLITUDE FOR SCAN = 0, THIRD SURFACE PHASE FOR SCAN = 0, PLUS FOCUS PROFILE ERROR (0.4 INCHES AT EDGE)

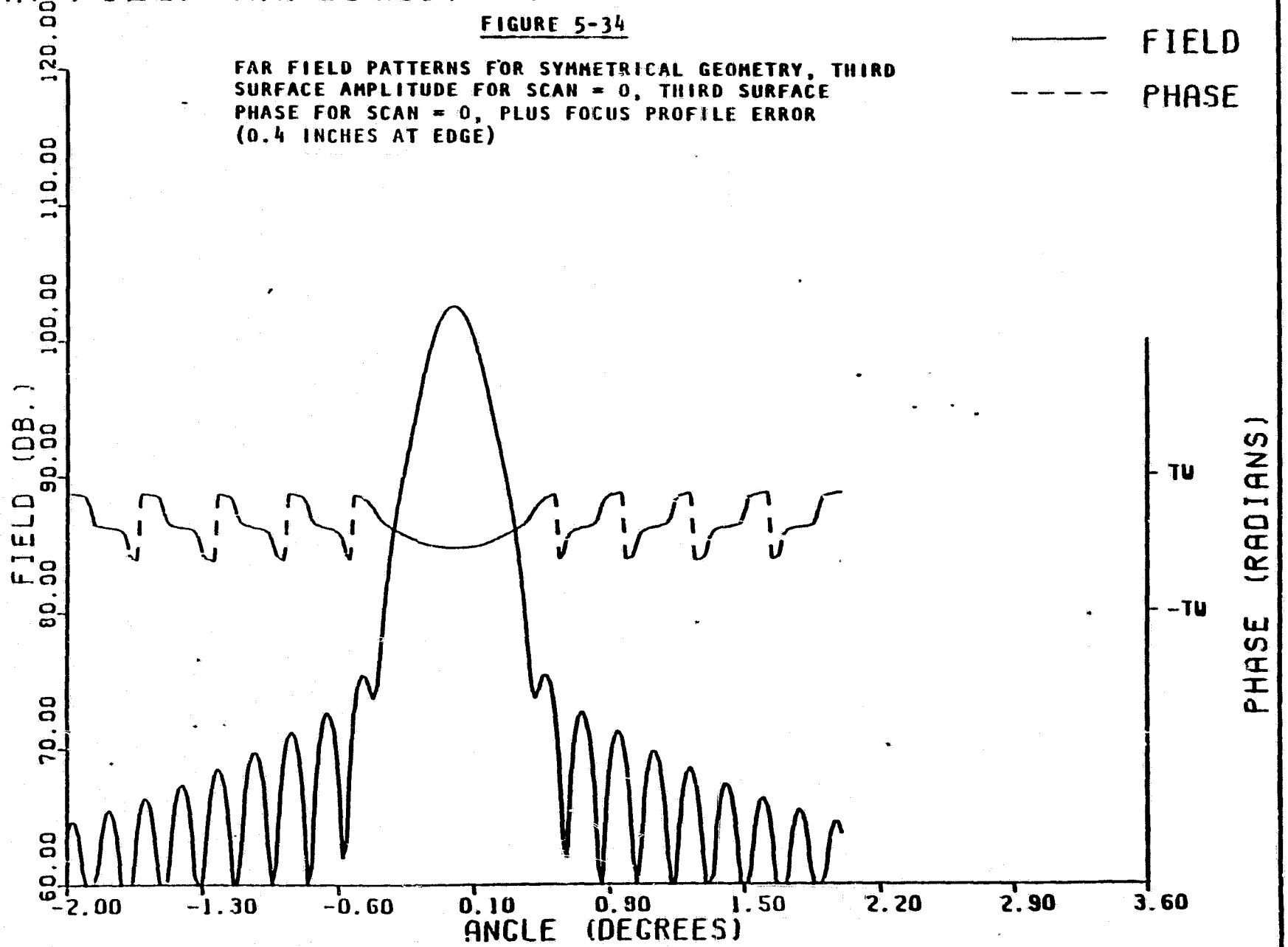

DATE: 01/29/82 TIME: 20.51.24.

AMP TAPER
20.00 0.00 80.00
PHASE FUNC
8.37 0.00 0.00

FAR FIELD AMPLITUDE AND PHASE PATTERN

FIGURE 5-35

FAR FIELD PATTERNS FOR SYMMETRICAL GEOMETRY, THIRD SURFACE AMPLITUDE FOR SCAN = +4 DEGREES, THIRD SURFACE PHASE FOR SCAN = +4 DEGREES, PLUS FOCUS PROFILE ERROR (0.4 INCHES AT EDGE)

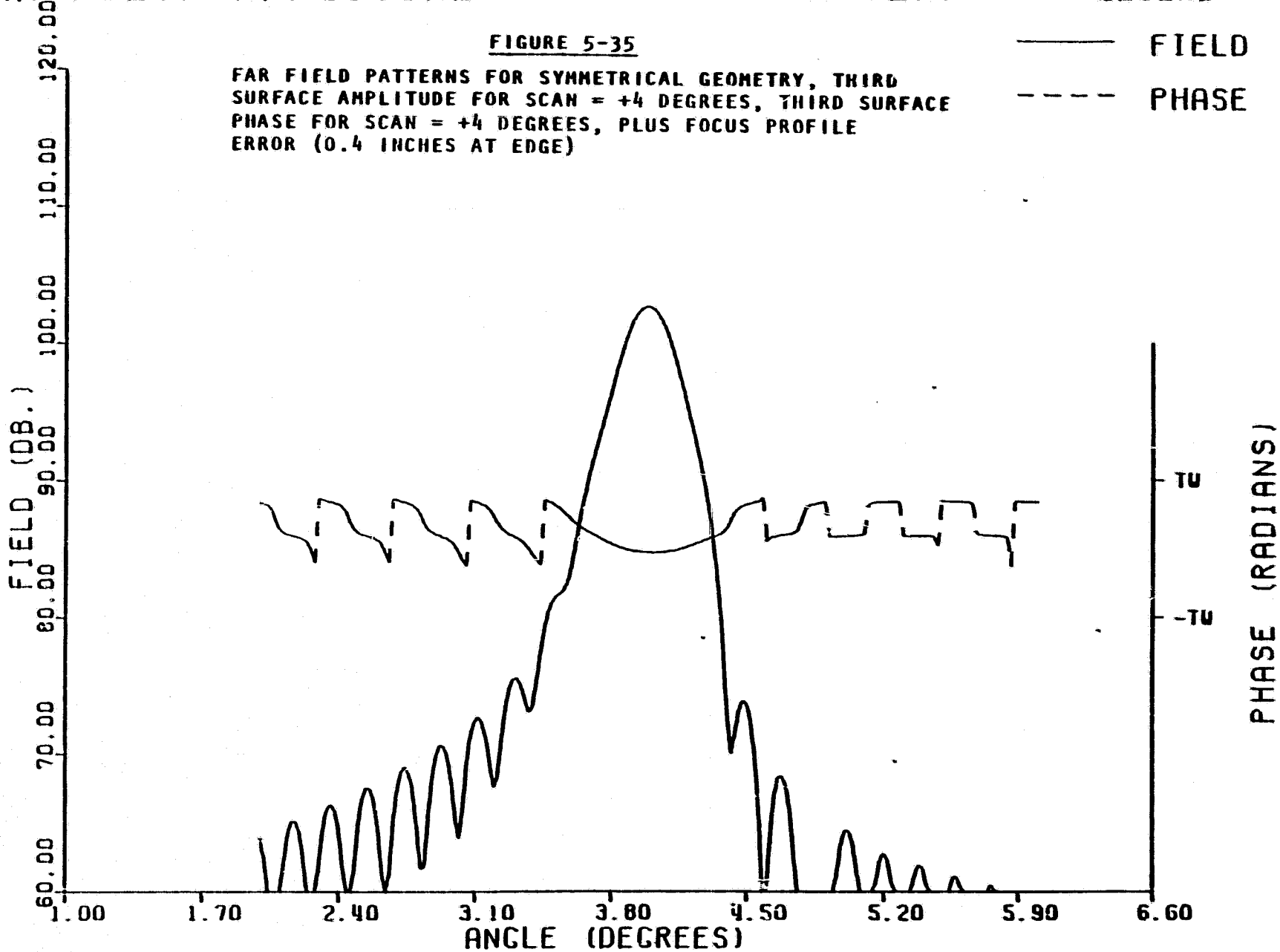

DATE: 01/28/82 TIME: 21.09.45.

AMP TAPER
20.00 0.00 80.00
PHASE FUNC
0.00 0.00 0.00

FAR FIELD AMPLITUDE AND PHASE PATTERN

FIGURE 5-36

FAR FIELD PATTERNS FOR SYMMETRICAL GEOMETRY, THIRD SURFACE AMPLITUDE FOR SCAN = 0, THIRD SURFACE PHASE FOR SCAN = 0, PLUS COMATIC PROFILE ERROR (0.4 INCHES AT EDGE)

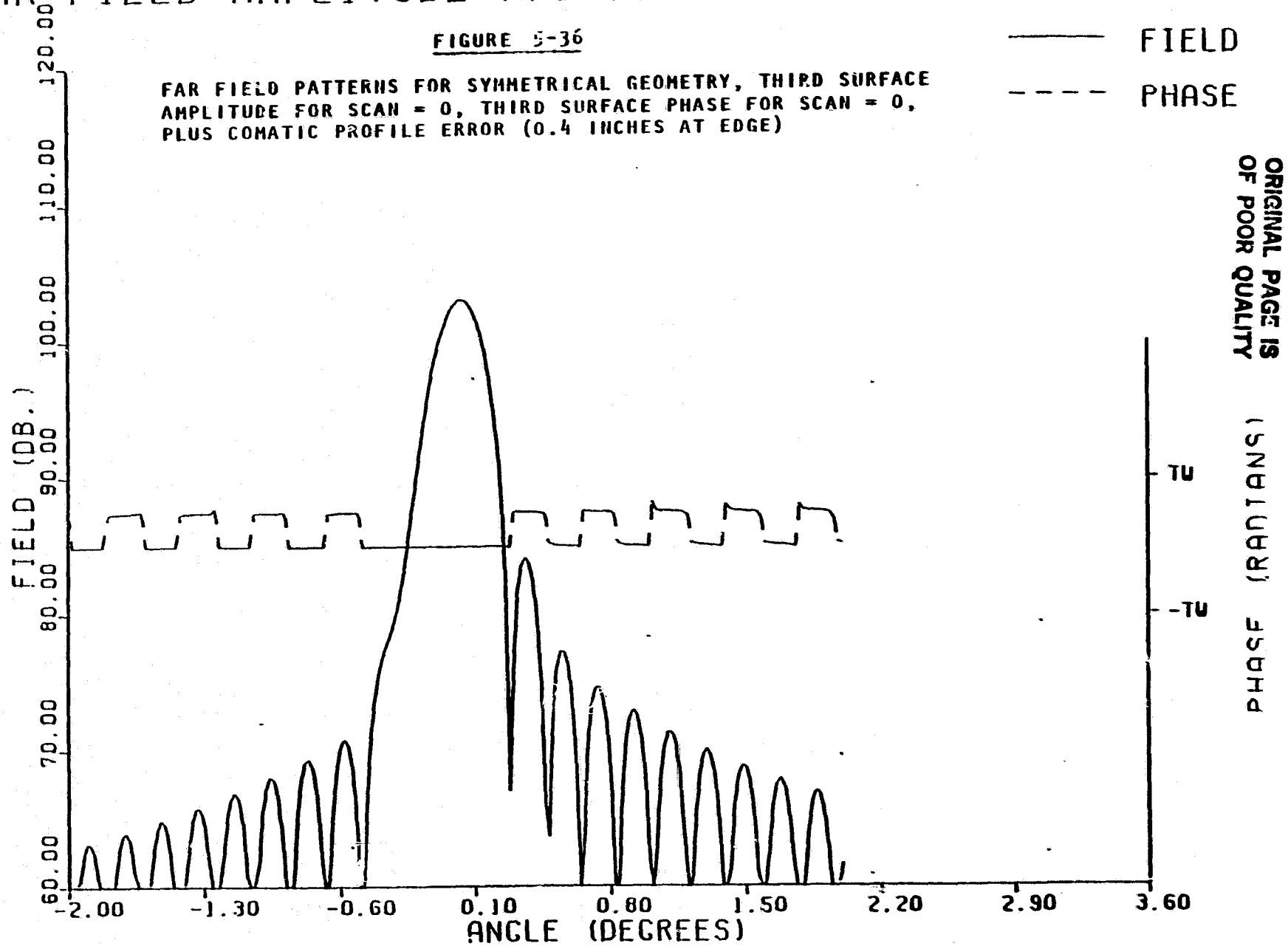

DATE: 01/28/82 TIME: 21.11.05.

AMP TAPER
20.00 0.00 80.00
PHASE FUNC
0.00 0.00 0.00

FAR FIELD AMPLITUDE AND PHASE PATTERN

LEGEND
——— FIELD
- - - - PHASE

FIGURE 5-37

FAR FIELD PATTERNS FOR SYMMETRICAL GEOMETRY, THIRD SURFACE AMPLITUDE FOR SCAN = 0, THIRD SURFACE PHASE FOR SCAN = 0, THREE CYCLE HARMONIC PROFILE ERROR (±0.2 RADIAN)

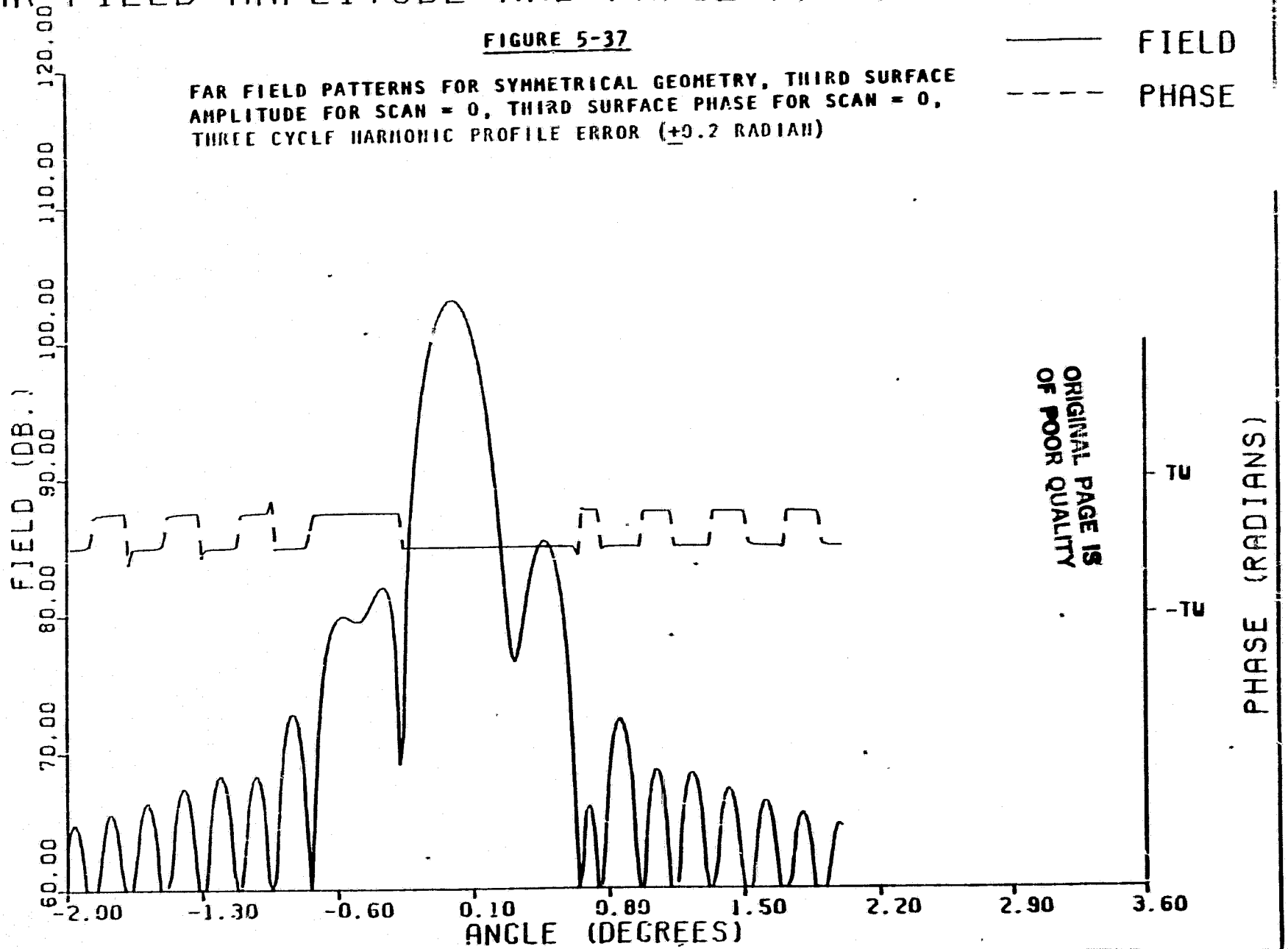

The evidence for this claim was derived from two bandwidth studies.

The first was an inbound-outbound set of calculations for the offset geometry at zero scan for frequencies of 29 and 20 GHz. The typically excellent far field results were obtained (Figures 5-38 and 5-39). The difference in level between the two patterns is not significant. The associated third surface distributions for the two frequencies (Figures 5-40 and 5-41) exhibit almost identical amplitudes and clearly related phases as indicated by the similar reversals of curvature near x = -8. The phase distributions of any diffraction integral are obtained from an arctangent routine and range over one wavelength or 2π radians. To convert them to more meaningful time delays requires that the phase information modulo 2π be adjusted to continuous data (Figure 5-42) before it is converted to the equivalent time delay (Figure 5-43). As indicated the time delay curves are identical over the array surface for this case of boresight incidence.

A second study included an inbound-outbound set of calculations for the same geometry and a +3 degree angle of incidence for frequencies of 30 and 20 GHz. Again, the amplitude and time-delay distributions on the surface of the array are practically identical (Figure 5-44).

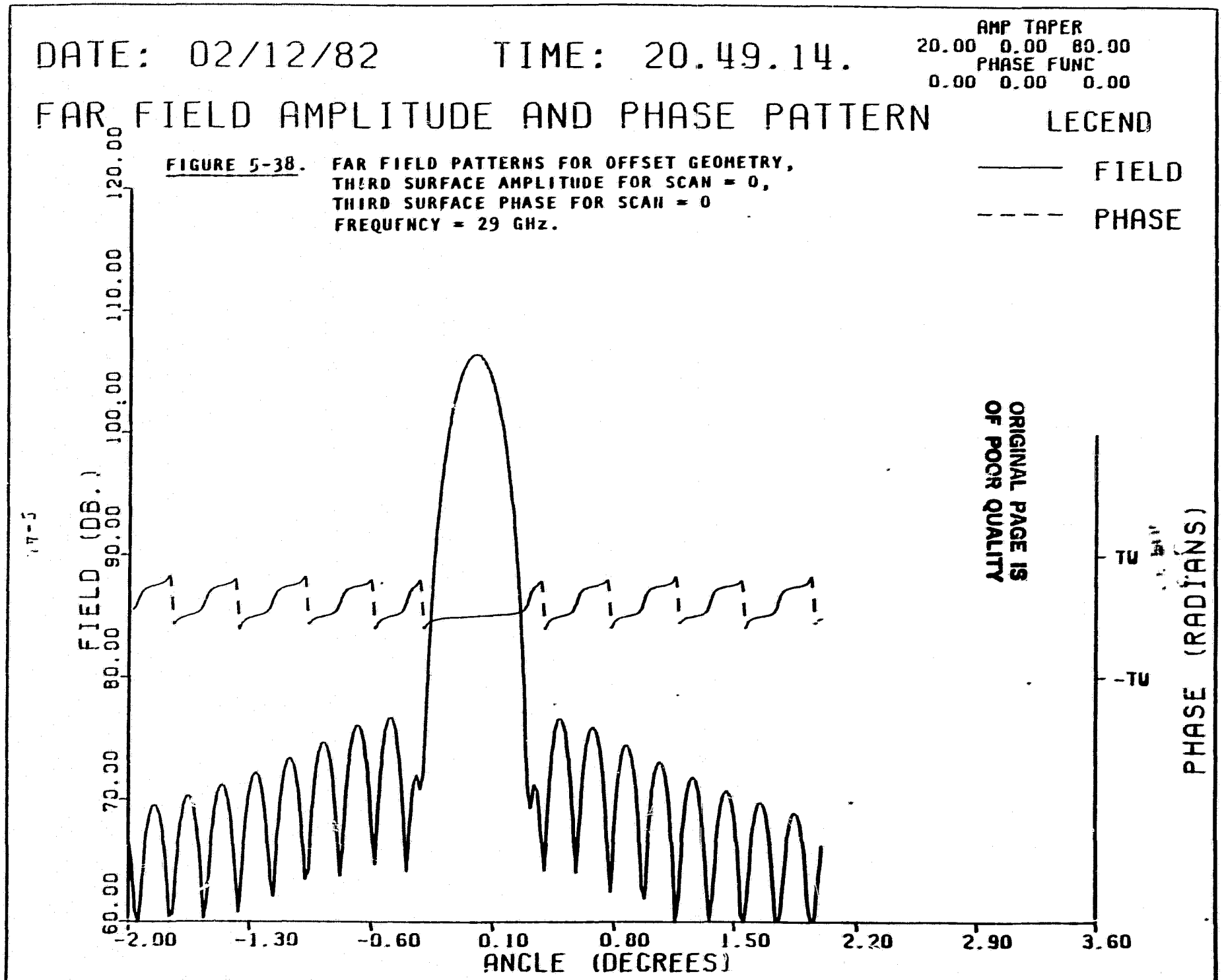
DATE: 02/12/82
TIME: 20.49.14.
AMP TAPER
20.00 0.00 80.00
PHASE FUNC
0.00 0.00 0.00
FAR FIELD AMPLITUDE AND PHASE PATTERN
LEGEND
FIELD
PHASE
FIGURE 5-38. FAR FIELD PATTERNS FOR OFFSET GEOMETRY, THIRD SURFACE AMPLITUDE FOR SCAN = 0, THIRD SURFACE PHASE FOR SCAN = 0 FREQUENCY = 29 GHz.
FIELD (DB.)
120.00
110.00
100.00
90.00
80.00
70.00
60.00
PHASE (RADIANS)
TU
-TU
-2.00
-1.30
-0.60
0.10
0.80
1.50
2.20
2.90
3.60
ANGLE (DEGREES)
ORIGINAL PAGE IS
OF POOR QUALITY

DATE: 02/12/82 TIME: 20.30.13.

AMP TAPER
20.00 0.00 80.00
PHASE FUNC
0.00 0.00 0.00

FAR FIELD AMPLITUDE AND PHASE PATTERN

LEGEND
——— FIELD
- - - - PHASE

FIGURE 5-39. FAR FIELD PATTERNS FOR OFFSET GEOMETRY, THIRD SURFACE AMPLITUDE FOR SCAN = 0, THIRD SURFACE PHASE FOR SCAN = 0, FREQUENCY = 20 GHz.

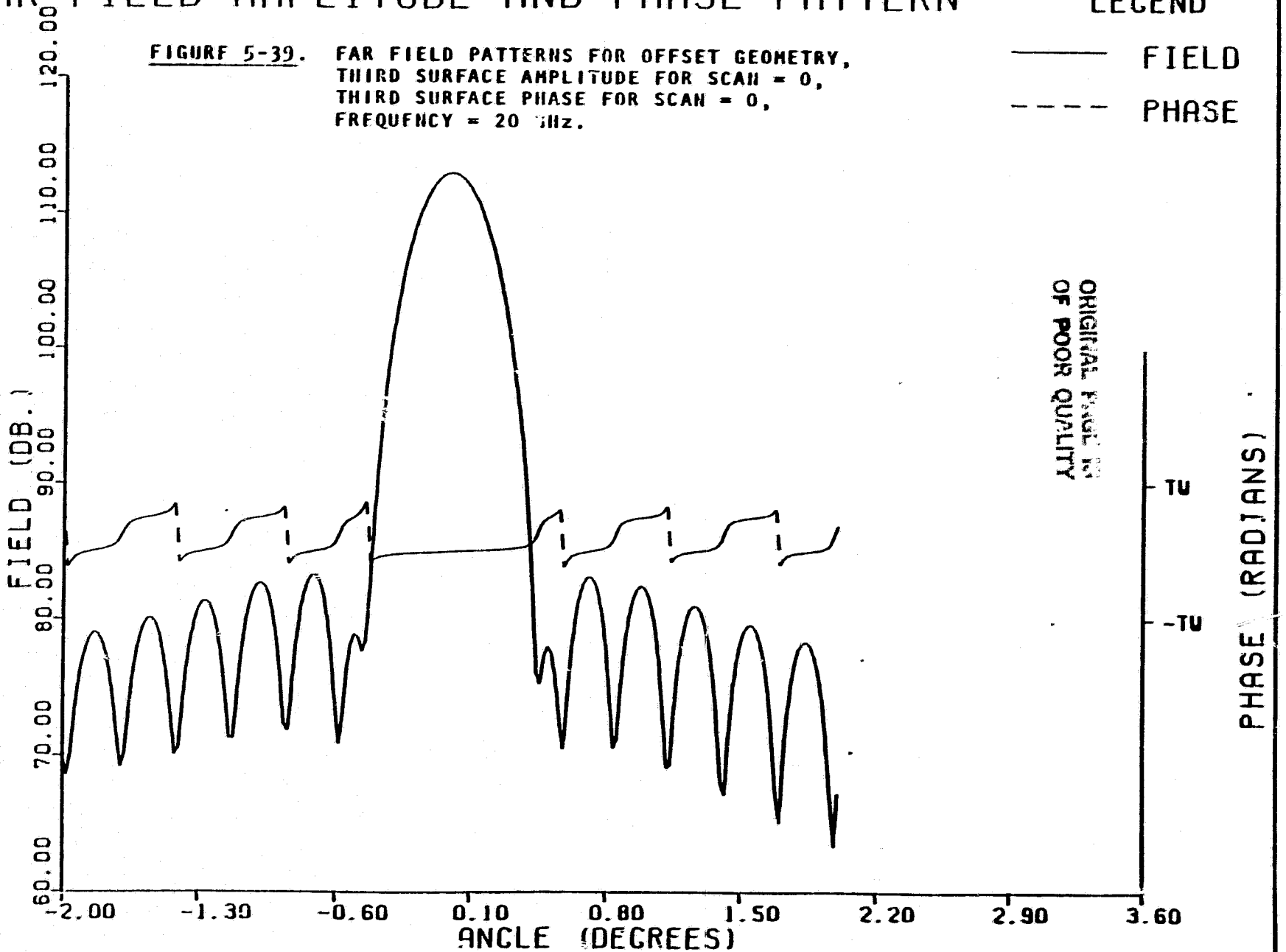

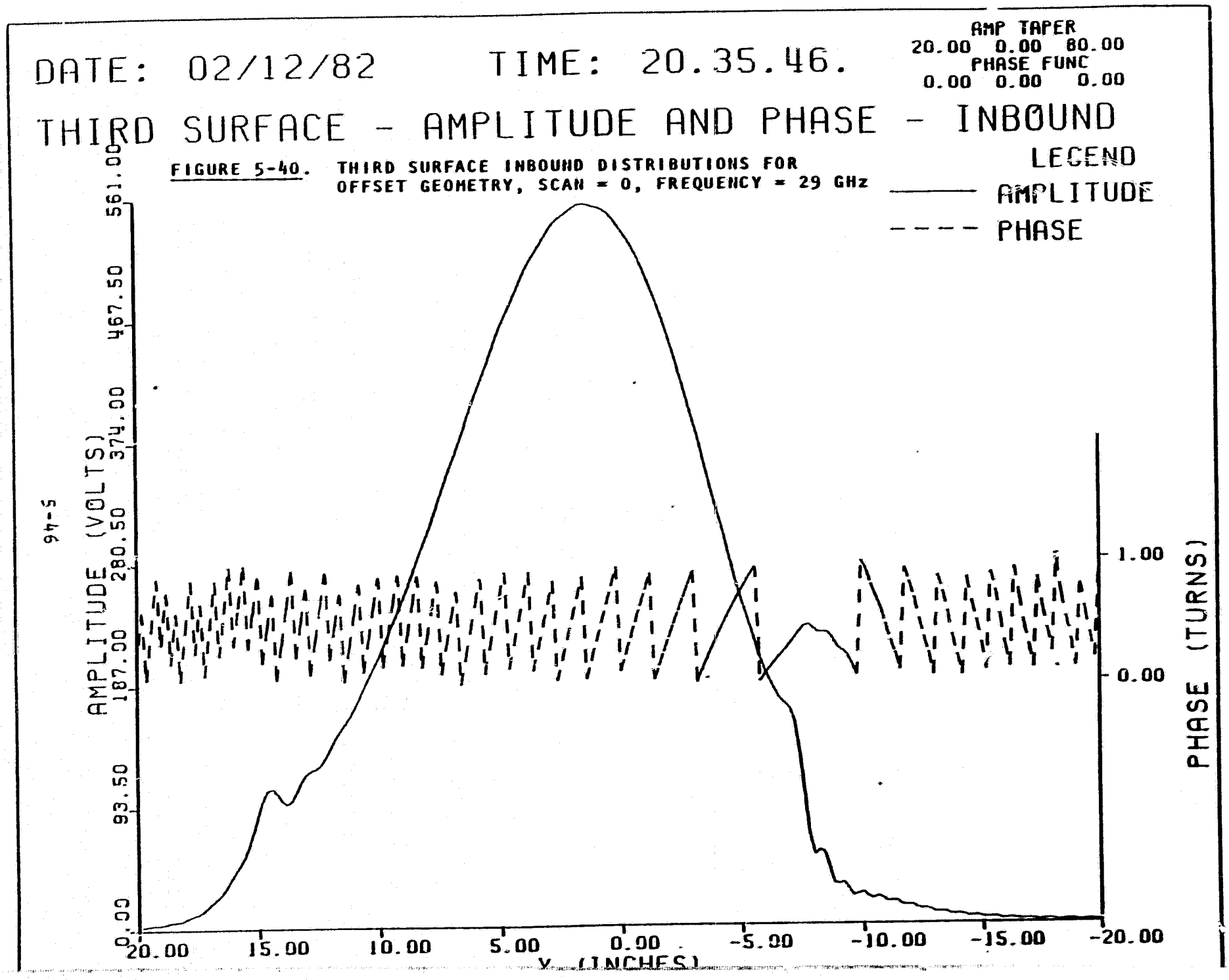

FIGURE 5-40. THIRD SURFACE INBOUND DISTRIBUTIONS FOR OFFSET GEOMETRY, SCAN = 0, FREQUENCY = 29 GHz

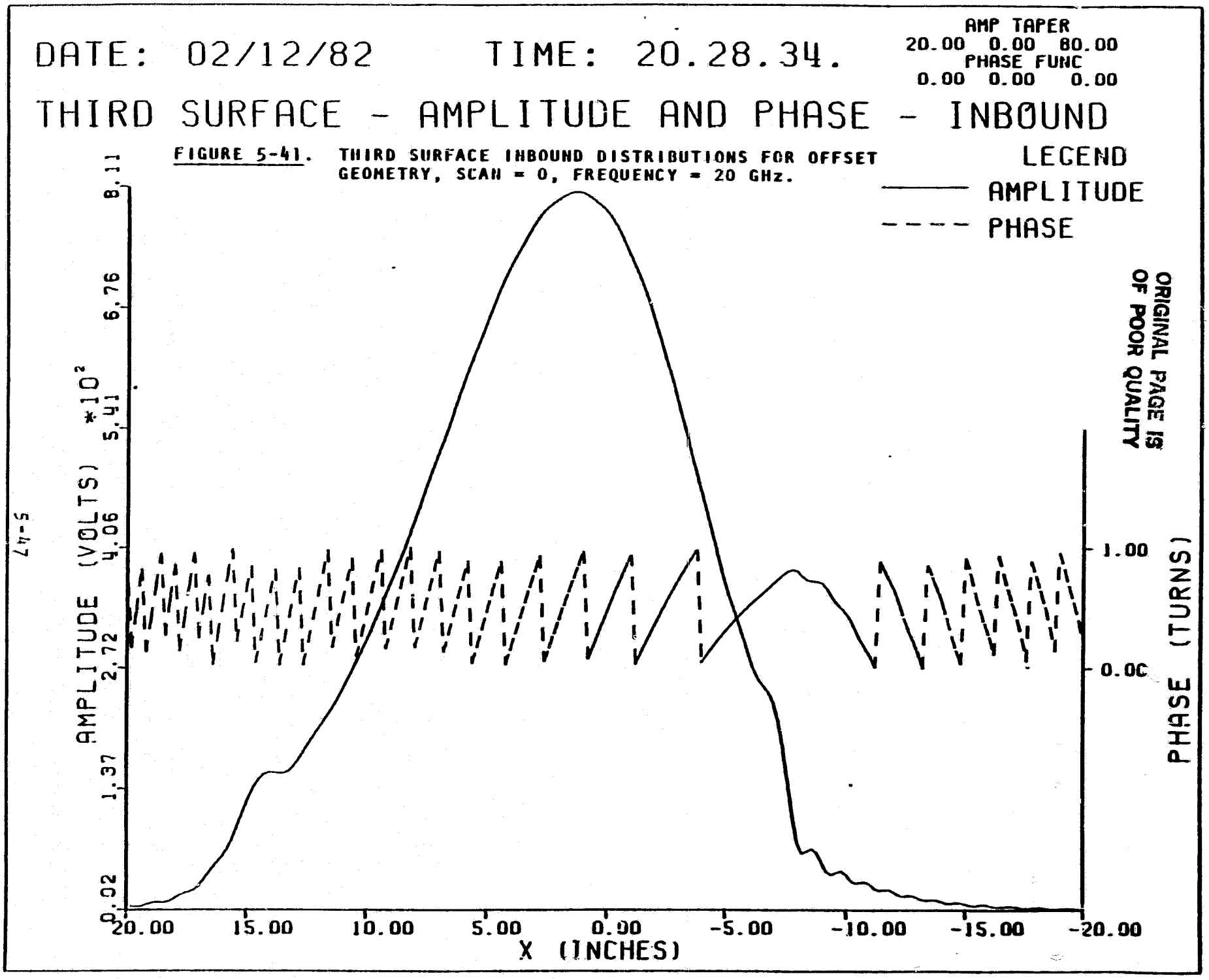
DATE: 02/12/82 TIME: 20.28.34.
AMP TAPER
20.00 0.00 80.00
PHASE FUNC
0.00 0.00 0.00
THIRD SURFACE - AMPLITUDE AND PHASE - INBOUND
FIGURE 5-41. THIRD SURFACE INBOUND DISTRIBUTIONS FOR OFFSET GEOMETRY, SCAN = 0, FREQUENCY = 20 GHz.
LEGEND
AMPLITUDE
PHASE
AMPLITUDE (VOLTS) *10²
0.02
1.37
2.72
4.06
5.41
6.76
8.11
PHASE (TURNS)
1.00
0.00
20.00
15.00
10.00
5.00
0.00
-5.00
-10.00
-15.00
-20.00
X (INCHES)
ORIGINAL PAGE IS OF POOR QUALITY
5-47

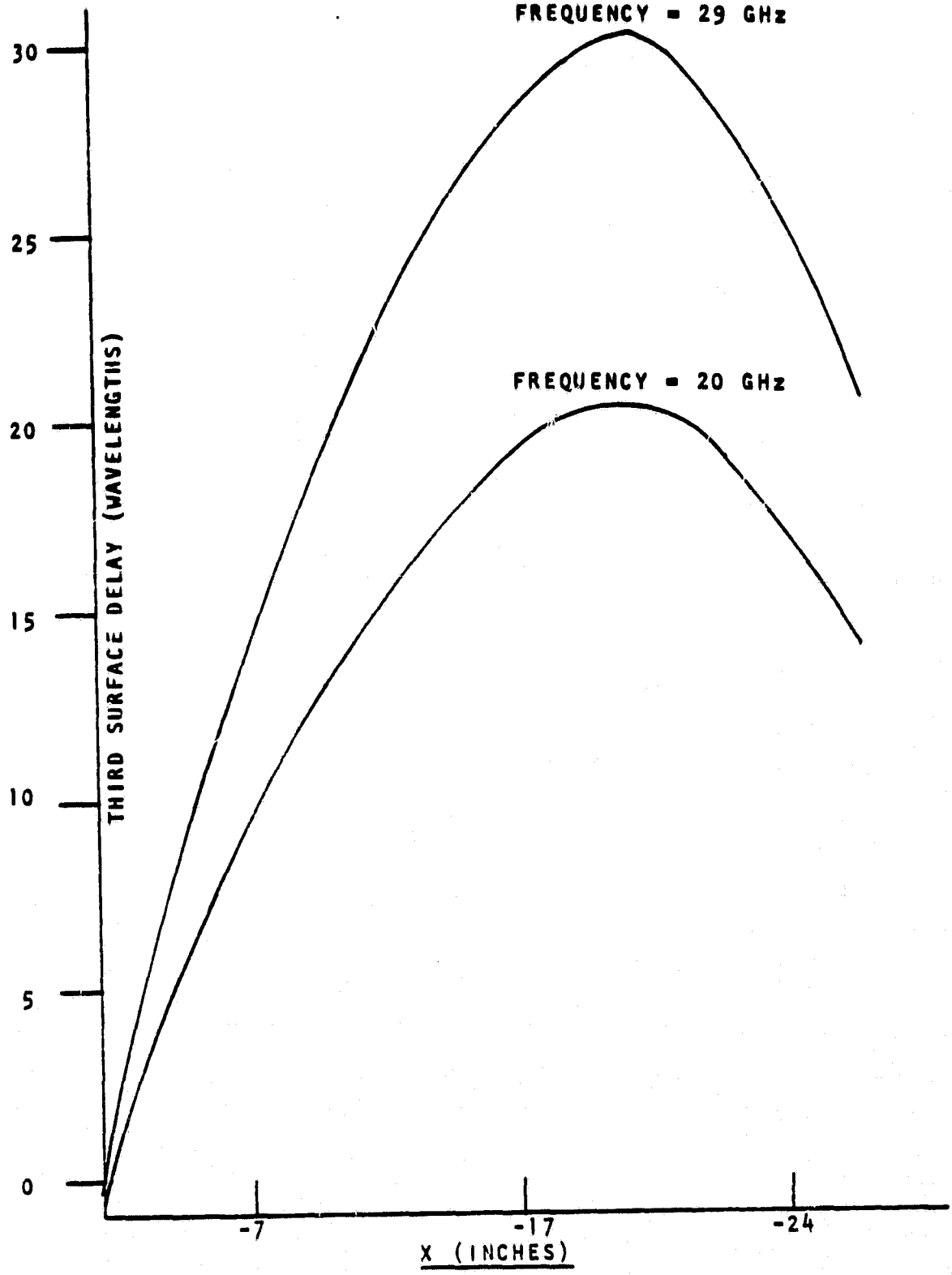

FIGURE 5-42. CONTINUOUS PHASE DISTRIBUTIONS FOR OFFSET GEOMETRY, SCAN = 0

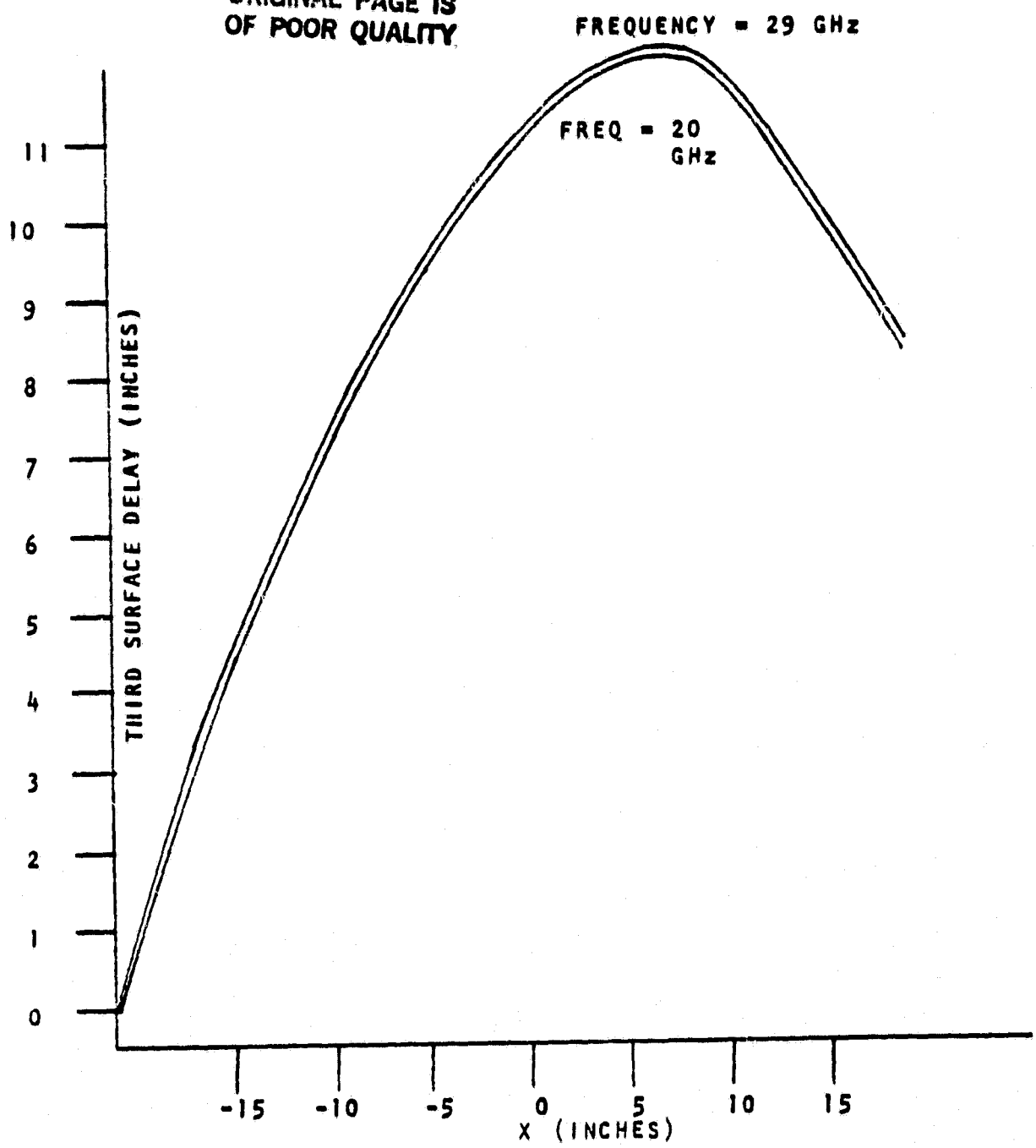

FIGURE 5-43
TIME DELAY DISTRIBUTIONS FOR OFFSET GEOMETRY, SCAN = 0

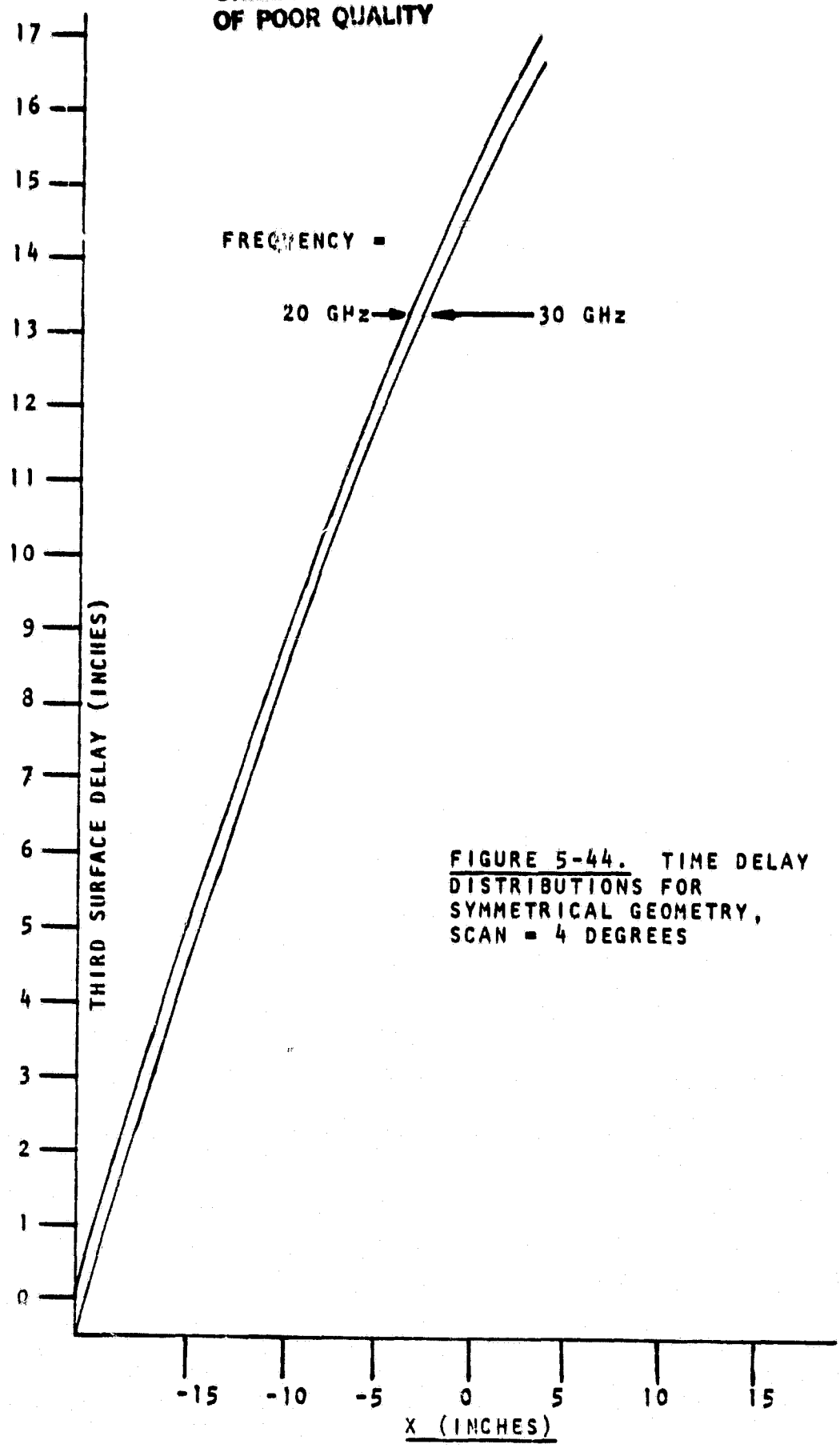

FIGURE 5-44. TIME DELAY DISTRIBUTIONS FOR SYMMETRICAL GEOMETRY, SCAN = 4 DEGREES

5.5 STEERING DELAY

An analysis was performed to determine the delay across the array required for scanning. For the symmetrical geometry the steering delay for scanning from zero to 4 degrees was calculated (Figure 5-45). For the offset geometry the steering delay for scanning from zero to 3 degrees was calculated (Figure 5-46).

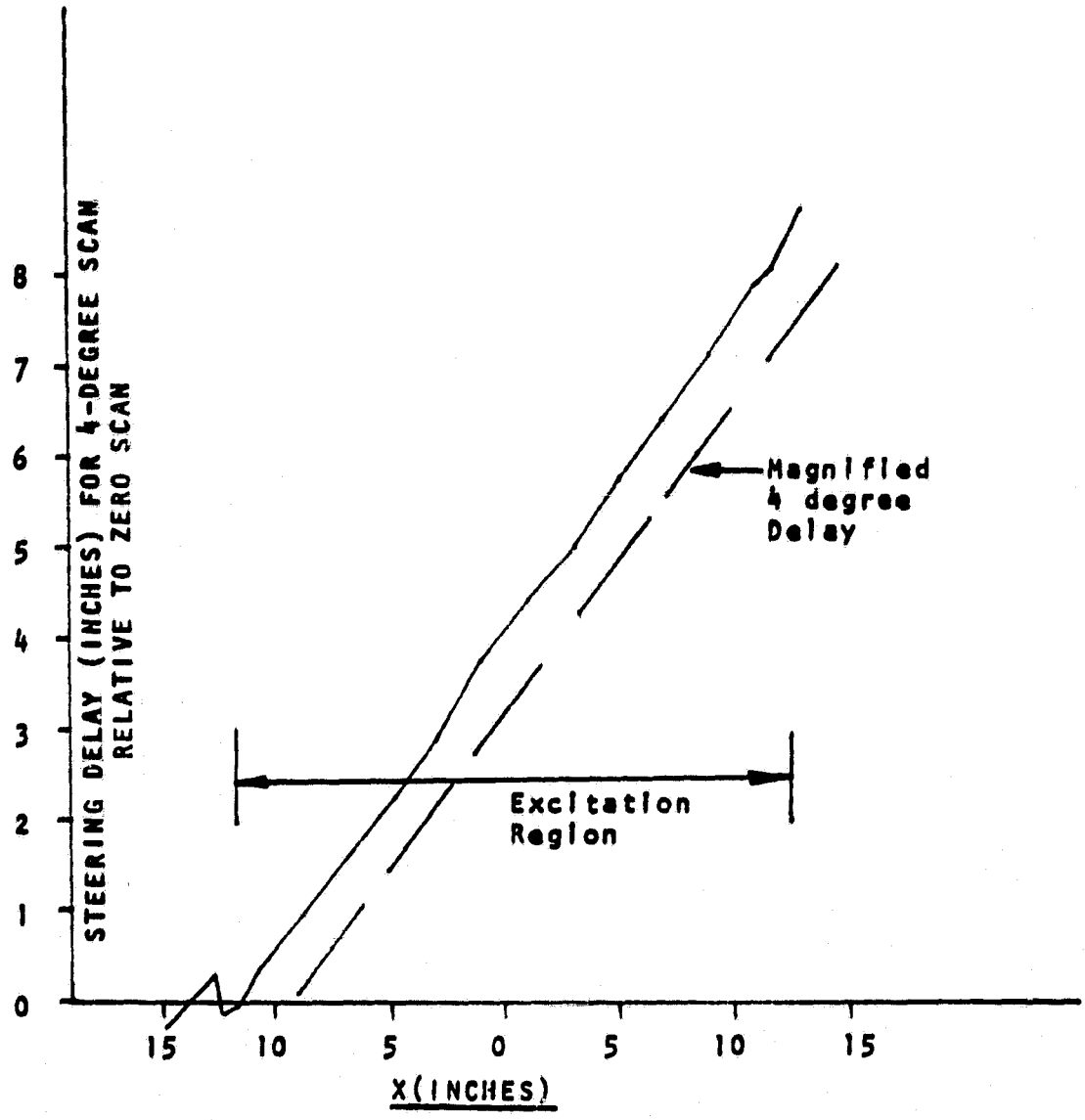

FIGURE 5-45
THIRD SURFACE DELAY FOR SYMMETRICAL GEOMETRY TO SCAN FROM ZERO TO 4 DEGREES, FREQUENCY = 30 GHz

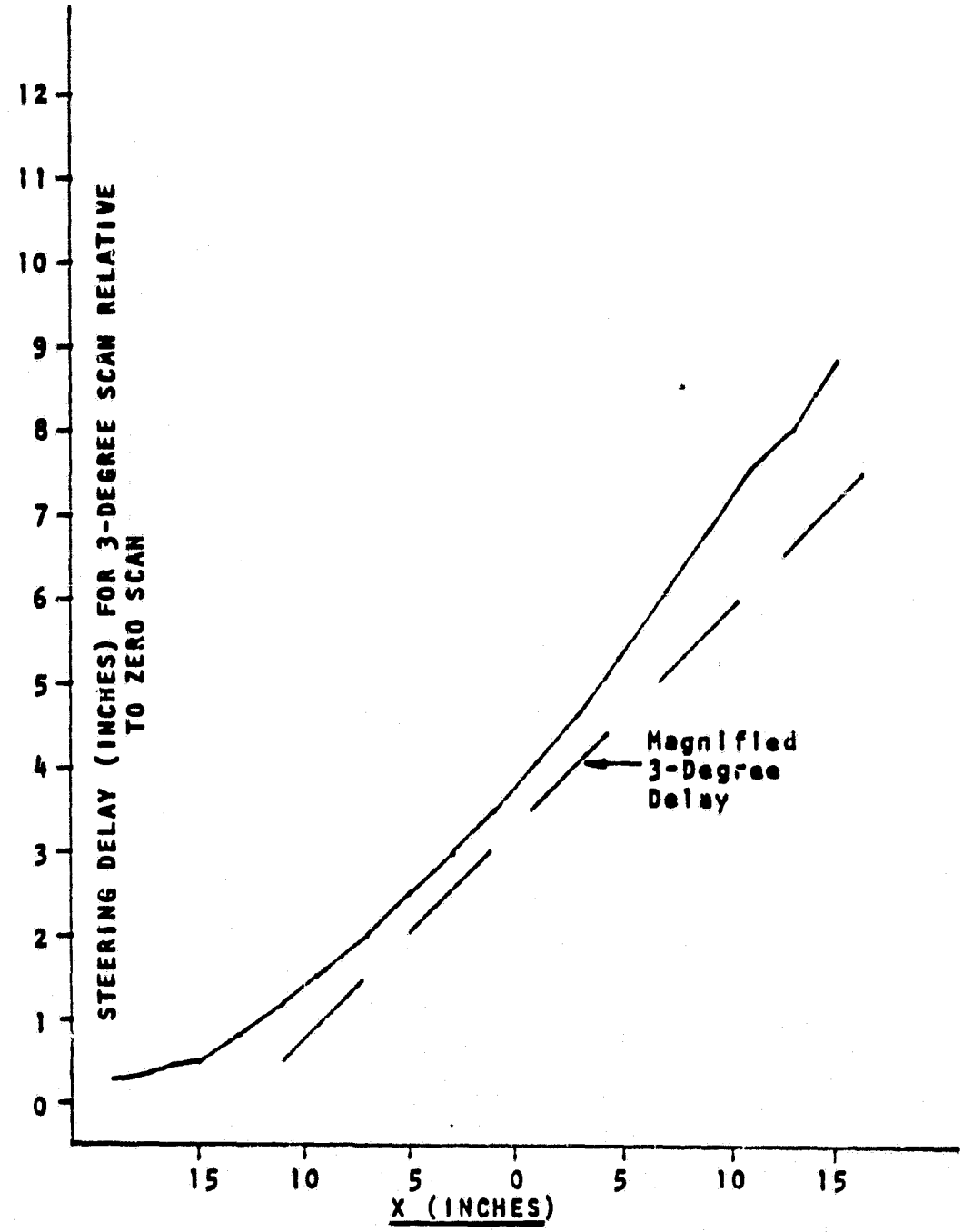

FIGURE 5-46
THIRD SURFACE DELAY FOR OFFSET GEOMETRY TO SCAN FROM ZERO TO 3-DEGREES, FREQUENCY = 20 GHz

6.0 REFERENCES

1. Robert J. Mailloux, "Phased Array Theory and Technology", RADC-TR-227, July 1981, Section 4.3.

2. W. D. White and L. K. DeSize, "Electronically Steerable Antenna Feed Techniques", 1963 PTGAP International Symposium, Boulder Colorado, July 1963.

3. L. K. DeSize, et. al., "Electronically Steerable Antenna Feed Techniques", RADC-TDR-63-121, March 1963.

4. L. K. DeSize, et. al., "Zoom Antenna Techniques", RADC-TR-66-300, May 1966.

5. D. Pride, "Zoom Antenna Techniques", RADC-TR-66-825, February 1967.

6. George Skahill, et. al., "Electronically Steerable Field Reflector Antenna Techniques", RADC-TR-66-354, August 1966.

7. W. Fitzgerald, "Limited Electronic Scanning with an Offset-Feed Near Field Gregorian System", ESD-TR-272, September 1971.

8. George Skahill an Walter Satre, "Reflector Antenna Zoom Techniques", RADC-TR-67-459, September 1967.

9. C. H. Tang and C. F. Winter, "A Study of the Use of a Phased Array to Achieve Pencil Beam over Limited Sector Scan", AFCRL-TR-73-0482, 1973.

10. A Rudge and M. Withers, "A New Technique for Beam Steering with Fixed Parabolic Reflectors", Proc. IEEE, Volume 118, No. 7, pp. 859 - 863.